

ANAEROBIC FERMENTATION OF BIOMASS  
GENERATED PRODUCER GAS TO  
ETHANOL

By

ROHIT PRADEEP DATAR

Bachelor of Engineering

University of Pune

Pune, India


1999

Submitted to the Faculty of the  
Graduate College of the  
Oklahoma State University  
in partial fulfillment of  
the requirements for  
the Degree of  
DOCTOR OF PHILOSOPHY  
December, 2003

ANAEROBIC FERMENTATION OF BIOMASS  
GENERATED PRODUCER GAS TO  
ETHANOL

Thesis Approved:

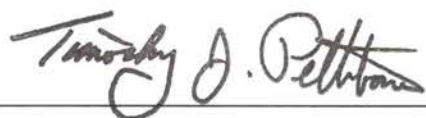
  
\_\_\_\_\_  
Thesis Adviser

  
\_\_\_\_\_

  
\_\_\_\_\_

  
\_\_\_\_\_

  
\_\_\_\_\_

  
\_\_\_\_\_

Dean of the Graduate College

## PREFACE

The development of low-cost, sustainable and renewable energy sources has been a major focus since the 1970's. Fuel-grade ethanol is one energy source that has a great potential for being generated from biomass. Considering the holistic approach of conversion of low cost biomass to ethanol and other products via gasification and fermentation, the undertaken research is a critical part to establish the viability of the process. The specific objectives of this research work, which continue to address several critical issues were: 1) integration of the gasifier-bioreactor system with assessment of the effect of biomass-generated producer gas on cell density and growth, pH, product profiles and substrate utilization, 2) assessment of the effects of individual gaseous impurities present in the biomass-generated producer gas on the above-mentioned parameters, 3) optimization of minerals, vitamins and metals to minimize liquid media cost and maximize cell concentration, and 4) development of a stable and efficient microbubble generation system for potential scale-up delivery of the producer gas. A novel clostridial bacterium, P7, was used for conversion of producer gas to ethanol. Fermentation studies were conducted on a four-liter bubble column bioreactor.

Keywords: Producer gas, syngas, ethanol, fermentation, clostridium, biomass.

## ACKNOWLEDGMENTS

My eternal gratitude goes to my parents, Pradeep Datar and Manik Datar, and to my brother, Rahul Datar for their love and support throughout my life. Their constant encouragement has been a source of my strength in realizing this long held dream of earning a PhD. I am also deeply indebted to my grandfather, Ravibhushan Datar and my late grandmothers, Leela Date and Aruna Datar, for instilling in me a solid foundation based on love, and making me realize the importance of success through “endurance and hard work”.

I also thank my sisters Aparna, Ashwini and Anuja, my brother-in-laws, Sandeep and Sudarshan, and my uncle and aunt, Arun and Ujwala Oka for their immense support during my education. Also, my uncle and aunt, Sanjeev and Mrunalini Date deserve a special mention.

I would like to thank my adviser, Dr. Randy Lewis for guiding me throughout this project. I could not have asked for a better adviser. During my four years with him, I have never seen him get angry or flustered, even though I had an occasional habit of breaking expensive glass electrodes. He was always a calm and patient person. There were times when research was slow and results were hard to get, but he always kept my motivation going with words of encouragement. His cogent and critical comments always stimulated a good discussion. He was never overbearing, but always firm and he respected and valued his students' thoughts and efforts. It was indeed a pleasure working with Dr.

Lewis. I am grateful to my doctoral committee members, Dr. AJ, Dr. Huhnke, Dr. Foutch and Dr. Bellmer for their support, comments and interest in my research work. I would also like to thank my friends in the Chemical Engineering office, Genny, Carolyn, Anne and Shirley for tolerating me and my numerous demands and for their help throughout my stay at OSU. I would also like to thank Dr. Pin-Ching from the National Renewable Energy Laboratory for her useful suggestions.

My friend and former colleague, Srinu deserves a special mention. He was of immense help during my early years on this project and he taught me all the tricks of running the bioreactor. I also thank my colleague Rustin for his support and suggestions. His company during our late night trips to Taco Bell and Sushi House was always fun. I sincerely appreciate the efforts of Matt, who helped me with the microbubble generator, and Jared and Asma, who were of great help during my media optimization studies.

This Ph.D would have been difficult without the help of my friends; Wayne Kiner and Robert Harshman at the Biosystems workshop who helped me build my bioreactor and microbubble generator.

The list is incomplete without thanking my infinitely long list of friends with whom I enjoyed cricket and racquetball, the potluck parties, although I rarely cooked and for all the great times we had together.

Also, I extend my special thanks to Bruno from Biosystems engineering for providing me producer gas and to Jack, Jason and Dr. Ralph Tanner from University of Oklahoma, Norman for giving me the “great smelling” bugs.

Last but not the least, I thank my fiancée, Shital and my extended family (Bala and Pramod Gaitonde and Neelesh and Tejal Chitnis) for their love, faith, trust and support during my Ph.D.

Finally, I thank all the sponsors of this research project, the Biomass Group at Oklahoma State University, and the Department of Chemical Engineering at OSU.

## TABLE OF CONTENTS

Chapter	Page
1. BIOMASS FERMENTATION TO ETHANOL: PAST, PRESENT AND FUTURE .....	1
1.1 Introduction.....	1
1.2 Environmental benefits of fuel-ethanol .....	6
1.1.1 Reduction/elimination in MTBE.....	6
1.1.2 Improvement in air quality.....	7
1.2 Economic and social benefits.....	9
1.3 National security and energy independence .....	10
1.4 Drawbacks of ethanol as a fuel .....	10
1.5 Ethanol manufacturing processes .....	11
1.5.1 Fermentation of sugar and starch crops .....	11
1.5.2 Ethanol from lignocellulosic feedstocks.....	12
1.6 A holistic approach for ethanol production via gasification.....	16
1.7 Objectives of this study.....	19
2. GASIFICATION AND PRODUCER GAS FERMENTATION: LITERATURE REVIEW .....	21
2.1 Introduction.....	21
2.2 Gasification of biomass.....	23
2.3 Producer gas fermentation .....	25
2.3.1 Biological catalysts .....	25
2.3.2 Principles of producer gas metabolism.....	27
2.3.3 Reactor configurations.....	31
2.3.4 Engineering aspects and media optimization.....	34
2.3.5 Microbubble generation system.....	37
2.4 Objectives of the study.....	39
3. INTEGRATION OF GASIFIER AND BIOREACTOR.....	40
3.1 Introduction.....	40
3.2 Objective of the study .....	41
3.3 Materials and Methods.....	41
3.3.1 Biomass preparation and properties.....	41
3.3.2 Gasifier operation and producer gas production.....	42

3.3.3	Biological catalyst.....	43
3.3.4	Culture medium .....	44
3.3.5	Bioreactor design and operation .....	49
3.3.6	Analytical procedures .....	55
3.4	Results and Discussion .....	60
3.4.1	Experiment 1 (with replenishment of liquid feed tank).....	60
3.4.2	Experiment 2 (with no replenishment of liquid feed tank) .....	73
3.4.3	Experiment 3 (gas clean up using 10% acetone) .....	86
3.5	Conclusions.....	95
4.	EFFECTS OF INDIVIDUAL GAS IMPURITIES.....	96
4.1	Introduction.....	96
4.2	Objectives of the study.....	97
4.3	Materials and Methods.....	98
4.3.1	Biological catalyst.....	98
4.3.2	Culture medium .....	98
4.3.3	Bioreactor operation.....	99
4.4	Results.....	100
4.4.1	Effect of O <sub>2</sub> on bioreactor performance.....	100
4.4.2	Effect of CH <sub>4</sub> on bioreactor performance .....	111
4.4.3	Effect of biomass-derived producer gas on pH of fermentation media .....	120
4.5	Discussion.....	120
4.5.1	Effect of O <sub>2</sub> introduction.....	120
4.5.2	Effect of CH <sub>4</sub> .....	122
4.5.3	Effect of producer gas on pH .....	123
4.6	Conclusions.....	123
5.	MEDIA OPTIMIZATION.....	124
5.1	Introduction.....	124
5.2	Objectives of the study.....	125
5.3	Materials and Methods.....	126
5.3.1	Biological catalyst.....	126
5.3.2	Culture Media .....	126
5.3.2	Experimental layout and operation .....	127
5.3.4	Analytical procedures .....	138
5.3.5	Experimental design.....	138
5.4	Results.....	139



Chapter	Page
5.4.1 Mineral optimization.....	139
5.4.2 Vitamin optimization .....	146
5.4.3 Trace metal optimization .....	160
5.5 Discussion.....	165
5.6 Conclusions.....	172
6. DESIGN OF A CONTINUOUS MICROBUBBLE GENERATION SYSTEM.....	176
6.1 Introduction.....	176
6.2 Objectives of the study.....	181
6.3 Materials and Methods.....	182
6.3.1 Design of Microbubble generator .....	182
6.3.2 Experimental layout and operation .....	185
6.3.3 Analytical procedures .....	188
6.4 Results.....	190
6.4.1 Microbubble quality and fractional incorporation .....	190
6.4.2 Volumetric material balance .....	191
6.4.3 Effect of surfactant concentration.....	197
6.4.4 Effect of salt addition.....	197
6.4.5 Effect of disc speed .....	201
6.4.6 Effect of gas flowrate.....	201
6.4.7 Effect of gas/liquid ratio .....	204
6.5 Discussion.....	204
6.6 Conclusions.....	209
7. CONCLUSIONS AND FUTURE WORK.....	210
7.1 Key research findings .....	211
7.2 Future studies .....	215
REFERENCES .....	218

## LIST OF TABLES

Table	Page
1.1. Common ethanolic motor-fuel formulations .....	3
1.2. Ethanol use in United States during 2002.....	5
2.1. Estimated biomass feedstock availability in the United States.....	22
3.1. Composition of stock mineral solution.....	46
3.2. Composition of stock vitamin solution.....	47
3.3. Composition of stock trace metals solution.....	48
3.4. Design specifications for bioreactor .....	51
5.1. Taguchi L <sub>12</sub> design for optimization of minerals.....	128
5.2. Factors and levels selected for various minerals.....	129
5.3. Taguchi L <sub>12</sub> design for optimization of vitamins.....	134
5.4. Factors and levels selected for various vitamins.....	135
5.5. Taguchi L <sub>12</sub> design for optimization of trace metals .....	136
5.6. Factors and levels selected for various trace metals .....	137
5.7. Cell concentrations (OD) for different mineral compositions .....	141
5.8. Y-hat model from first regression for mineral optimization.....	143
5.9. Residuals using regression analysis for mineral optimization.....	147
5.10. Cell concentrations (OD) for different vitamin compositions .....	150
5.11. Y-hat model from first regression for vitamin optimization.....	152
5.12. Y-hat model from second regression for vitamin optimization.....	154

Table	Page
5.13. Residuals using second regression analysis for vitamin optimization.....	156
5.14. Cell concentrations (OD) for different trace metal compositions.....	161
5.15. Y-hat model from first regression for trace metal optimization .....	163
5.16. Y-hat model from second regression for trace metal optimization.....	164
5.17. Residuals using second regression analysis for trace metal optimization .....	166
5.18. Cost analysis for original and optimized mineral composition .....	173
5.19. Cost analysis for original and optimized vitamin composition .....	174
5.20. Cost analysis for original and optimized trace metal composition.....	175
6.1. Design specifications for the microbubble generator .....	184

## LIST OF FIGURES

Figure	Page
1.1. Historic U.S. fuel ethanol production .....	4
1.2. Carbon dioxide recycle .....	8
1.3. Ethanol production strategy .....	17
2.1. Acetyl-CoA pathway for production of ethanol from producer gas .....	29
3.1. Biological catalyst, P7, used for producer gas fermentation .....	45
3.2. Bioreactor design .....	50
3.3. Schematic of experimental layout.....	54
3.4. Dry cell weight versus cell concentration (OD units).....	57
3.5. Cell concentration profile for experiment 1 .....	61
3.6. Batch growth curve for experiment 1 .....	62
3.7. pH profile for experiment 1 .....	64
3.8. Inlet and outlet CO profiles for experiment 1 .....	65
3.9. Inlet and outlet H <sub>2</sub> profiles for experiment 1 .....	66
3.10. Ethanol and butanol profiles for experiment 1 .....	68
3.11. Inlet and outlet CO <sub>2</sub> profiles for experiment 1 .....	69
3.12. Observed and predicted OD assuming cell washout for experiment 1 .....	71
3.13. Cell OD, pH, and product profiles from Day 0 to 8.5 for experiment 2.....	74
3.14. Batch growth curve for experiment 2 .....	75
3.15. Inlet and outlet CO profiles for experiment 2 .....	76

Figure	Page
3.16. Inlet and outlet H <sub>2</sub> profiles for experiment 2 .....	77
3.17. Inlet and outlet CO <sub>2</sub> profiles for experiment 2.....	79
3.18. Cell OD, pH, and product profiles from Day 8.5 to 11.5 for experiment 2.....	80
3.19. Cell OD, pH, and product profiles from Day 11.5 to 20 for experiment 2.....	82
3.20. Cell OD, pH, and product profiles from Day 0 to 18 for experiment 3.....	85
3.21. Inlet and outlet CO profiles for experiment 3.....	87
3.22. Inlet and outlet H <sub>2</sub> profiles for experiment 3 .....	88
3.23. Cell OD, pH, and product profiles from Day 18 to 24 for experiment 3.....	89
3.24. Observed and predicted OD assuming cell washout for experiment 3.....	91
3.25. Cell OD, pH, and product profiles from Day 24 to 29 for experiment 3.....	92
4.1. Cell OD profiles for 1000 ppm and 1900 ppm O <sub>2</sub> concentrations.....	101
4.2. pH profiles for experiment with O <sub>2</sub> introduction.....	103
4.3. NaOH consumption profile for experiment with O <sub>2</sub> introduction .....	104
4.4. Inlet and outlet CO profiles for experiment with O <sub>2</sub> introduction.....	106
4.5. Inlet and outlet H <sub>2</sub> profiles for experiment with O <sub>2</sub> introduction .....	107
4.6. Inlet and outlet CO <sub>2</sub> profiles for experiment with O <sub>2</sub> introduction.....	109
4.7. Ethanol and butanol profiles for experiment with O <sub>2</sub> introduction.....	110
4.8. Cell OD profiles for experiment with CH <sub>4</sub> introduction.....	112
4.9. pH profiles for experiment with CH <sub>4</sub> .....	113
4.10. NaOH consumption profile for experiment with CH <sub>4</sub> .....	114
4.11. Inlet and outlet CO profiles for experiment with CH <sub>4</sub> .....	116
4.12. Inlet and outlet H <sub>2</sub> profiles for experiment with CH <sub>4</sub> .....	117

Figure	Page
4.13. Inlet and outlet CO <sub>2</sub> profiles for experiment with CH <sub>4</sub> .....	118
4.14. Product profiles for experiment with CH <sub>4</sub> .....	119
4.15. pH profile with biomass-derived producer gas .....	121
5.1. Design of gassing manifold .....	131
5.2. Experimental layout for nutrient optimization.....	133
5.3. Average cell OD for gross mineral optimization.....	140
5.4. Average OD and standard deviation plot for mineral optimization.....	142
5.5. Y-hat pareto of coefficients for minerals .....	145
5.6. Observed cell concentrations (OD) and absolute residuals from regression analysis for minerals.....	148
5.7. Y-hat marginal means plot for minerals .....	149
5.8. Average OD and standard deviation plot for vitamin optimization.....	151
5.9. Y-hat pareto of coefficients for vitamins from first regression .....	153
5.10. Observed cell concentrations (OD) and absolute residuals from regression analysis for vitamins.....	157
5.11. Y-hat marginal means plot for vitamins .....	158
5.12. Cell OD for vitamin confirmation experiments.....	159
5.13. Average OD and standard deviation plot for trace metals optimization.....	162
5.14. Observed cell concentrations (OD) and absolute residuals from regression analysis for trace metals .....	167
5.15. Y-hat pareto of coefficients for trace metals from first regression.....	168
5.16. Y-hat marginal means plot for trace metals .....	169
6.1. Resistances involved in gas transport from bulk gas to reaction site in cell.....	178
6.2. Structure of a microbubble (colloidal gas aphron) .....	180

Figure	Page
6.3. Experimental layout for microbubble generation system .....	183
6.4. Design of microbubble generator.....	186
6.5. Total volumetric gas balance around the microbubble generator when inlet gas flow rate was controlled using a rotameter.....	192
6.6. Total volumetric liquid balance around the microbubble generator.....	193
6.7. Total volumetric balance around the microbubble generator when the gas flow was controlled by a rotameter.....	194
6.8. Total volumetric gas balance around the microbubble generator when inlet gas flow rate was controlled using a mass flow meter .....	195
6.9. Total volumetric balance around the microbubble generator when the gas flow was controlled by a mass flow meter.....	196
6.10. Volumetric gas balance for different gas flow rates .....	198
6.11. Effect of surfactant concentration of microbubble quality and gas incorporation	199
6.12. Effect of salt addition on microbubble quality and gas incorporation at different surfactant concentrations .....	200
6.13. Effect of disc speed on microbubble quality and gas incorporation.....	202
6.14. Effect of inlet gas flow rate on quality of microbubbles and gas incorporated ....	203
6.15. Effect of inlet gas flow/liquid flow ratio on percentage of gas incorporated .....	205

## NOMENCLATURE

ccm	cubic centimeters
CH <sub>4</sub>	methane
CMC	critical micelle concentration (ppm)
CO	carbon monoxide
CO <sub>2</sub>	carbon dioxide
D	dilution rate (hr <sup>-1</sup> )
FID	flame ionization detector
f <sub>G</sub>	gas fraction in microbubbles
f <sub>L</sub>	liquid fraction in microbubbles
GC	gas chromatograph
G <sub>i</sub>	flow rate of total gas incorporated into microbubbles (ml/min)
G <sub>in</sub>	total inlet gas flow rate (ccm)
g/L	grams per liter
G <sub>u</sub>	flow rate of total unincorporated gas from the microbubble generator (ccm)
hp	horse power
H <sub>2</sub>	hydrogen
IC	ion chromatograph
L <sub>in</sub>	total inlet liquid flow rate (ml/min)
L <sub>out</sub>	total outlet liquid flow rate (ml/min)



NaCl	sodium chloride
NaOH	sodium hydroxide
N <sub>2</sub>	nitrogen
O <sub>2</sub>	oxygen
P	ethanol concentration (g/L)
P <sub>i</sub>	ethanol concentration when non-growth associated ethanol production starts (g/L)
ppm	parts per million
Q <sub>a</sub>	volumetric flow rate of microbubbles (ml/min)
rpm	revolutions per minute
t	time (s)
TCD	thermal conductivity detector
V	volume of microbubbles (ml)
V <sub>L</sub>	volume of liquid (ml)
vol	volume (ml)
X	cell concentration (OD units)
X <sub>0</sub>	cell concentration before washout begins
Y <sub>N</sub>	cell concentration of N <sup>th</sup> bottle in a set of 3
α	growth associated constant for specific rate of ethanol production
β	non-growth associated constant for specific rate of ethanol production (g/L/day/OD)
μ	specific cell growth rate (hr <sup>-1</sup> )
μm	microns

## **CHAPTER 1**

### **BIOMASS FERMENTATION TO ETHANOL: PAST, PRESENT AND FUTURE**

#### **1.1 Introduction**

Since the energy crisis of the 1970's, the development of low-cost, sustainable and renewable energy sources has been a major focus. Fuel-grade ethanol and other valuable commercial products can be produced by utilizing biomass as a starting raw material. Ethanol can be used as a supplement to gasoline or as an alternative transportation fuel, which is beneficial in light of diminishing petroleum reserves. Typically, in the United States ethanol is used as an additive to gasoline and not as a stand-alone transportation fuel. Some of the common ethanolic motor-fuel formulations (Wheals et al., 1999) that are being used around the world are indicated in Table 1.1.

The United States has an extensive transportation system that is very critical to the economy of the nation. The total energy used for fuel by such a large transportation system in the United States was about 27.1 quadrillion Btu (quads) in 2001. Of this huge energy requirement, 99% was obtained by burning fossil fuels of which 97% of this was derived from petroleum (Greene and Schafer, 2003). Approximately 70% of the oil in the US is used for transportation. Currently, the United States imports about 57% of the total oil consumed and it is projected that oil imports will grow to about 68% by 2025 (Ethanol Industry Outlook, 2003). It has been estimated that the total worldwide reserves of fossil

fuels (proven and undiscovered) would last for about 46 years at a current worldwide energy consumption of  $10^{12}$  J/year (Kosaric and Velikonja, 1995). It is therefore critical to obtain energy from renewable resources such as inexpensive agricultural crops and residues. In addition to the reduction in oil dependence, ethanol obtained from renewable sources helps maintain and reduce global greenhouse gas emissions as compared to fossil fuels (Hohenstein and Wright, 1994). Therefore, there is a tremendous potential for conversion of underutilized low-cost biomass to liquid fuels such as ethanol and other useful products in lieu of traditional fossil fuels.

The Clean Air Acts Amendments (CAA) of 1990 mandated the reduction of toxic gaseous pollutants and volatile organic compounds from emissions of motor vehicles (Yacobucci and Womach, 2000). This act stipulated the use of either reformulated gasoline with at least 2% oxygen by weight or oxygenated fuels, which contain at least 2.7% oxygen by weight (Ahmed, 2001). The predominantly used oxygenates are MTBE (Methyl Tertiary Butyl Ether) and to a lesser extent ethanol, although MTBE is being slowly phased out due to potential health hazards and toxic combustion emissions. But over the last few years, there has been a tremendous growth in the U.S. ethanol industry fueled by a growing demand for renewable fuels. In 2002, the total ethanol produced in the United States was 2.13 billion gallons, representing a 20% increase over 2001 and a 45% increase over 1999 (Ethanol Industry Outlook, 2003). Fuel ethanol production in the United States for the past two decades is shown in Figure 1.1. The figure illustrates a steady increase in ethanol production in response to the growing use and market opportunities for ethanol. The primary ethanol uses in 2002 are shown in Table 1.2. According to the major uses, ethanol-based fuels have a great potential to supplement

<b>Fuel*</b>	<b>Ethanol content (%v/v)</b>
Hydrous ethanol (Alcool) (Brazil)	95.5
E85 (North America)	85
Gasoline (Brazil)	24
E10 (Gasohol) (North America)	10
Oxygenated fuel (USA)	7.6
Reformulated Gasoline (USA)	5.7
Biodiesel (Sweden)	15

\*Hydrous ethanol contains 4.5% (v/v) water. The other formulations contain hydrocarbons and a trace of water

Table 1.1. Common ethanolic motor-fuel formulations (Wheals and Basso, 1999)

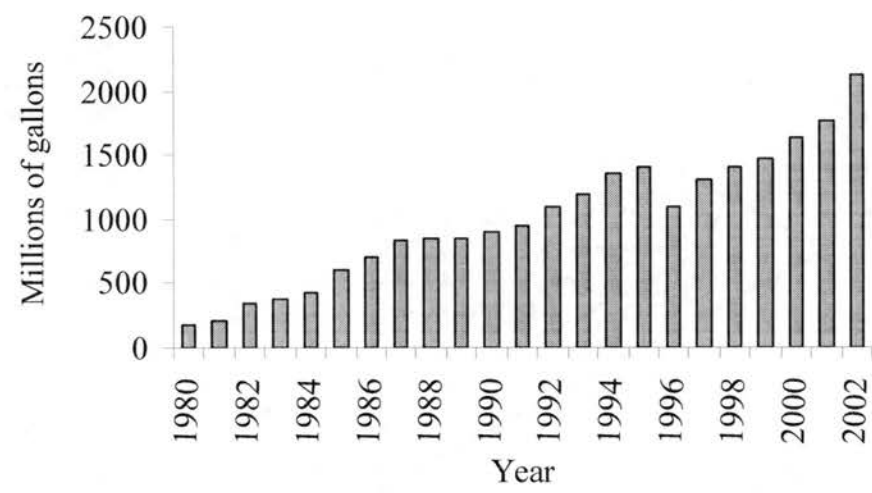


Figure 1.1. Historic U.S. fuel ethanol production (Ethanol Industry Outlook, 2003)

Market	Purpose	Million gallons
Federal reformulated gasoline	Oxygenate	700
Federal winter oxygenated fuels	Oxygenate	250
Minnesota oxygenated fuels	Oxygenate	250
Conventional gasoline	Octane enhancer	900

Table 1.2. Ethanol use in United States during 2002

or even replace gasoline in the future (Yacobucci and Womach, 2000). There are several economic, environmental, social benefits of ethanol as a fuel, each of which is described below in detail.

## **1.2 Environmental benefits of fuel-ethanol**

### **1.2.1 Reduction/elimination in MTBE**

MTBE has been traditionally used as an oxygenate in gasoline because of its high octane number, low sulfur content and relatively low production cost as compared to other high octane components (Ahmed, 2001). In 1998, the United States consumed about 4.3 billion gallons of MTBE, 1.5 billion gallons of which was imported (Ethanol Industry Outlook, 1999). MTBE has been shown to be a potential carcinogen in humans and animals (Nadim et al., 2001). Also, exhaust gas emissions containing MTBE have shown to irritate lungs and eyes (Poulopoulos and Philippopoulos, 2001). MTBE is also much difficult to degrade and hence a source of ground and surface water contamination (He et al., 2002). Ethanol has about 35% oxygen by weight, twice as much as in MTBE. Thus, ethanol is a very strong candidate to replace MTBE in the future despite the higher cost, since it is environmentally friendly and can be produced domestically from renewable sources.

### 1.2.2 Improvement in air quality

Ethanol is a preferred motor fuel since it reduces harmful vehicle emissions, thus protecting the environment. The addition of ethanol to gasoline also facilitates the reduction or removal of toxic air components like 1,3 butadiene and benzene, which are commonly found additives in gasoline (Blackburn and Teague, 1998).

*Reduction in ground level ozone precursors:* After the Clean Air Act Amendments of 1990 were established, the addition of oxygenates to gasoline was required to reduce the formation of harmful ground-level ozone (photochemical smog) in urban areas. The chemical reaction of hydrocarbons and oxides of nitrogen produce ozone in the presence of sunlight. This ozone causes a variety of health related problems in humans and also damages agricultural crops. The use of ethanol as part of the fuel results in emissions that are less reactive in the presence of ultraviolet radiation than those produced by burning gasoline. Thus, there is a lower potential for the formation of such damaging ground-level ozone.

*Reduction in greenhouse gas emissions:* Emissions of carbon dioxide (CO<sub>2</sub>), the primary greenhouse gas, have steadily increased and the transportation sector alone accounts for 33% of the total emissions (Greene and Schafer, 2001). The greenhouse gases, which include CO<sub>2</sub>, methane and oxides of nitrogen, contribute to global warming thus affecting weather patterns and causing increased aridity in fertile areas. The production and use of ethanol from biomass, unlike gasoline, is CO<sub>2</sub> neutral (Figure 1.2). The CO<sub>2</sub> formed during combustion of ethanol is utilized during the growth of plants used to produce ethanol. Thus, the use of renewable fuels like ethanol does not increase atmospheric CO<sub>2</sub> levels, as do the petroleum fuels. Moreover, the likelihood of a



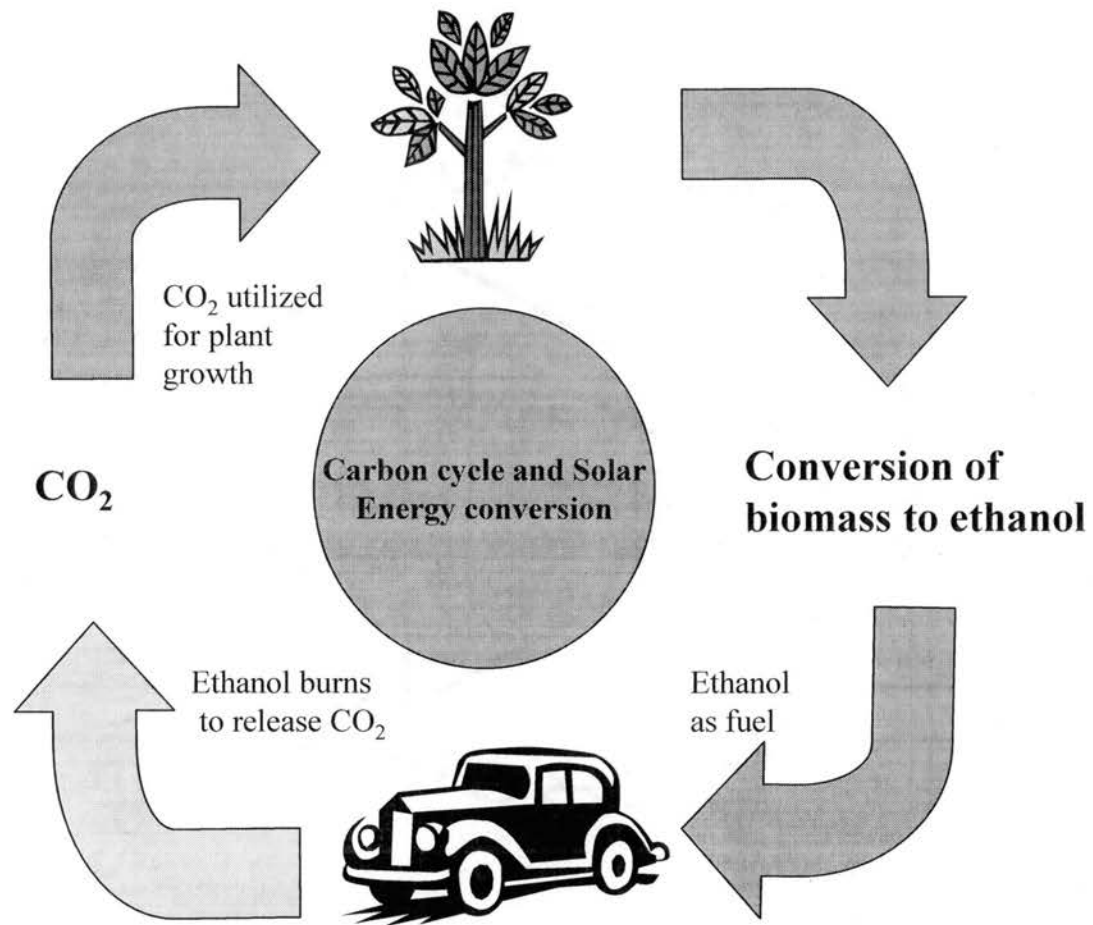


Figure 1.2 Carbon dioxide recycle (Ethanol Industry Outlook, 2003)

net reduction in CO<sub>2</sub> levels increases since CO<sub>2</sub> is formed into organic matter that goes back to the soil, thereby increasing soil fertility and reducing erosion. It is estimated that an 85 % ethanol fuel would reduce greenhouse gas emissions by as much as 37%, while a 10% ethanol blend would reduce emissions by about 3.9% (DOE Report, 1999).

*Particulates, nitrogen oxides and carbon monoxide (CO) emissions:* Particulates are emissions of soot and particles of partially combusted fuel components. They are of concern in diesel engines. It is estimated that ethanol-blended fuels would reduce such emissions by as much as 40% (Ethanol Industry Outlook, 2003). There have also been significant reductions in sulfur dioxide emissions by use of ethanol-blended diesel or neat ethanol. With the use of E85 (85% ethanol, 15% gasoline) or E95 (95% ethanol, 5% gasoline), there would be a 20% reduction in nitrogen oxide emissions. Also, a 10% ethanol blend would reduce CO emissions by about 25-30% as a result of better fuel combustion (DOE Report, 1999).

### **1.3 Economic and social benefits**

Currently, the United States imports about 57% of its oil, creating a \$66 billion trade deficit, which is expected to rise to \$170 billion by 2020 (NREL Report, 1999). It is estimated that a 40 million gallon per year ethanol plant would provide a one-time monetary boost of \$142 million during the construction of such a plant. Additionally, the ethanol plant would add 694 permanent jobs and generate at least \$1.2 million in tax revenue for local and state governments. Also, the construction of such an ethanol manufacturing facility would increase the local economic base of the community by \$110 million (Ethanol Industry Outlook, 2003).

#### **1.4 National security and energy independence:**

The United States continues to be reliant on overseas oil resources for its domestic consumption. It is projected that oil imports would grow to 68% in 2025, thus increasing the dependence on crude oil from potentially unstable regions around the world. Thus it is essential to increase the local energy production via fuels from renewable sources to prevent sudden energy disruptions that could have severe economic ramifications. It is estimated that a 10% ethanol blend would cause a 3% reduction in fossil energy, while the use of E95 could reduce the fossil energy requirement by as much as 44% (Yacobucci and Womach, 2000).

#### **1.5 Drawbacks of ethanol as a fuel**

There have been ongoing arguments over the use of ethanol as a fuel. Some of the drawbacks include:

- Ethanol can be corrosive to some metals, gaskets and seals in car engines (Yacobucci and Womach, 2000)
- The heating value of ethanol is 76,000 Btu/gallon as compared to 115,000 Btu/gallon for gasoline; hence more ethanol is required to travel the same distance. There have been conflicting reports on the statement mentioned above, since some experts argue that there is statistically no mileage difference due to a higher combustion efficiency of ethanol as compared to gasoline (DOE Report, 1999).
- Ethanol-blended fuels increase the emission of aldehydes and acetic acid and may contribute to acid rain formation (Zervas et al., 2001).

- Some argue that the cost of ethanol is too high to be used as an additive or replacement to gasoline and that the ethanol industry would not survive without tax incentives. With a current subsidy of \$ 0.53/gallon, it is estimated that the Highway Trust Fund would lose revenue of \$1.2 billion.

Arguably, ethanol as a fuel would not be able to compete with gasoline unless cheaper routes for ethanol production are investigated and developed.

## **1.6 Ethanol manufacturing processes**

### **1.6.1 Fermentation of sugar and starch crops**

Almost all of the current commercial production of ethanol (in United States and Brazil) is from the fermentation of sugar crops (sugar cane and sugar beet) and from starchy crops (maize, wheat and corn). In the United States, the production of ethanol from corn grew to about 1.9 billion gallons in 2001 (Ugarte and Walsh, 2002). This accounted for 90% of the total ethanol production and an estimated 615 million bushels of corn (6.2% of total corn produced) were consumed. The remaining 10% of the total ethanol production was from fermentation of grain sorghum, barley, wheat, cheese whey and potatoes. The basic steps for conversion of such crops to ethanol are:

- The biomass either undergoes a grinding process (dry milling) or is chemically treated (wet milling) to reduce the size of the feedstock.
- The starch is converted to sugars by enzymatic treatment.
- The sugars are fermented to ethanol by special strains of yeast.
- The ethanol is purified from the fermentation broth by distillation.

- The remaining solid residue is then used for cattle feed or in some cases is used as a fuel for boilers.

This process often occurs in geographic locations within the corn belt area because of lower transportation costs of the feedstock supply. Hence, ethanol production is generally economically feasible (with tax subsidy) only in such regions, since feedstock contributes a major share in the total costs. Therefore, to expand ethanol production throughout the United States, alternate raw materials like underutilized biomass or low cost cellulosic feedstock are being investigated.

### **1.6.2 Ethanol from lignocellulosic feedstocks**

There is a tremendous supply of lignocellulosic feedstock around the world. It is estimated that  $20 \times 10^8$  tons/year of lignocellulosic biomass is available (Szczodrak and Fiedurek, 1995). The most common lignocellulosic materials are corn stover, grasses, wood chips, paper wastes and agricultural residues. In the United States alone, the estimated feedstock availability is about 360 million dry tons/year, with corn stover contributing about 43% of the amount (Kadam and McMillan, 2003). The advantage of such materials is the abundant unused supply. Also, lignocellulosic feedstocks, such as switchgrass and Bermudagrass, can be cultivated on marginal, under-utilized lands for a very low cost. Lignocellulosic materials are characterized by varying amounts of cellulose, hemi-cellulose, lignin and small quantities of other extractives. Typically, the composition by weight is 40-50% cellulose, 20-40% hemi-cellulose and 10-30% lignin (McKendry, 2002, Sun and Cheng, 2002). Cellulose is a linear polymer of glucose with a  $\beta$  1-4 linkage. The average molecular weight is about 100,000. Hemi-cellulose is a

branched polysaccharide, consisting primarily of five carbon sugars such as xylose and arabinose in addition to glucose and mannose. The average molecular weight is less than 30,000. Lignin is a group of amorphous, high molecular weight compounds.

The following processes are currently utilized for the production of ethanol from lignocellulosic materials and are explained below.

- Dilute acid hydrolysis followed by fermentation
- Concentrated acid hydrolysis followed by fermentation
- Dilute acid pretreatment followed by enzymatic hydrolysis and fermentation
- Ammonia disruption, hydrolysis and fermentation
- Steam disruption, hydrolysis and fermentation
- Gasification of biomass followed by fermentation

*Dilute acid hydrolysis followed by fermentation:* In this process, ground biomass is treated with a dilute sulfuric acid (2-5%) at about 160 °C under a pressure of about 10 atmospheres to break down the cellulose and hemi-cellulose components to fermentable sugars (Iranmahboob et al., 2002). The lignin fraction is separated from the hydrolyzate. The five and six carbon sugars are then fermented to ethanol using genetically engineered organisms like *Escherichia Coli* (Ingram et al., 1997), *Saccharomyces* yeast (Krishnan et al., 1997) and *Zymomonas Mobilis* (Picataggio et al., 1997). Ethanol is then separated from the fermentation broth by distillation. One major drawback is the fact that this process results in low glucose yields (50-60%) from cellulose and hence gives low ethanol yields (Himmel et al., 1997).

*Concentrated acid hydrolysis followed by fermentation:* A concentrated acid solution (10-30%) is used at 100 °C (Clausen and Gaddy, 1993) and atmospheric pressure to hydrolyze the hemi-cellulose and cellulose. The concentrated acid hydrolysis process is preferred over the dilute acid hydrolysis process because of lower operating temperatures and pressures as well as the higher yields. Commercial resins are then used to separate the acid from sugar and the solution is neutralized with lime to precipitate residual acid to hydrated gypsum (Hawaii Report, 1994). A challenging issue in both the dilute acid hydrolysis and concentrated acid hydrolysis processes is the disposal of lignin, although it can be used as a fuel. Also, a major disadvantage is the formation of unwanted byproducts like hydroxymethyl furfural (Slaff, 1984).

*Enzymatic hydrolysis followed by fermentation:* The feedstock is first pretreated with a dilute acid to break down the lignocellulose into lignin, hemi-cellulose and cellulose. The cellulose and hemi-cellulose are then treated with special enzymes called cellulases and xylanases to break down the cellulose and hemi-cellulose fractions into six and five carbon sugars respectively, which are then fermented to ethanol. The pretreatment of lignocellulose with dilute acid followed by enzymatic breakdown of cellulose and hemi-cellulose has shown to maximize the overall process yields as compared to processing with dilute acid alone. The disadvantage of this method is the high cost and requirement of enzymes. Also, this process is complicated by accumulation of soluble products like cellobiose and cellotriose which act as competitive inhibitors of hydrolysis (Ingram et al., 1997).

*Ammonia disruption, hydrolysis and fermentation:* The lignocellulosic biomass is exposed to ammonia at a high pressures and temperatures of about 25-90 °C. The

elevated pressure and temperature causes swelling and decrystallization of the biomass. The pressure is then suddenly lowered, causing the biomass to explode. This makes the biomass accessible to enzymes during hydrolysis. The extracted fiber is then hydrolyzed to sugar using enzymes and then fermented to ethanol.

*Steam disruption, hydrolysis and fermentation:* Biomass is fed into a high-pressure cylinder and treated with steam. The biomass is then passed into a flash tank, causing an explosion due to the sudden pressure change. This causes autohydrolysis of the hemicellulose to xylose, while the cellulose is treated with enzymes to form glucose. The sugars are then fermented to ethanol. A disadvantage of the process is that volatile organics are formed (e.g. furfural) which are toxic to the microbial catalysts.

*Gasification followed by fermentation:* Gasification converts biomass to a gas mixture by partial oxidation at high temperature in the presence of a medium such as air, oxygen or steam (McKendry, 2002). This gaseous mixture can then be fermented to ethanol using anaerobic microbial catalysts such as *Clostridium ljungdahlii* (Gaddy and Clausen, 1992), *Clostridium acetoethanogenum* (Abrini et al., 1994) and *Acetobacterium woodii* (Buschhorn et al., 1989). Unlike other processes described previously in which the lignin fraction of lignocellulose remains unutilized, it is possible to convert all the carbon present in lignocellulosic substrate to a gaseous mixture (Reed and Jantzen, 1979). A large variety of biomass substrates, including solid municipal waste and waste paper, can be converted to fermentable gas by this method. Typically, gasification of biomass using air as a fluidization medium yields a gas mixture primarily composed of carbon monoxide (CO), carbon dioxide (CO<sub>2</sub>), hydrogen (H<sub>2</sub>) and nitrogen (N<sub>2</sub>). The composition of gas obtained depends on the gasification medium used. The gas can also



be converted to ethanol by chemical catalysts, but microbial catalysts offer several advantages. Biocatalysts require significantly lower temperature and pressure conditions (usually atmospheric conditions) and hence are economically more viable due to lower processing costs. Microbial catalysts also show a higher specificity and yield and are also less susceptible to poisoning, the disadvantages being longer processing times (Klasson et al., 1992, Vega et al., 1990, Grethlein et al, 1992). Although the gasification-fermentation approach seems very promising, it is characterized by some problems. The gaseous substrate has to transfer to active sites on the microbial catalyst for efficient conversion to ethanol and other products. The constituents of producer gas such as CO and H<sub>2</sub>, have aqueous solubilities of 60% and 4%, respectively as compared to O<sub>2</sub> on a mass basis and hence such processes are often mass transfer limited (Bredwell et al., 1995 and 1999).

### **1.7 A holistic approach for ethanol production via gasification**

A holistic approach is being employed at Oklahoma State University to investigate the process of converting low-cost underutilized biomass to ethanol and other useful products using the gasification process. This holistic approach encompasses all aspects, including growth, handling, transportation, storage, gasification, fermentation and separation of final products. A schematic of the overall ethanol production strategy is shown in Figure 1.3.

Switchgrass, a native Oklahoma tall grass, is being used as a model crop for the gasification study because of its abundance and low cost. However, the gasifier is capable of using a wide spectrum of lignocellulosic feedstocks like corn residues, saw dust, wood

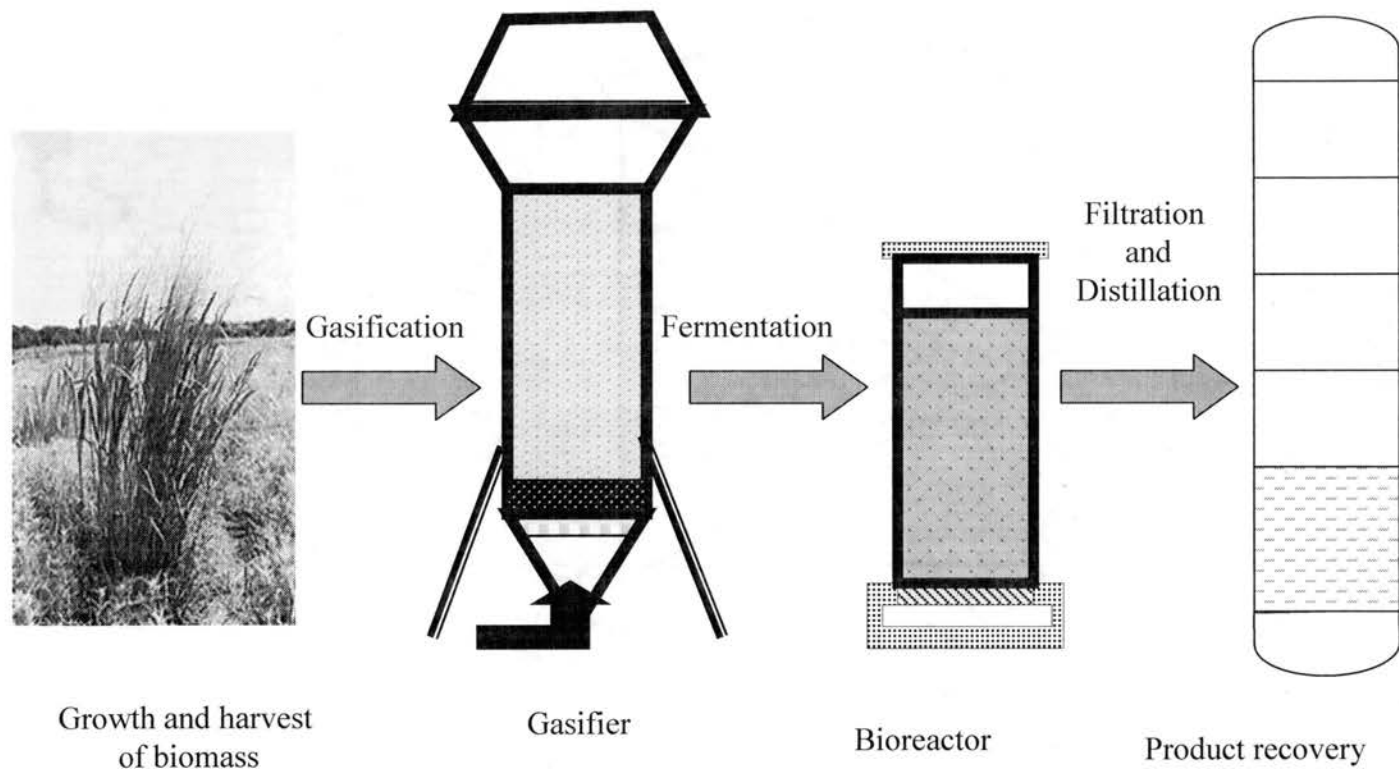


Figure 1.3 Ethanol production strategy

chips and Bermudagrass. A pilot-plant scale fluidized bed gasifier is being operated at Oklahoma State University, Stillwater, for gasification of switchgrass. The composition of producer gas can be altered by changing the medium used for gasification with minor modifications in the heating system of the existing gasifier. Steam gasification can be used when CO and H<sub>2</sub> are the predominantly required gases. Currently, the gasifier is operated under controlled amounts of air to maximize CO production and minimize oxygen production. However, significant amounts of CO<sub>2</sub> and N<sub>2</sub> are produced in this process as compared to steam gasification (Sadaka et al., 2002, Gil et al., 1999). Typically, the producer gas obtained from gasification of switchgrass) contains N<sub>2</sub>, CO<sub>2</sub>, CO, H<sub>2</sub>, methane and trace quantities of light hydrocarbons (Cateni et al., 2000 and 2003). The producer gas also contains solid particulates like ashes and condensable tars that must be separated before the fermentation process.

A novel clostridial acetogen, denoted as P7, is currently being used for the fermentation of producer gas to ethanol. The bacterium operates under anaerobic conditions and follows the Wood-Ljungdahl pathway (Wood et al., 1986, Phillips et al., 1994) for autotrophic growth. The overall biochemical reactions using different gaseous substrates are summarized as follows, assuming ethanol (C<sub>2</sub>H<sub>5</sub>OH) as the sole product.

- CO as substrate:  $6 \text{ CO} + 3 \text{ H}_2\text{O} \rightarrow 4 \text{ CO}_2 + \text{C}_2\text{H}_5\text{OH}$
- CO<sub>2</sub> and H<sub>2</sub> as substrates:  $6 \text{ H}_2 + 2 \text{ CO}_2 \rightarrow \text{C}_2\text{H}_5\text{OH} + 3 \text{ H}_2\text{O}$
- CO and H<sub>2</sub> as substrates:  $6 \text{ H}_2 + 6 \text{ CO} \rightarrow 2 \text{ C}_2\text{H}_5\text{OH} + 2 \text{ CO}_2$

Note that the last reaction is just a combination of the first two reactions. With CO as the sole carbon substrate, 33% of the carbon can be theoretically converted to ethanol, while the theoretical carbon conversion to ethanol would be 100% for a 3:1 molar ratio of H<sub>2</sub> to

CO<sub>2</sub>. For an equimolar mixture of H<sub>2</sub> and CO, 67% of the carbon from CO could be converted to ethanol. Obviously, the ethanol yield would depend on the composition of producer gas. Although ethanol can be theoretically produced from CO alone, previous studies with P7 have shown that an external supply of CO<sub>2</sub> is required in addition to CO to sustain cell growth and ethanol formation, although CO<sub>2</sub> is generated during the fermentation process (Rajagopalan, 2001). The stoichiometric reactions for other products like acetic acid (CH<sub>3</sub>COOH) and butanol (C<sub>4</sub>H<sub>9</sub>OH) are shown below.

- $4 \text{ CO} + 2 \text{ H}_2\text{O} \rightarrow \text{CH}_3\text{COOH} + 2 \text{ CO}_2$
- $4 \text{ H}_2 + 2 \text{ CO}_2 \rightarrow \text{CH}_3\text{COOH} + 2 \text{ H}_2\text{O}$
- $12 \text{ CO} + 5 \text{ H}_2\text{O} \rightarrow \text{C}_4\text{H}_9\text{OH} + 8 \text{ CO}_2$
- $12 \text{ H}_2 + 4 \text{ CO}_2 \rightarrow \text{C}_4\text{H}_9\text{OH} + 7 \text{ H}_2\text{O}$

### 1.8 Objectives of this study

The ultimate goal of the holistic research is to develop a process for conversion of lignocellulosic feedstocks into fuel ethanol, at a price competitive to that of gasoline. The production of ethanol by gasification-fermentation is a new technology and there is very limited knowledge about such integrated gasification-fermentation systems. Because of the wide scope of this research, a multi-disciplinary, multi-task team consisting of agricultural engineers, biochemists, economists, microbiologists, agronomists and chemical engineers are studying the individual aspects of this process.

A four-liter bubble column bioreactor has been designed and set-up for conversion of producer gas to ethanol. Bubble columns are preferred because of their simple and inexpensive construction and operational characteristics (Bailey and Ollis, 1986). A

fritted disc has been used for dispersion of gases into tiny bubbles to enhance and eliminate mass transfer limitations during producer gas fermentation, although such a design may be unsuitable for larger reactors due to a high pressure drop across the disc. Experiments using clean bottled gas (containing only CO, H<sub>2</sub>, CO<sub>2</sub>, and N<sub>2</sub> from compressed gas sources) have previously been conducted, addressing critical engineering issues like cell concentration and stability, pH and temperature effects on cells and specific production rates of products (Rajagopalan, 2001).

The objectives of this work, which continue to address several critical issues, include:

1. Integration of the gasifier-bioreactor system with assessment of the effect of biomass-generated producer gas on cell density and growth, pH, product profiles and substrate utilization.
2. Assessment of the effects of individual gaseous impurities present in the biomass-generated producer gas on the above-mentioned parameters.
3. Optimization of minerals, vitamins and metals to maximize cell concentration while minimizing the liquid media cost.
4. Development of a stable and efficient microbubble generation system for potential scale-up delivery of the producer gas.

## **CHAPTER 2**

### **GASIFICATION AND PRODUCER GAS FERMENTATION: LITERATURE**

#### **REVIEW**

##### **2.1 Introduction**

Conversion of biomass and biologically renewable resources to fuel ethanol and other products has tremendous potential and could contribute significantly to our energy needs. The United States consumes about 94.2 quads of energy, of which about 3.5 quads is from biomass. (Chum and Overend, 2001). The major sources of biomass feedstock are low-cost residues, wastes and by-products such as corn stover, wheat and rice straw, municipal solid waste, sawdust (Kadam and McMillan, 2003) and dedicated energy crops like switchgrass, hybrid poplars, hybrid willows (Ugarte and Walsh, 2002), and agricultural crops like corn and sugarcane (Krishnan et al., 2000, Wheals and Basso, 1999). The total estimated availability of usable biomass feedstocks in the United States is about 360 million dry tons/year (Table 2.1). It is estimated that there will be a 58-188% increase in energy produced from biomass by the year 2010 in the United States (Hohenstein and Wright, 1994). Thus a considerable effort has been devoted towards developing energy crops to meet the estimated increase in energy requirement (Tolbert and Wright, 1998, Wright, 1994). An estimated 549 million acres of land would be available to grow such crops based on estimates by Oak Ridge National

Feedstock type	Estimated availability (million dry tons/yr)
Corn stover	153
Other agricultural residues	58
Corn fiber	4
Energy crops	70
Wood coproducts	72

Table 2.1. Estimated biomass feedstock availability in the United States  
(Kadam and McMillan, 2003)

Laboratory- Biofuels Feedstock Development Program. The use of herbaceous energy crops, like switchgrass, for the production of ethanol also offers a significant energy gain as compared to corn. The ratio of total available energy to the total energy input for harvesting and handling is 4.43 and 1.21 for switchgrass and corn, respectively, translating to energy gains of 343% and 21% respectively (McLaughlin and Walsh, 1998). In addition to its energy gain, switchgrass has been chosen as the model crop for biomass utilization because of its higher productivity over a wide geographic range, ability to grow on marginal lands, low water and nutrient requirements and environmental benefits like improved soil conservation (Sanderson et al., 1996).

Extensive research is being conducted at Oklahoma State University for characterization of an optimal system for growth, harvest, transportation, storage and processing of switchgrass to ethanol. An estimated 27 million acres of native rangeland and 8.5 million acres of cropland exists in Oklahoma for cultivation of energy crops like switchgrass and bermudagrass with dry biomass yields of about 3-6 tons/acre (Taliaferro, 1975).

## **2.2 Gasification of biomass**

Gasification is a heterogeneous thermochemical process in which a carbon based feedstock is converted to a gaseous product by means of a gasification agent. The gaseous product is usually a mixture of carbon monoxide, carbon dioxide, hydrogen, methane, water (steam), some higher hydrocarbons, inert gases like nitrogen, and various contaminants like char particles, ash and tar (Bridgewater, 1994). Gasification can be classified into indirect and direct gasification. Direct gasification involves the use of an



oxidizing agent, either air or oxygen, to partially oxidize the feedstock, while indirect gasification occurs in the absence of oxygen. Steam is a common gasifying agent for indirect gasification (Belgiorno et al., 2003, Gil et al., 1997). The type of gasifier depends on many factors such as the type and size of biomass, the desired composition of product gas, and the scale of operation. Some common gasifier configurations include fixed bed gasifiers, moving bed gasifiers and fluidized bed gasifiers. Though simple and inexpensive to operate, fixed bed gasifiers have disadvantages like channeling and limited scale-up capacity (Bridgewater, 2003, McKendry, 2002b). Fluidized bed gasifiers offer excellent heat and mass transfer rates between biomass and the gas stream and have been used for a variety of feedstocks like sawdust, sugarcane bagasse, rice husk, woodchips and solid waste (Narvaez et al., 1996, Natarajan, et al., 1998). Since switchgrass is a small particle feedstock with a tendency to agglomerate in other types of gasifiers, fluidized bed gasifiers offer a reliable alternative. Fluidized bed gasifiers can also be scaled-up easily for industrial operations (Bridgewater, 2003). Typically, the producer gas obtained via biomass gasification consists primarily of CO, CO<sub>2</sub>, N<sub>2</sub>, CH<sub>4</sub>, H<sub>2</sub>, water and trace amounts of higher hydrocarbons (Belgiorno et al., 2003), ammonia, oxides of nitrogen, cyanide (Furman et al., 1993) and various contaminants like ash and tars.

## 2.3 Producer gas fermentation

### 2.3.1 Biological catalysts

A large number of bacterial strains have been isolated which have the ability to convert producer gas (or syngas) to ethanol, acetic acid and other useful liquid products. (Madhukar et al., 1996). Some of the acetogens capable of producer gas fermentation to acids and alcohols are *Clostridium thermoaceticum*, *Clostridium ljungdahlii*, *Peptostreptococcus productus*, *Eubacterium limosum*, *Clostridium autoethanogenum*, *Acetobacterium woodii* and *Butyribacterium methylotrophicum*.

*Clostridium ljungdahlii* was the first recognized organism to form ethanol autotrophically from components of bottled synthesis gas (Klasson et al., 1992, Gaddy, 1997). The organism favors the production of acetate at a higher pH (5-7), but ethanol is the dominant product at pH between 4 and 4.5 (Klasson et al., 1992 and 1993). The ethanol to acetate ratio was also altered by use of different nutrient sources and reducing agents (Klasson et al., 1992). Ethanol and acetate concentrations of 48 g/L and 3 g/L respectively were reported after 560 hours of operation in a continuous stirred tank reactor (CSTR) with cell recycle. The maximum cell concentration observed during this period with a cell recycle system was about 4 g/L as compared to a maximum of 1.5 g/L without the use of cell recycle. The CO and H<sub>2</sub> conversions were about 90% and 70% respectively (Klasson et al., 1993, Vega et al., 1989). In addition to producer gas components, *Clostridium ljungdahlii* can also utilize sugars like arabinose, xylose and fructose for growth (Klasson et al., 1992).

*Butyribacterium methylotrophicum* has been used to produce acetate, butyrate and butanol, but is capable of producing ethanol in very low concentrations from components of producer gas. Acetate was the major product when the bacteria were grown on H<sub>2</sub>/CO<sub>2</sub> or CO alone with doubling times of nine and twelve hours respectively. Typically, with 100% CO as the substrate, steady state acetate, butyrate and cell concentrations in a continuous mode were about 0.86, 0.086 and 0.248 g/L respectively. The molar yield coefficients (mol of product / mol CO consumed) reported for CO<sub>2</sub>, acetate, butanol and ethanol were 0.522, 0.158, 0.011 and 0.007 respectively, while the cell yield was about 0.108 g/mol CO (Grethlein et al., 1990, Worden et al., 1989). This organism is capable of growing on multicarbon compounds like glucose, lactate and pyruvate as well as C-1 compounds like H<sub>2</sub>/CO<sub>2</sub>, CO, formate or methanol (Worden et al., 1991).

*Eubacterium limosum* utilizes CO to predominantly produce acetate with ethanol and butyrate as the minor products (Genthner and Bryant, 1982). Under batch conditions, 5.4 g/L of acetate was produced in 65 hours with negligible ethanol and butyrate. During continuous fermentation, the acetate concentration varied from 16.5 mM (1 g/L) to 35 mM (2.1 g/L), depending upon the dilution rates in the chemostat mode. The cell concentration observed in the continuous mode with cell recycle was about 3.5-4 g/L (Chang et al., 2001).

*Peptostreptococcus productus* has been isolated and utilized to produce ethanol, acetate and methane from components of producer gas (Lorowitz and Bryant, 1984). The organism utilized CO for growth, while CO and CO<sub>2</sub>/H<sub>2</sub> was used in acetate production. Also, the bacteria did not utilize any CO<sub>2</sub>/H<sub>2</sub> in the absence of CO, while H<sub>2</sub> utilization was observed only under batch conditions and not in the continuous mode. The molar

yield of acetate under batch conditions was 0.25 mol / mol CO utilized, while the cell yield was about 0.952 g/mol CO (Vega et al., 1989a).

*Clostridium autoethanogenum*, a strict anaerobe, can metabolize producer gas and other carbon sources like pyruvate, L-glutamate, xylose, arabinose, rhamnose, fructose to produce ethanol and acetate. With at 60% CO substrate, the maximum ethanol and acetate concentrations observed under batch conditions were 0.35 and 0.47 g/L respectively (Abrini et al., 1994).

A novel clostridial acetogen, P7 (*Clostridium carboxidovorans*), capable of converting producer gas to ethanol, butanol, acetate and butyrate using the acetyl-coA pathway was used in this research (Rajagopalan et al., 2002, Tanner, 2003). Initial studies have shown product yields (mol C consumed/mol CO utilized) for ethanol, butanol and acetic acid as 0.15, 0.075 and 0.025 respectively (Rajagopalan et al., 2002). The typical cell yields were in the range of 0.45-0.59 g/mol CO. Although P7 is a net CO<sub>2</sub> producer, external CO<sub>2</sub> is required for initiating and sustaining cell growth. In addition to CO<sub>2</sub>, P7 also requires 0.1-1 ppm of sulfide for growth and stability. Preliminary studies conducted in a 1-liter reactor indicate that P7 can grow on H<sub>2</sub>/CO<sub>2</sub>, but no significant H<sub>2</sub> utilization was observed in a 5-liter reactor (Rajagopalan, 2001).

### **2.3.2 Principles of producer gas metabolism**

Several anaerobic bacteria are capable of autotrophic growth for efficient conversion of components of producer gas to ethanol and other products (Phillips et al., 1994). Autotrophic organisms are those which use CO (or CO<sub>2</sub>) as the sole source of carbon for growth. An autotrophic pathway is characterized by the distinct mechanism by

which CO<sub>2</sub> is utilized for the synthesis of an organic compound from which succeeding anabolic reactions proceed (Wood et al., 1986). The metabolic pathway by which CO or CO<sub>2</sub> are utilized for acetate production has been elucidated by Wood and Ljungdahl and is called the Wood-Ljungdahl pathway or the acetyl-CoA pathway (Drake, 1994).

The acetyl-CoA pathway was first studied and demonstrated in *Clostridium thermoaceticum*. The distinctive features of formation of ethanol and other products from components of producer gas via the acetyl-CoA pathway are as follows (Phillips et al., 1994, Shanmugasundaram et al., 1993).

- Formation of a methyl moiety of acetate on tetrahydrofolate from either CO or CO<sub>2</sub>.
- Transfer of the methyl group to carbon monoxide dehydrogenase (CODH) via a corrinoid protein.
- CODH catalyzed condensation of the methyl group with a CO- derived carbonyl group in presence of coenzyme A to form acetyl-CoA.
- Formation of ethanol and acetate from acetyl-CoA.

A simplified scheme for the production of ethanol from producer gas using the acetyl-CoA pathway is illustrated in Figure 2.1. The most important enzymes involved in the acetyl-CoA pathway for the formation of ethanol from components of producer gas are CODH, hydrogenase, formate dehydrogenase and ethanol dehydrogenase. Other key enzymes for butanol and butyrate production are butyrate kinase, crotonase, butanol dehydrogenase and butyryl-CoA dehydrogenase (Grethlein and Jain, 1992).

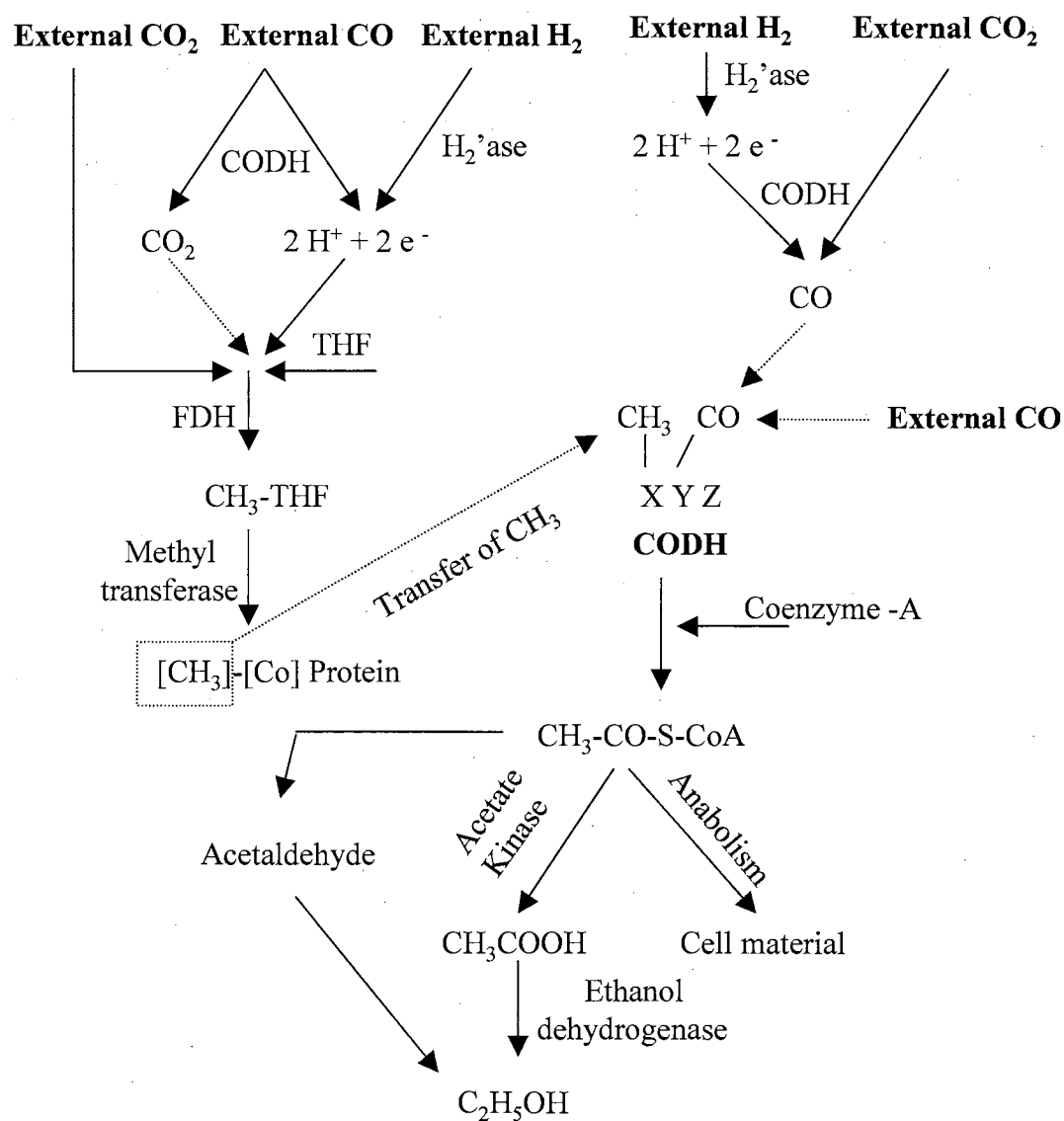


Figure 2.1. Acetyl-CoA pathway for production of ethanol from producer gas (Drake, 1994, Vijjeswarapu et al., 1985)

CODH is a highly multifunctional enzyme. CODH can catalyze the reversible oxidation of CO to CO<sub>2</sub> to generate electrons according to the equation illustrated below (Pezacka and Wood, 1984).



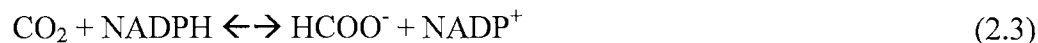
The electrons can be used for generating the acetyl-CoA at the expense of generating unusable carbon in the form of CO<sub>2</sub>. CODH is also responsible for the synthesis of acetyl-CoA from CO (in the form of a CO- derived carbonyl group), coenzyme A and the CO- or CO<sub>2</sub>-derived methyl group originating from methyltetrahydrofolate (Xia et al., 1996, Hu et al., 1982). Clostridial CODH contains three active sites containing iron, sulfur, cobalt and nickel (Lynd et al, 1982, Russell and Lindahl, 1998).

Hydrogenase is responsible for hydrogen uptake and electron formation (Menon and Ragsdale, 1996) via catalyzing the following reversible reaction



The electrons generated by oxidation of external hydrogen by hydrogenase are utilized to produce acetate and ethanol (Ljungdahl, 1986). This is why H<sub>2</sub>, which can generate electrons via hydrogenase, is desired for ethanol production since carbon would not be lost at the expense of generating electrons (shown in Equation 2.1).

Formate dehydrogenase is a metalloenzyme containing both selenium and tungsten or molybdenum. The enzyme catalyzes the reversible reaction of CO<sub>2</sub> and formate as follows (Ljungdahl and Andersen, 1975).



CO<sub>2</sub> is reduced by formate dehydrogenase and enzymes of the tetrahydrofolate pathway to form methyl tetrahydrofolate. CODH, hydrogenase and formate dehydrogenase are all very sensitive to oxygen (Laurinavichene et al., 2001, Prince et al., 1985).

The transfer of the methyl group to corrinoid iron-sulfur protein and then to CODH is catalyzed by methyltransferase (Doukov et al., 2000, Menon and Ragsdale, 1997). The formation of the carbonyl group from CO/CO<sub>2</sub> is not well understood. If CO<sub>2</sub> is the feed source, it is proposed that CO<sub>2</sub> is reduced to CO within CODH and the CO is then channeled within the enzyme to another active site (Seravalli and Ragsdale, 2000). Condensation of the methyl and carbonyl groups takes place on CODH in the presence of coenzyme A to form acetyl-CoA, an intermediate used for building cell materials and production of ethanol, acetate, butanol and butyrate. A simplified scheme for the production of ethanol from producer gas using the acetyl-CoA pathway is illustrated in Figure 2.1.

### **2.3.3 Reactor configurations**

The transport of gases to the bulk liquid through the liquid film around the gas bubble is the rate-limiting step in most fermentation processes that involve sparingly



soluble gaseous substrates. Producer gas fermentations are primary examples of such mass transfer limited fermentations. At mild temperatures, CO and H<sub>2</sub> have aqueous solubilities of 60% and 4% respectively as compared to oxygen on a mass basis (Bredwell et al., 1999). These low solubilities result in low concentration gradients, and hence low volumetric mass transfer rates. The choice of a suitable reactor for producer gas fermentations depends on matching the operational capabilities of different reactors to the reaction kinetics of the system (Cowger et al., 1992). A good reactor design is that which can achieve high mass transfer rates and high cell density under mild temperature and pressure conditions in a small reactor volume with minimum operational difficulties and costs.

Continuous stirred tank reactors (CSTR) have been routinely employed for producer gas fermentations. High mass transfer rates have been achieved by the use of an agitator system (Klasson et al., 1992). Increasing the operating pressure also significantly increases the CO uptake in producer gas fermentations, leading to a reduced reactor volume (Vega et al., 1990). The reactor may also be fitted with an array of impellers. Such a multiple impeller design offers superior gas hold-up, mass transfer, and power consumption numbers compared to a single impeller design (Gogate et al., 2000), although contamination possibilities are potentially higher at numerous entry points of the impellers (Shuler and Kargi, 1992). A two-stage reactor system has also been used to maximize ethanol production and minimize the formation of by-products. CO and H<sub>2</sub> conversions of 90% and 70%, respectively, were observed in the first reactor, while they were about 70% and 10% in the second reactor. High ethanol to acetate ratios were achieved by the use of such a dual reactor system (DOE, 1994). The use of stirred tanks

with agitators would not be economically viable for industrial fermentations because the power consumption increases with impeller diameter to the fifth power and the impeller rate to the third power (McCabe and Smith, 1956, Worden et al., 1997).

A comparative study was performed between a CSTR and a bubble column reactor for CO fermentation using *Peptostreptococcus productus*. Higher conversion rates of CO were observed with the bubble column without the use of any additional agitation (Vega et al., 1990). Producer gas fermentation with packed bubble columns and trickle bed reactors has also been studied. The packed bubble columns offer large liquid retention times, high interfacial area, high mass transfer coefficients, and minimum costs without the need for mechanical agitation, the disadvantage being a large amount of back mixing, foaming, and coalescence. The trickle bed reactor has a low pressure drop and liquid hold-up and the conversion rates were the highest compared to CSTR and bubble columns (Klasson et al., 1992).

Bubble columns are also commonly used for industrial fermentations. The gas is dispersed either by spargers or porous discs in bubble column bioreactors. Sparging rings provide a smaller bubble size initially with better gas dispersion, but single orifice spargers are preferred because they are less resistant to plugging. Bubble columns are used for low viscosity Newtonian fluids and provide higher gas efficiency than stirred tanks, since the energy requirement to overcome the pressure drop across the sparger (or porous disc) and hydrostatic fluid head is not very high (Shuler and Kargi, 1992). Bubble columns also offer low shear environments as compared to agitated reactors and hence are a preferred option for bacteria that are shear sensitive. However, bubble columns cannot be scaled-up easily to industrial-sized reactors because of high-pressure drops

across the spargers, but this drawback can be overcome by the use of several small bubble columns for industrial operations.

Immobilized cell reactors have also been studied for producer gas fermentation (Chatterjee et al., 1996). Immobilization of the microbial catalysts offers advantages of high cell density as compared to batch or continuous stirred tank reactors and ease of cell separation from fermentation broth (Gaddy and Sitton, 1982). These reactors can also be operated at dilution rates that exceed the maximum cell growth rate, without resulting in cell washout, but mass transfer of gaseous reactants is a disadvantage in such reactors.

#### **2.3.4 Engineering aspects and media optimization**

Commercialization of producer gas fermentations is currently hindered by low productivity in the bioreactor. Several factors like low cell density, lack of regulation of metabolic pathways to yield only the desired product, inhibition of the biological catalysts by products and substrates and low gas-liquid mass transfer need to be addressed to establish the economic feasibility of producer gas fermentations (Worden et al., 1997).

High cell densities can be achieved in bioreactors using a cell recycle system (Riesenberg and Guthke, 1999, Parekh and Cheryan, 1994). It was reported that there was a 5-20 fold increase in cell density and product concentration with cell recycle relative to a continuous system without cell recycle for CO fermentation with *Butyrubacterium methylophilicum*. Acetate, butyrate and butanol concentrations increased from 0.86, 0.086 and 0 to 8, 4 and 1.4 g/L respectively (Grethlein et al., 1990, Worden et al., 1991). Similarly, increased gas conversion rates have been observed with the use of centrifuges,

hollow fiber membranes, and other ultrafiltration techniques for cell recycle (Gaddy, 1997). Increased ethanol concentrations were reported with enhanced cell concentrations (3 to 5 times) with a tangential flow filter for producer gas fermentations using *C. ljungdahlii* (Klasson et al., 1993).

Alteration of fermentation conditions, like the pH, has also drastically affected the product concentrations (Grupe and Gottschalk, 1992). Research with *C. ljungdahlii* has shown that at high pH values (5.5–6), acetate was the dominant product while at a lower pH (4–4.5), there was a drastic shift in the production of ethanol (Klasson et al., 1993). This concept has been used for maximizing the ethanol production in a two-stage reactor. The first reactor is operated at a higher pH, favoring the production of acetate and cells. The effluent from the first reactor is fed to the second reactor, which operates at a lower pH, thus converting all the acetate to ethanol (DOE Report, 1994). Thus, higher productivity and selectivity can be achieved by the use of such dual reactor systems (Nishiwaki, 1997, DOE Report, 1994) and by regulation of the fermentation broth pH (Grethlein et al., 1990, Klasson et al., 1993).

Inhibition by end products or intermediates is a principal factor that limits metabolic rates and final product concentrations in many fermentation processes (Yang and Tsao, 1994), thus making it uneconomical for commercialization (Marlatt and Datta, 1986). It was observed that growth of *Butyribacterium methylotrophicum* was inhibited at alcohol concentrations of 5g/L (Worden et al., 1997), while the clostridial strain P7 initially tolerated 0.5 M (2.3 g/L) ethanol (Liou et al., 2002). These concentrations are very low as compared to concentrations needed for establishing an economically viable process. Efforts have been made to eliminate drawbacks of inhibition by improvement of

bacterial strains to tolerate higher product concentrations or/and by use of novel separation coupled fermentation processes like pervaporation, extraction, perstraction, (Qureshi et al., 1999) and membrane separation (Schroen and Woodley, 1997). Recent studies performed at University of Oklahoma, indicate that P7 was adapted to grow in ethanol concentrations of about 78 g/L (Liou et al., 2002), which is well above the concentration for an economically feasible process.

Optimization of nutrient media is also critical to achieve high cell growth and maximize product concentrations. It has been reported that the addition of reducing agents resulted in enhanced cell growth and product distribution (Rao and Mutharasan, 1988). Specifically to clostridial fermentations, the presence of reducing agents increases the solvent formation (Rao and Mutharasan, 1987). Selectivity of ethanol was doubled by addition of various reducing agents like methyl viologen, benzyl viologen, sodium thioglycolate and ascorbic acid. Other nutrient sources like cellobiose and galactose also increased cell concentrations (Klasson et al., 1992). Enhancement of ethanol production with significant suppression of acetic acid was observed in the presence of sodium azide and polyethylene glycol in *C. thermocellum* (Rani et al., 1994 and 1997) and with 30mM flouroacetate for P7 (Liou et al, 2002). Thus optimal nutrient levels must be investigated because attempts to double cell concentration by simply doubling the nutrients have failed, suggesting inhibition of cell growth at excessively high nutrient concentrations (Phillips et al., 1993).

Research on producer gas fermentations using P7 with a bubble column bioreactor has been ongoing at Oklahoma State University. Past studies (Rajagopalan, 2001) have indicated that the bioreactor is limited by the intrinsic kinetics of P7 (nutrient limitations)

and not by the mass transfer rate of CO from the bulk gas phase to the cells. No increase in the cell concentration was observed by incorporating a hollow tangential flow membrane filter for cell recycle. Sodium sulfide (0.1-1 ppm) and CO<sub>2</sub> were necessary to sustain cell growth, although CO<sub>2</sub> was produced during the fermentation process.

### **2.3.5 Microbubble generation system**

Mass transfer can potentially be a severe problem for producer gas fermentations in large-scale bioreactors. Microbubble dispersions offer an excellent alternative, providing high interfacial area at a low power input. It is estimated that the power requirement for producer gas fermentations using microbubbles is 0.01 kW/m<sup>3</sup> as compared to 1 kW/m<sup>3</sup> for commercial stirred tank fermenters and 2 kW/m<sup>3</sup> for producer gas fermentations using conventional sparging in stirred tanks (Bredwell and Worden, 1998). Microbubbles or colloidal gas aphrons are surfactant-stabilized bubbles with diameters of about 50-100 µm (Sebba, 1987). The word “aphron” is derived from the greek word for foams and can be defined as a phase bounded by an encapsulating soapy film. The surfactant layer surrounding the bubble imparts an electric double layer that prevents them from coalescing and hence the microbubbles are stable enough to be pumped like liquids (Bredwell et al., 1995). Microbubbles can be produced in a separate small vessel and then pumped to the bioreactor. Colloidal gas aphrons have been used in a large variety of applications, such as removal of metals (Ciriello, 1982) and dyes (Roy et al., 1992), flotation of cells (Hashim and Gupta, 1998, Hashim et al., 1998), protein recovery (Jauregi and Varley, 1998 and 1999, Jauregi et al., 1997), biodegradation (Jenkins et al.,

1993) and enhancement of mass transfer in aerobic (Kaster et al., 1990) and anaerobic fermentations (Bredwell and Worden, 1998).

Microbubbles were first produced using a modified glass aspirator (Sebba, 1971). Microbubbles were formed upon the rapid flow of a dilute surfactant solution through the venturi throat at which a gas is admitted. But this method was unsatisfactory for production of microbubbles on a large scale and hence an improved design consisting of a spinning disc was used (Sebba, 1985). The generator consists of a high speed spinning disc with baffles at close proximity creating a high shear zone. Other methods for the production of microbubbles involve the use of ultrasound (Bjerknes et al., 1997) and electric current (Burns et al., 1997). It has been reported in previous studies that the microbubbles typically consisted of 50-65% gas by volume with the remaining fraction as liquid (Sebba, 1985, Bredwell and Worden, 1998).

The research efforts to date have been focused towards production of ethanol and other useful liquid products via fermentation of clean bottled producer gas. Clearly, there is a need to demonstrate the integration of a gasifier-bioreactor system and assess the effects of biomass-derived producer gas with regards to cell growth and viability and product formation for future commercialization.

For establishing the economic feasibility of producer gas fermentations, there is also a need to maximize product yields at the lowest nutrient cost. Hence, it is essential to optimize and identify the concentration of each nutrient to maximize the cell concentration (assuming each cell produces the same amount of product) and thereby the product yields.

Although mass transfer has been enhanced previously using a microbubble generator (Kaster et al., 1990, Bredwell and Worden, 1998), it is necessary to identify the total gas incorporation into microbubbles and increase the microbubble quality to justify the economics of using such a system.

## **2.4 Objectives of the study**

Considering the holistic approach of conversion of low cost biomass to ethanol and other products, the undertaken research is a critical part to establish the viability of the process. As explained in Chapter 1, the specific objectives of this research work, which continue to address several important issues are:

1. Integration of the gasifier-bioreactor system with assessment of the effect of biomass-generated producer gas on cell density and growth, pH, product profiles and substrate utilization.
2. Assessment of the effects of individual gaseous impurities present in the biomass-generated producer gas on the above-mentioned parameters.
3. Optimization of minerals, vitamins and metals to maximize cell concentration while minimizing the liquid media cost and.
4. Development of a stable and efficient microbubble generation system for potential scale-up delivery of the producer gas.



## **CHAPTER 3**

### **INTEGRATION OF GASIFIER AND BIOREACTOR**

#### **3.1 Introduction**

The ultimate aim of the study is to produce ethanol and other useful liquid products by fermentation of producer gas generated by gasification of low cost biomass. The conversion of producer gas to ethanol using microbial catalysts is a very complex heterogeneous process. In this chapter, the effects of biomass-generated producer gas on cell concentration, hydrogen uptake, and acid/alcohol production in a continuous bubble column bioreactor are shown. Previous work has assessed the same parameters using “clean” bottled gases rather than biomass-generated producer gas (Phillips et al., 1994, (Rajagopalan et al., 2002).

It is essential to investigate and establish continuous operations at stable conditions with biomass-derived producer gas before scale-up and commercialization. Switchgrass was chosen as the model crop for gasification to producer gas, and a recently discovered clostridial bacteria, P7, was used as the biocatalyst. Initial studies have shown that P7 is a stable ethanol producer. The operating conditions for P7, like pH and temperature, have also been identified in previous studies.

### **3.2 Objective of the study**

The specific objective of the study is as follows:

- Integration of the gasifier-bioreactor system with assessment of the effect of biomass-generated producer gas on cell density and growth, pH, product profiles and substrate utilization. The parameters are compared with experiments using clean bottled gas.

### **3.3 Materials and Methods**

#### **3.3.1 Biomass preparation and properties**

(The work described in this section and in section 3.3.2 was not a part of my dissertation research, but has been included in this chapter because it offers more insight into the overall integration of the gasifier and bioreactor).

Producer gas was generated from switchgrass, a native Oklahoma tall grass. The switchgrass was harvested, baled, and stored until the moisture content was below 15%. The bale was chopped in a tub grinder with a ½ inch screen for size reduction. The resulting material had a density of around 130 kg/m<sup>3</sup> and most particulates had a length between ½ and 1 inch. The material was dusty and tended to agglomerate very easily, creating feeding problems which were eventually overcome. The elemental analysis of switchgrass (moisture and ash free) was 44.9% C, 5.7% H, 0.9% N, and 48.5% O. The moisture content was 13%.

### **3.3.2 Gasifier operation and producer gas production**

The pilot-scale fluidized bed gasifier at Oklahoma State University was constructed utilizing an initial design developed by Carbon Energy Technology, Inc., and the Center for Coal and the Environment at Iowa State University (Ames, IA). The design had been modified for the gasification of switchgrass. The gasifier consists of a fuel hopper, feed auger, injection auger, reactor, ignition system and a gas clean up system.

The fluidized-bed gasifier is 10 inches in diameter and is constructed of mild steel with a two-inch refractory lining (Cateni et al., 2003). The fluidized reactor bed is one foot high and contains sand particles to aid in the biomass conversion process. The air for fluidization is fed through a distribution plate at the bottom of the bed via uniformly spaced holes. The air, supplied by piston compressors, was injected through an electric air heater maintained at 25 °C into the plenum underneath the distribution plate. The biomass was pushed into the gasifier with an injection auger, rotating at a constant speed. The plate is covered with a 40 by 40 mesh metallic wire cloth to prevent entrainment of the sand particles below the plate when the bed is not fluidized. The maximum feed rate capacity of the gasifier is 34 kg/h (75 lb/h).

During startup, propane gas was combusted to heat the reactor to about 800 °C. The optimum operating temperature is between 650 and 700 °C (Cateni et al., 2000). The gasification process was monitored via numerous sensors, all of which were connected to a computer for process supervision and data acquisition. A load cell was used to monitor fuel hopper weight, which served as an indicator of switchgrass mass flow rate into the gasifier. To measure airflow, an electronic mass flow meter was used. A differential pressure gauge indicated the pressure drop through the bed. Several thermocouples were

added to the gasifier: one in the plenum, ten in and above the fluidized zone, three at the top of the gasifier and one before the venturi meter. A differential pressure gauge was placed across a venturi meter in the outlet gas stream to indicate the temperature-compensated gas flow rate. The gas was then directed either to a flare or a clean up system.

The producer gas exited at the top of the gasifier and was passed through two cyclones to separate particulates from the gas stream. Ash was collected at the bottom of the cyclones. The cyclones were fitted with 2-inch diameter airlocks to prevent gas from exiting through the bottom of the cyclones. After the cyclones, the producer gas passed through condensation towers to remove a large portion of the tars. The towers are closed cylinders divided longitudinally by a vertical fin water-cooled heat exchanger with a heat transfer area of 1320 in<sup>2</sup>. The gas was then passed through a series of vertical water scrubbers to condense residual tars.

The “clean” producer gas was then sent to a Quinsy piston compressor to store the gas at a pressure of 120 psi. The two storage tanks have a total capacity of about 650 liters. Gas samples were collected from the exhaust of the gasifier and storage tanks and analyzed using a GC. Typically, the gas was stored for 1-3 weeks before being utilized. The stored gas provided over 15 days of feed gas to the bioreactor. Compositional changes in the producer gas were not noticeable during the storage period.

### **3.3.3 Biological catalyst**

The biological catalyst used was a recently discovered novel clostridial bacteria, P7. The novel status has been confirmed by DNA-DNA hybridization studies and 16S rRNA

sequence analysis (Tanner et al., 1998). P7 is a gram-positive, motile rod shaped anaerobic acetogen that sporulates occasionally (Figure 3.1). The bacterium was first isolated from an agricultural lagoon by Ralph Tanner, University of Oklahoma. The organism was cultured and grown using strict anoxic techniques (Bryant, 1972, Dowel, 1981) in a nutrient media described below. The growth media contained (per liter) 1.0 g ammonium chloride, 0.8 g sodium chloride, 0.1 g potassium chloride, 0.1 g potassium monophosphate, 0.2 g magnesium sulfate, 20 mg calcium chloride, 1.0 g sodium bicarbonate, 1.0 g yeast extract, 0.2 g cysteine hydrochloride and 0.2 g sodium sulfide. Vitamins and trace metals (10 ml each; described in following section) were also added. Enrichments were established in a mineral medium under a 100% CO headspace at 37 °C. Bromoethanesulfonic acid (20 mM) was also added to inhibit the growth of methanogenic bacteria. In addition to components of producer gas like CO/CO<sub>2</sub> and H<sub>2</sub>, P7 can also utilize and grow on sugars (Liou and Tanner, 2002). The optimal pH range for growth is between 5 and 6. P7 has been recently named as *Clostridium carboxidovorans* and preliminary studies indicate that it can also directly ferment switchgrass (Tanner, 2003).

### **3.3.4 Culture medium**

A culture medium containing Pfennig's minerals, trace metals, and vitamins was used as a nutrient source to cultivate and grow cells in the bioreactor. The nutrient media contained (per liter) 30 ml of stock mineral solution (Table 3.1), 10 ml of stock vitamin solution (Table 3.2), 10 ml of stock trace metals solution (Table 3.3), 0.5 g yeast extract, 5 g N-morpholinoethanesulfonic acid (MES), and 5 ml of 4% cysteine-sulfide (reducing

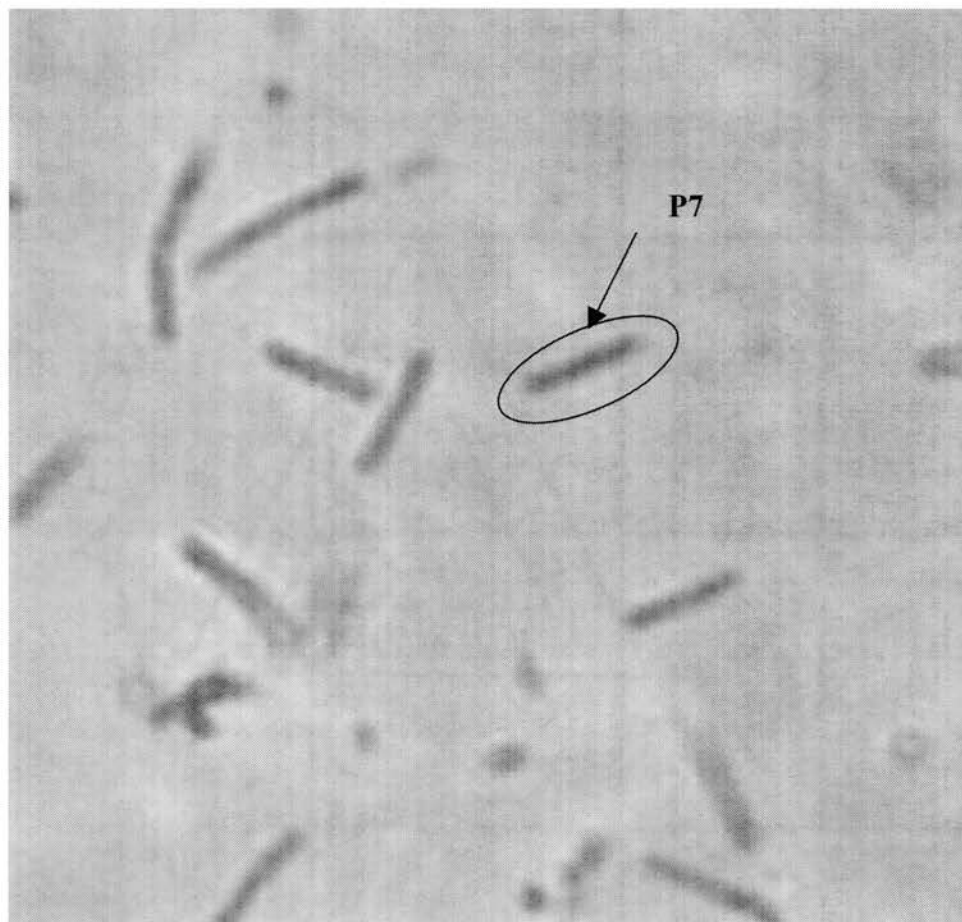


Figure 3.1. Biological catalyst, P7(*Clostridium carboxidovorans*), for producer gas fermentation.

<b>Component</b>	<b>Amount (g/L)</b>
Sodium chloride	80
Ammonium chloride	100
Potassium chloride	10
Potassium phosphate monobasic	10
Magnesium sulfate	20
Calcium chloride	4

Table 3.1. Composition of stock mineral solution

<b>Component</b>	<b>Amount (g/L)</b>
Pyridoxine	0.01
Thiamine	0.005
Riboflavin	0.005
Calcium Pantothenate	0.005
Thioctic acid	0.005
p-Amino benzoic acid	0.005
Nicotinic acid	0.005
Vitamin B <sub>12</sub>	0.005
d-Biotin	0.002
Folic acid	0.002
Mercaptoethanesulphonic acid (MESNA)	0.01

Table 3.2. Composition of stock vitamin solution



<b>Component</b>	<b>Amount (g/L)</b>
Nitrilotriacetic acid	2
Manganese sulfate	1
Ferrous ammonium sulfate	0.8
Cobalt chloride	0.2
Zinc sulfate	0.2
Cupric chloride	0.02
Nickel chloride	0.02
Sodium molybdate	0.02
Sodium selenate	0.02
Sodium tungstate	0.02

Table 3.3. Composition of stock trace metals solution

agent) solution. MES is a biological buffer (pH range 5-6) and was added to avoid excessive pH fluctuations in the fermentation broth during experimentation although the pH was controlled using a pH controller. Cysteine-sulfide was added to lower the redox potential of the media and maintain anoxic conditions in the bioreactor. Resazurin, a redox potential indicator was also added (0.1 ml of 0.1% solution) to indicate the presence of oxygen. All the chemicals were purchased from Sigma Chemical Company, St. Louis, MO.

### **3.3.5 Bioreactor design and operation**

The bioreactor is a bubble column reactor made of stainless steel and glass with a height of two feet and diameter of 4.5 inches and operating volume of 4 –4.5 liters and was constructed at the Biosystems workshop at Oklahoma State University. The detailed design and specifications are as shown in Figure 3.2 and Table 3.4. A sintered glass fiber porous disc (Ace Glass Inc., Vineland, NJ) with a pore size of 4-8 microns is fitted at the bottom to disperse the inlet feed gas into tiny bubbles. The reactor is fitted with a pressure relief valve (F.C. Kingston Company, LA) to avoid excessive pressure build up due to the potential blockage of the gas outlet (previously observed because of snow and excessive foaming). The fermentation broth is kept well mixed by externally recirculating the liquid at 200-300 ml/min with a ¼-inch plastic tubing attached to a peristaltic pump (Cole Parmer, Vernon Hills, IL). A portion of the recycle stream, containing both media and cells, was withdrawn as product during the continuous phase at 1.5 ml/min, resulting in a dilution rate of  $0.0225\text{ h}^{-1}$  and liquid residence time of 44 hours. Fresh media was added at the same flow rate during continuous operation.

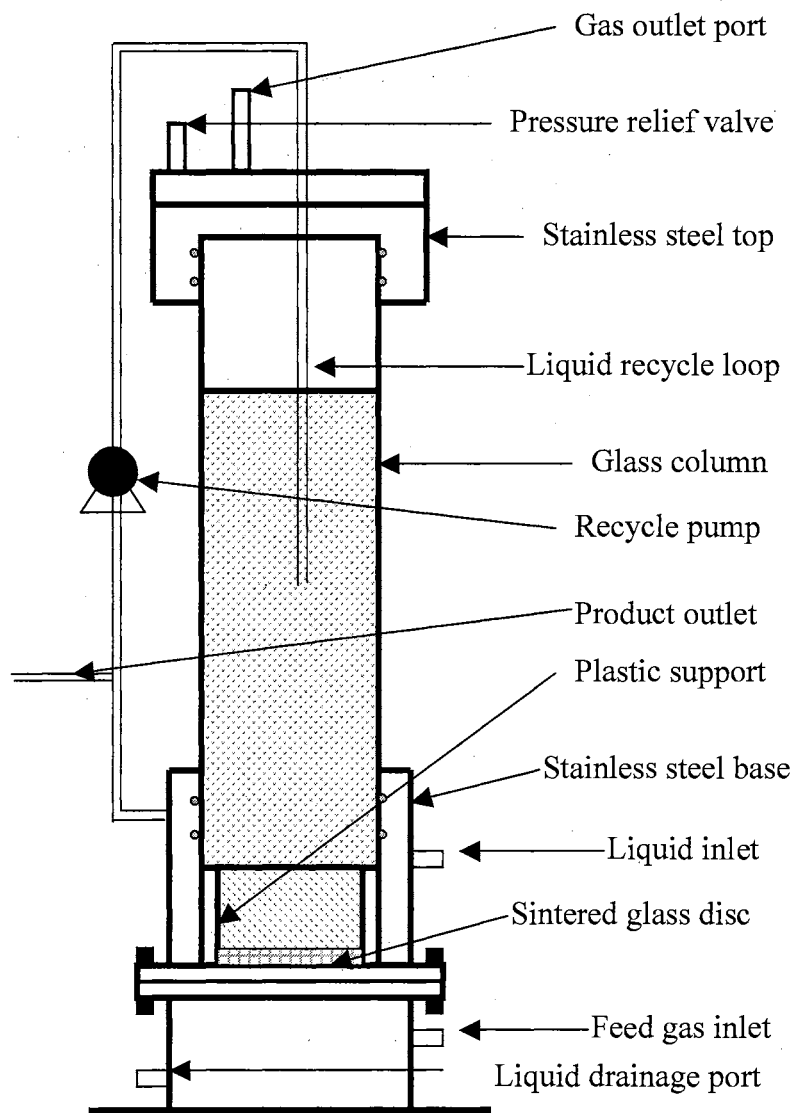


Figure 3.2. Bioreactor design

<b>Bioreactor</b>	<b>Specifications</b>
Maximum liquid volume	4.5 liters
Operational volume	4 liters
Height (Glass column)	14.5 inches
Diameter (Glass column)	4.5 inches
Height (Stainless steel base)	5.5 inches
Diameter (Stainless steel base)	6 inches
Height (Stainless steel top)	2 inches
<b>Sintered glass fiber disc</b>	<b>Specifications</b>
Diameter	150 mm
Thickness	12 mm
Pore size	4-8 microns

Table 3.4. Design specifications for bioreactor

The liquid media was prepared in 5-gallon glass tanks. All the media components described in the previous section were mixed together (except for cysteine-sulfide) and the pH was measured using a portable pH meter with an epoxy electrode (Beckmann Instruments, Fullerton, CA). The starting pH was increased from 4.5 (usually observed value) to 5.9 using a 5 N NaOH solution. The media was boiled, cooled, and pumped into the sterile bioreactor using a sterile 0.5  $\mu\text{m}$  pore size filter and allowed to deoxygenate under continuous nitrogen bubbling. Media required during the continuous operation, was boiled, cooled and deoxygenated in glass feed tanks and kept under a positive nitrogen pressure. Two tanks were alternately used to provide an uninterrupted fresh feed supply to the bioreactor (while one was in use, the other was being deoxygenated). Cysteine-sulfide was added to cooled media using a sterile 0.2  $\mu\text{m}$  filter to prevent stripping during boiling. The bioreactor (with all accessories attached) was sterilized with steam for 30 minutes at 110 °C using a steam generator (Scott Engineering Services, Pompano Beach, FL). The individual bottled gases (Air-Gas Co., Tulsa, OK) were mixed using mass flow controllers (Porter Instruments, PA) and passed into the bioreactor through a 1/4-inch stainless steel tubing (Swagelok, Solon, OH) at a total gas feed rate of 180 ccm at 3.5 psig. The gases were sterilized using a 0.2  $\mu\text{m}$  microporous membrane filter. The temperature of the reactor was measured using a digital thermometer and maintained at 37 °C by wrapping an electric heating tape (Thermolyne, Dubuque, IA) around the glass column. The heating tape was connected to a powerstat (Superior Electric Company, Bristol, CT). The heat load was manually adjusted and controlled using the powerstat to the desired temperature of 37 °C. The reactor was covered with insulation to minimize heat loss and temperature fluctuations.

The mixed gas composition (CO, CO<sub>2</sub>, and H<sub>2</sub>) was similar to that in the producer gas obtained from the gasifier. Before starting the experiment, gas from the storage tanks was analyzed for N<sub>2</sub>, CO, CO<sub>2</sub>, and H<sub>2</sub> and the composition was confirmed with values obtained during the initial storage. Constituents like methane, trace quantities of oxygen, ethane, ethylene, and acetylene (present in the producer gas) were replaced with nitrogen in the bottled gas experiments.

After the media became anoxic (indicated by change of color of the solution from pink to pale yellow), flow of the bottled CO, CO<sub>2</sub> and H<sub>2</sub> was initiated in addition to the N<sub>2</sub>. Inoculum was withdrawn from a 250 ml serum bottle (Wheaton, Millville, NJ) using a sterile 60 ml luer-lok syringe and 20 G, 1.5-inch needle (Becton-Dickinson, Franklin Lakes, NJ) and transferred to the bioreactor under sterile and anoxic conditions. After inoculation, the bioreactor was operated under semi-batch mode with liquid in the batch phase and gas in continuous phase until the cell concentration began to stabilize. Continuous liquid feed and product removal at 1.5 ml/min was then started. Once the cell concentration reached steady state in the continuous mode, the feed gas was switched from the bottled gas mixture to the stored producer gas.

The flow rate of producer gas was controlled using a rotameter (Cole Parmer IL). A 4-way stainless steel valve (Swagelok, Solon, OH) was used to change between bottled and producer gas. The feed gas lines were purged for 10 minutes with producer gas before switching between the two gas sources, to eliminate residual oxygen in the gas lines from entering the bioreactor. The pH of the bioreactor was maintained at the desired value using a computer controlled pH controller (Camile TG) with an anoxic 1 N

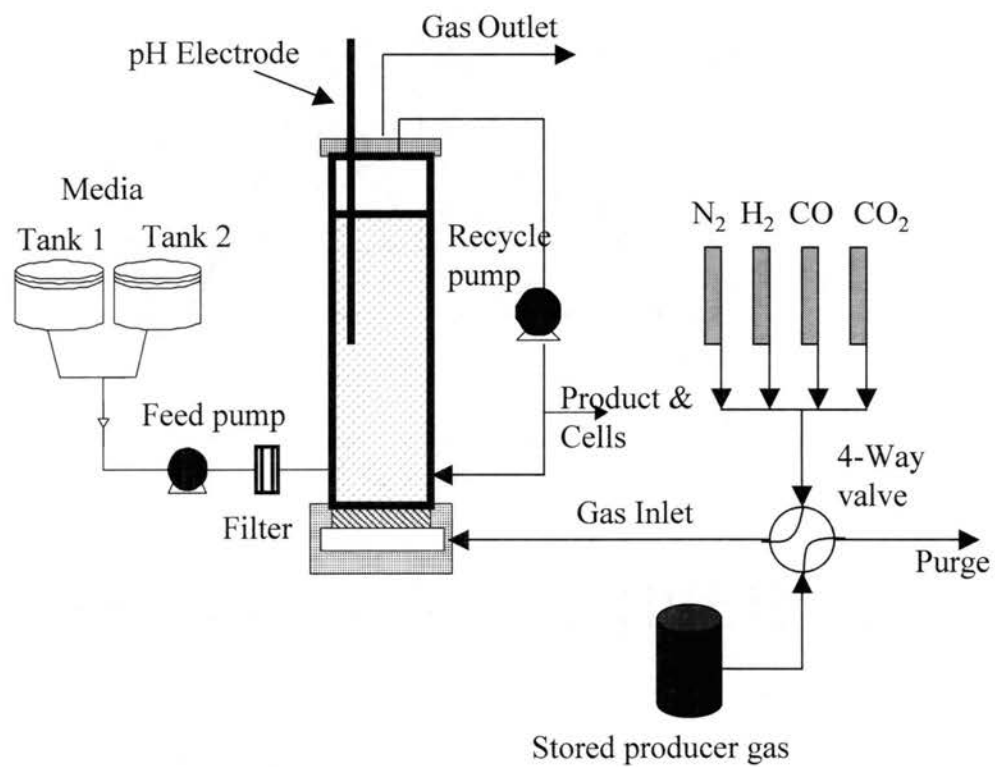


Figure 3.3. Schematic of experimental layout

NaOH/HCl solution. The NaOH/HCl solution was prepared in 500 ml glass cylinders and continuously bubbled with nitrogen gas to maintain anoxic conditions. Carbon monoxide (Nighthawk) and hydrogen monitors (Arrgh Manufacturing Company, Novato, CA) were used to detect possible gas leaks. The experimental layout of the entire system is shown in Figure 3.3. All fittings on the bioreactor exposed to the media are made of stainless steel (to avoid corrosion) and were purchased from Swagelok Company, Solon, OH

### **3.3.6 Analytical procedures**

*Cell concentration:* The optical density (OD), which is proportional to the cell concentration (includes vegetative cells as well as spores), was determined using a Genway 6300 spectrophotometer (Cole Parmer, Vernon Hills, IL). Cell samples were withdrawn from the bioreactor using sterile 10-ml Luer-lok syringes and collected in 4-ml plastic cuvettes. The OD was measured at a wavelength of 660 nm. Samples with an OD greater than 0.4 units were diluted appropriately such that the OD value obtained was within the linear calibration range of 0 to 0.4 OD units. A calibration chart was developed to relate the OD to the dry cell weight (mg/L). All the graphs in this study are reported in OD units.

*Calibration of cell OD versus dry cell weight:* One liter of reactor broth from a terminated experiment was collected in a glass bottle. 1 ml of sample was withdrawn and diluted 4 times by addition of 3 ml distilled water to measure the cell OD of the reactor broth. Serial dilutions were performed with distilled water to obtain solutions of different cell OD. The cell OD of each diluted sample was measured as described earlier. The diluted samples were transferred to 10-ml centrifuge tubes and centrifuged for 30



minutes. The supernatant was withdrawn and an identical amount of distilled water was added and the solution was recentrifuged. This procedure was repeated twice. After the second centrifuge cycle, the solutions were transferred to small aluminum pans. The initial weight of the aluminum pans was determined by heating them in an oven overnight (to dry them completely) and then measuring the pan on a weighing scale (Denver Instruments, Arvada, CO). The aluminum pans, filled with diluted cell solutions were heated overnight in an oven (Model # OV-12A, Blue M, Blue Island, IL) at 110 °C. The aluminum pans were weighed again and the difference in weight was used to estimate the dry cell weight (DCW). The DCW (mg/L) was plotted against the cell OD (shown in Figure 3.4). The relationship between the dry cell weight and cell OD is

$$\text{DCW} = 427.94 * \text{OD} + 1.47$$

*Gas analysis:* Gas samples were withdrawn from the outlet and inlet lines of the bioreactor in 5-ml gas tight syringes (VICI, Valco Instruments Company Inc, Houston, TX). The gas compositions were determined using a gas chromatograph (3800-CP, Varian Co., CA) with a Hayesep-DB column (Hayes Separations Inc, Bandera, TX) connected to a thermal conductivity detector (TCD) with argon as the carrier gas. The TCD oven and filament were maintained at 140 °C and 200 °C respectively. The column oven was operated at 40 °C for 6 minutes, after which the temperature was ramped up to 140 °C at 100 °C/min for 20 minutes. The GC was calibrated using premixed gases (Airgas Co., Tulsa, OK and Matheson Tri-gas, Twinsburg, OH). Calibration charts, thus obtained, were used to calculate the inlet and outlet gas compositions (vol% basis).

*Liquid analysis:* The liquid samples (4 ml) withdrawn from the product line were centrifuged (International Equipment Company, MA) at 4000 rpm for 30 minutes. The

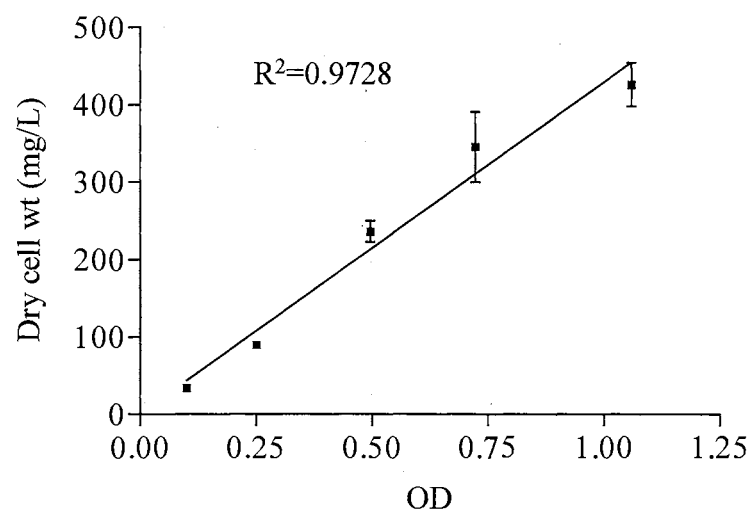


Figure 3.4. Dry cell weight versus cell concentration (OD units)

cell free supernatant was collected in 4-ml glass vials and frozen at  $-20^{\circ}\text{C}$  until further analysis. The liquid products were analyzed for alcohols using an Ion Chromatograph (Dionex, Sunnyvale, CA). The samples were prepared by diluting the samples 10 times using deionized (DI) water. The diluted samples were then passed through a Chelex-100 resin (100-200 mesh, sodium form, Biorad Labs, CA) to remove heavy trace metals that might interfere with the alcohol analysis. A 500-mM NaOH solution was used as an eluant. The samples were analyzed using an autosampler. Samples were interspersed with standards to verify the calibration of the instrument throughout the analysis. An electrochemical detector was used with a Dionex Carbopac, MA1 (4 X 250) column. The analysis time was about 17 minutes for one sample. This method was later discontinued because of the interference of MES buffer (resulting in poor resolution of peaks) while measuring acids and long sample preparation times. Product profiles for experiment 1 were obtained by using this method.

The newer method for simultaneous analysis of acids (butyrate, acetate and propionate) and alcohols (ethanol, butanol and propanol) utilized an Agilent 6890N gas chromatograph with a 7683 series autosampler and injector (Agilent Technologies, Palo Alto, CA). An 8' X 1/8" AT steel packed column (Alltech Associates, Deerfield, IL) with 80-100 mesh Porapak® QS packing and phosphoric glass wool at inlet and outlet was connected to a flame-ionization detector (FID). The operating temperatures for the injection port, FID oven, and detector were 220, 200, and 250  $^{\circ}\text{C}$ , respectively. Nitrogen was used as the carrier gas at a flow rate of 25.7 ml/min. The hydrogen and air flowrates in the detector were set at 30 and 400 ml/min, respectively. All the samples were injected

using an autosampler with an injection volume of 1.0  $\mu$ l. Liquid analysis for experiment three was performed using this method.

The liquid broth for experiment two was analyzed using a 3400 Varian Gas Chromatograph (Varian, Sugar Land, TX.), equipped with a FID and a 6-ft glass column packed with Carbopack B DA 80/20 4 % Carbowax 20 M resin (Supelco, Bellefonte, PA). Liquid analysis for experiment 2 was performed using this method.

*Sulfide analysis:* 25 ml of fermentation broth was withdrawn from the bioreactor periodically and the sulfide concentration was measured using a CHEMET sulfide assay kit (Chemetrics, Calverton, VA). The sulfide concentration was maintained above 0.1 ppm by addition of a sterile cysteine-sulfide solution.

Several continuous experiments were performed, in which cells were grown on clean bottled gas and shifted to actual producer gas after a steady cell concentration was observed. The basic experimental protocol for all experiments was identical. However, the exact inlet gas compositions and some minor changes for each of the three experiments are discussed below:

*Experiment 1:* The operational volume of the bioreactor was 4.5 liters. The producer gas composition was 58.1% N<sub>2</sub>, 17.5% CO, 15.5% CO<sub>2</sub>, 4.4% H<sub>2</sub>, and 4.5% CH<sub>4</sub>. The feed media (stored in the feed tank) was also replenished during the course of the experiment.

*Experiment 2:* The producer gas composition for this study was 56.8% N<sub>2</sub>, 14.7% CO, 16.5% CO<sub>2</sub>, 4.4% H<sub>2</sub>, and 4.2% CH<sub>4</sub>. The reactor volume was reduced to 4 liters, after the glass column cracked near the top following experiment 1. The media in the feed tank was sufficient for the entire experiment, eliminating the need to replenish the tank.

*Experiment 3:* The producer gas used for this experiment was cleaned with a 10% acetone solution prior to storage in the tanks. The producer gas composition for this study was 59.9% N<sub>2</sub>, 14.9% CO, 15.5% CO<sub>2</sub>, 4.9% H<sub>2</sub>, and 4.8% CH<sub>4</sub>.

### 3.4 Results and Discussion

#### 3.4.1 Experiment 1 (with replenishment of liquid feed tank)

##### Days 0 to 11 (with bottled gas)

**Cell concentration:** As seen in Figure 3.5, the cells started to grow after a lag phase of 4 days. The term cell growth (as used in this study) indicates the increase in cell population and not the structural size of an individual cell. During the growth phase, the concentration increased exponentially under batch conditions with clean bottled gas. The cell OD reached a maximum of 1.3 on Day 6. The net cell growth rate ( $\mu$ ) in the batch mode was approximately 0.0215 hr<sup>-1</sup> (shown in Figure 3.6 as the slope). Continuous liquid feed and product removal (with cells) at 1.5 ml/min was started on Day 6 and continued throughout the remainder of the experiment. The cell OD remained steady at 1.2 for the next 4 days, until Day 10. The liquid feed source tank (pH = 5.75) was changed on Day 10. The cell material balance in the continuous mode shows

$$\frac{dX}{dt} = \mu X - DX \quad (\text{Eq. 3.1})$$

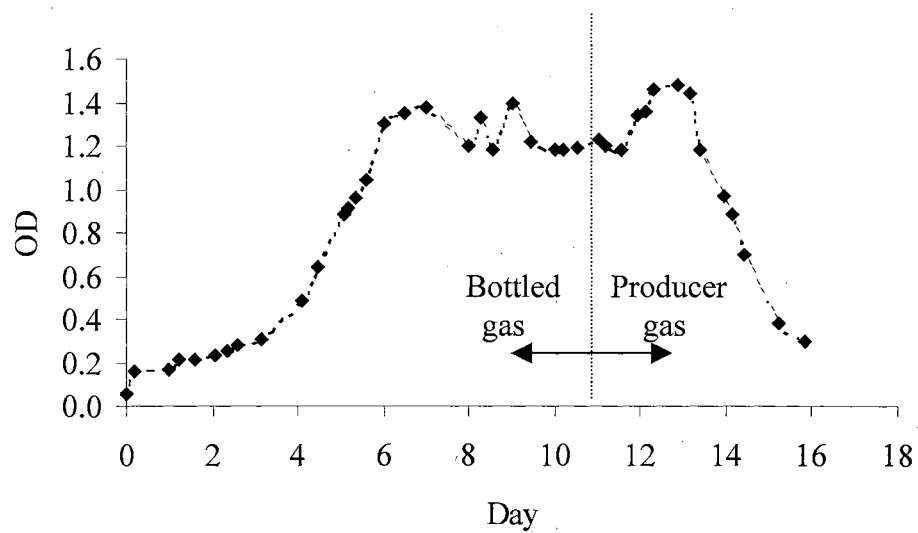


Figure 3.5. Cell concentration profile for experiment 1. The reactor was operated with liquid in batch mode until Day 6 and in a continuous mode till Day 16. Gas was always continuous

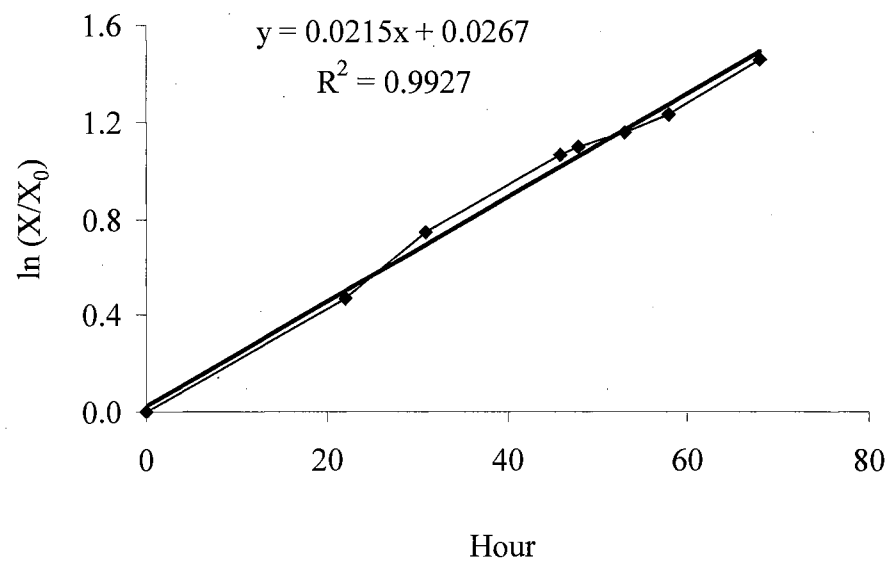


Figure 3.6. Batch growth curve for experiment 1.

X represents the OD, which is proportional to the cell concentration.

where  $X$  (which is proportional to OD) is the cell concentration and  $D$  is the dilution rate (liquid feed rate/liquid volume). At a steady state cell concentration,  $\mu = D$ . Thus,  $\mu = D = 0.023 \text{ hr}^{-1}$ , which is slightly greater than the growth rate during the batch mode.

*pH:* An automatic pH controller was used to set and control the pH. Due to the inability of the controller to simultaneously pump acid and base, the controller was set to operate with a lower pH control. NaOH was used as the base at all times. The pH was initially set at 5.9 from Day 0 to Day 4 and lowered progressively throughout the experiment to 5.7 (Day 4 to Day 8), 5.5 (Day 8 to Day 9), 5.25 (Day 9 to Day 11) and 5.1 (Day 11 to Day 16). As shown in Figure 3.7, the observed pH profile followed the set point until Day 11.

*CO and H<sub>2</sub> utilization:* As shown in Figure 3.8, the consumption of CO commenced on Day 2 and steadily increased with the increase in cell OD over the next 4 days. This established the dependence of CO consumption on the cell concentration in the bioreactor. The inlet and outlet CO concentrations remained steady at about 17.5 vol % and 10 vol % respectively.

As seen in Figure 3.9, negligible H<sub>2</sub> consumption was observed until Day 5. The H<sub>2</sub> consumption steadily increased to about 27% of the feed H<sub>2</sub> on Day 9 and remained steady until Day 11. Hydrogenase is a multifunctional enzyme that catalyzes the reversible reaction of protons into H<sub>2</sub>. The existence of multiple hydrogenases within a single living organism has been shown, with each expressed under certain physiological conditions, depending on the energy needs of the organism (Maness and Weaver, 2001). H<sub>2</sub> utilization was not observed on a 5-liter scale in the previous studies with clean bottled gases (Rajagopalan, 2001). Although no intentional changes in the operation of



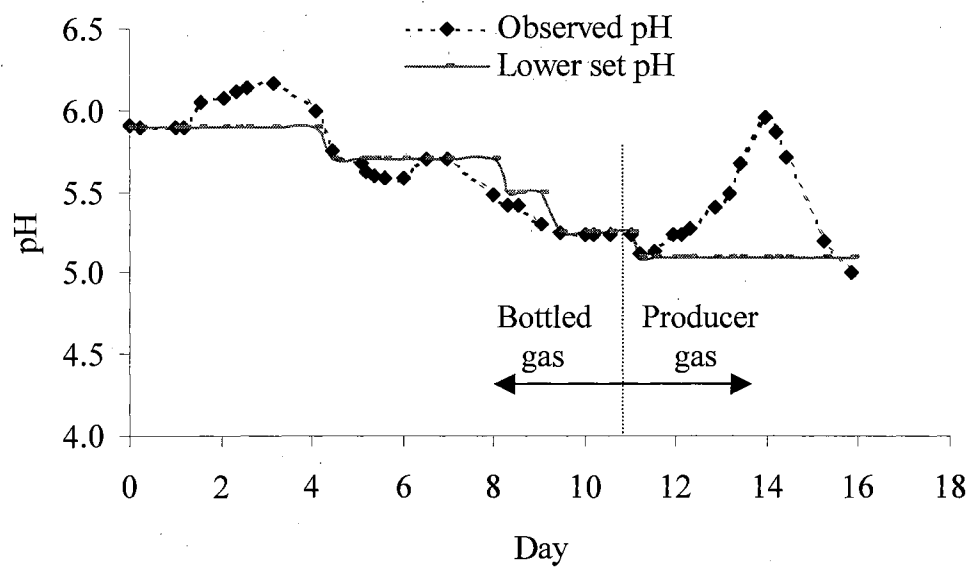


Figure 3.7. pH profile for experiment 1

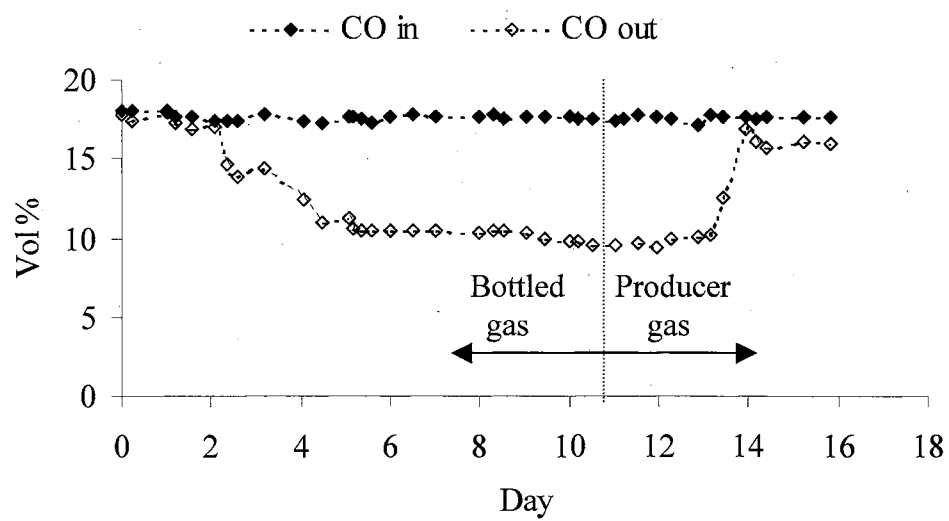


Figure 3.8. Inlet and outlet CO profiles for experiment 1

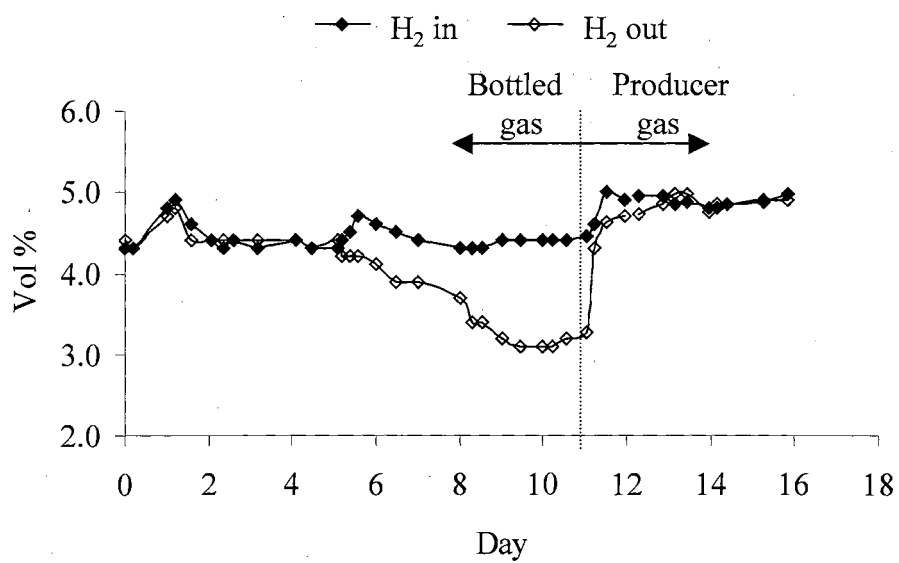


Figure 3.9. Inlet and outlet  $\text{H}_2$  profiles for experiment 1

the bioreactor were made, utilization of  $H_2$  was observed with clean bottled gases in this experiment. Recent research studies have indicated that the hydrogenase activity in clostridial P7 is almost twice at a pH of 6 as compared to a pH of 5 (Shenkman, 2003). The hydrogenase activity in many bacteria including *Clostridium acetobutylicum* (Kim et al., 1984) and *Clostridium thermoaceticum* (Drake, 1982) was inhibited by CO. The  $H_2$  utilization can possibly be attributed to a lower partial pressure of CO, as well as lower pH in these studies as compared to those reported by Rajagopalan (2001).

*Product formation:* The ethanol and butanol profiles are shown in Figure 3.10. No significant ethanol and butanol production was observed until Day 4. The butanol concentration increased to 0.3 wt% on Day 6 and remained steady until Day 8. On Day 8, the butanol increased slightly to 0.35 wt% and a steady profile was observed until Day 11. A similar trend in ethanol concentration was observed until Day 11, with a steady state ethanol concentration of 0.05 wt % (Day 6 to Day 8) and 0.08 wt% (Day 8 to Day 11). The inlet and outlet  $CO_2$  profiles, as shown in Figure 3.11, showed that the generation of  $CO_2$  was dependant on the cell concentration and CO consumption in the bioreactor. A steady rise in the production of  $CO_2$  was observed from Day 2 to Day 6. At steady state, for an inlet concentration of about 15.6 vol %, the outlet  $CO_2$  concentration was 21.5 vol% from Day 6 to Day 11.

#### **Days 11 to 16 (using biomass-generated producer gas)**

*Cell concentration:* As shown in Figure 3.5, the bottled gas feed was replaced by actual producer gas on Day 11 and continued until Day 16. The cell OD increased slightly from 1.2 to 1.4. The cell OD remained steady at 1.4 for 2 days, until Day 13. The

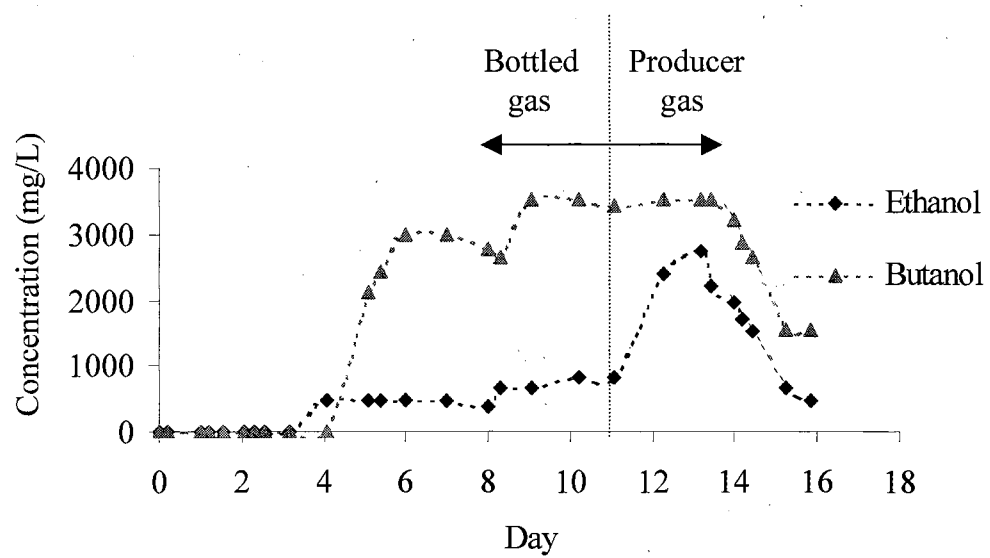


Figure 3.10. Ethanol and butanol profiles for experiment 1

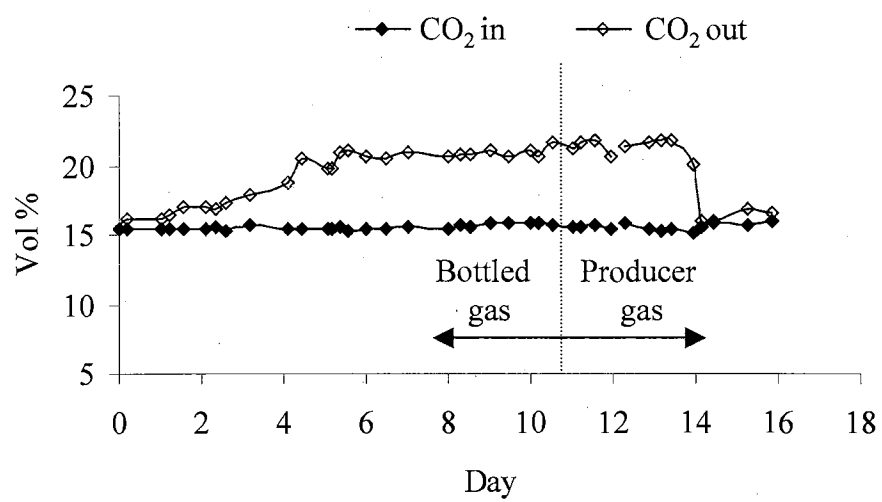


Figure 3.11. Inlet and outlet  $\text{CO}_2$  profiles for experiment 1

liquid nutrient source (pH = 5.75) was again replenished on Day 12.5. The OD began steadily decreasing from 1.45 on Day 13 and dropped to 0.3 on Day 16. The experiment was terminated on day 16. The steady state cell concentration during the first two days (Days 11 to 13) is indicative that the cell growth was balanced by cells leaving the reactor in the product stream. However, the cell decline beginning on Day 11 indicated that cells were dying and/or cells were washing out as a result of no cell growth. With  $D=0.02 \text{ hr}^{-1}$  and assuming no net growth ( $\mu=0$ ), integration of Equation 3.1 for the OD (which is proportional to  $X$ ) beginning on Day 11 with an initial OD of 1.45 yields:

$$X = X_0 \exp(-Dt) \quad (\text{Eq. 3.2})$$

where  $X_0$  is the cell OD when cells started disappearing. The predicted OD, which agrees very well with the measured OD, is shown in Figure 3.12. The excellent agreement suggests that the cell growth stopped (with negligible death) beginning on Day 11 and that the cell decrease was due to washout. The liquid feed tank was changed on Day 12.5 (just before washout began). Although, the chances of cell washout due to faulty media were low, the experiment was repeated to eliminate this possibility.

*pH:* Following the introduction of producer gas on Day 11, an instant and rapid rise in pH was observed (Figure 3.7). The pH went up from 5.1 on Day 11 to 6.0 on Day 14, after which the pH steadily dropped to 5.1 on Day 16. Since no acid profiles were available for this experiment, the cause of the pH rise and drop could not be established.

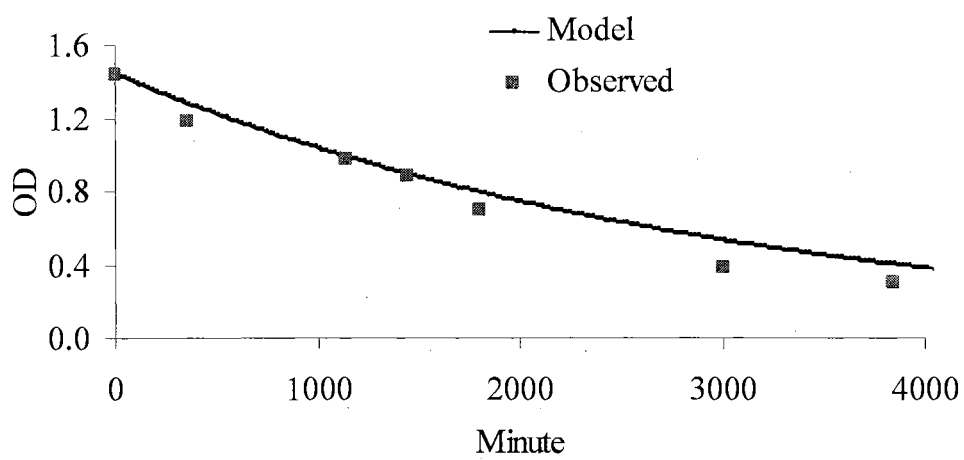


Figure 3.12. Observed and predicted cell OD assuming cell washout for experiment 1. Equation 3.2 was used to predict the washout rate.



*CO and H<sub>2</sub> utilization:* The introduction of biomass-generated producer gas on Day 11 had no immediate effect on the consumption of CO (Figure 3.8). A sharp decline in CO consumption was observed on Day 13, corresponding to a decline in cell OD during that period. Negligible CO consumption was observed from Day 14 to Day 16, because of a low cell OD. The consumption of H<sub>2</sub> ceased almost instantly on Day 11, after the introduction of producer gas and was near zero for the remainder of the experiment (shown in Figure 3.9). The decrease in H<sub>2</sub> uptake after introduction of producer gas is likely explained by the inactivation or inhibition of hydrogenase. Previous studies have shown that nitric oxide, acetylene and oxygen are strong inhibitors of this enzyme (Tibelius and Knowles, 1984), all of which have been identified in the producer gas.

*Product formation:* As seen in Figure 3.10, the butanol concentration remained steady at 0.35 wt% until Day 14. A gradual drop in the butanol concentration was observed after Day 14, corresponding to the drop in cell OD after Day 14. A jump in ethanol concentration was observed on Day 11, after introduction of producer gas from about 0.08 wt% to 0.27 wt % on Day 13. However, the constant cell OD during this period suggested the non-growth associated production of ethanol following introduction of producer gas. The ethanol concentration decreased with the decrease in cell OD, from Day 13 to Day 16. A negligible production in CO<sub>2</sub> was observed from Day 14 to Day 16, corresponding to a minimal CO consumption during this period.

### 3.4.2 Experiment 2 (with no replenishment of liquid feed tank)

#### Days 0 to 8.5 (with bottled gas)

*Cell concentration:* The reactor was operated during the first 6.5 days with liquid in the batch mode and gas (using bottled gas) in the continuous mode. As shown in Figure 3.13, the cells started growing with bottled gas after a lag phase of about four days. The net cell growth rate ( $\mu$ ) in the batch mode was approximately  $0.04 \text{ hr}^{-1}$  (shown as the slope in Figure 3.14). The cell OD started to plateau on Day 6 at a cell OD of 1.1. At this point, continuous liquid feed and product removal was initiated at 1.5 ml/min and the cell OD leveled off at approximately 1.2. Analysis of the cell concentration shown by Equation 3.1, indicates that  $\mu = D = 0.023 \text{ hr}^{-1}$ , which is about one-half the growth rate during the batch mode.

*CO and H<sub>2</sub> utilization:* The CO (shown in Figure 3.15) and H<sub>2</sub> (shown in Figure 3.16) utilization increased on Day 4, which is when the cells began to grow. The steady state CO utilization was about 22% of the feed CO, while the H<sub>2</sub> utilization was approximately 21% of the feed H<sub>2</sub>. Obviously, increasing the cell concentration, changing the gas feed rate, and/or adjusting the reactor size can affect the utilization.

*Product formation:* Ethanol, butanol, butyrate and acetate were the major products formed during fermentation. As shown in Figure 3.13, there was a rapid rise in acetate and butyrate formation beginning on Day 4 (when the cells started to grow). Thus, the acid formation is growth-associated. Following a change to the continuous mode on Day 6.5, the acetate concentration began to diminish, likely due to acid leaving the reactor at a greater rate than it was being produced. The butyrate concentration remained steady at

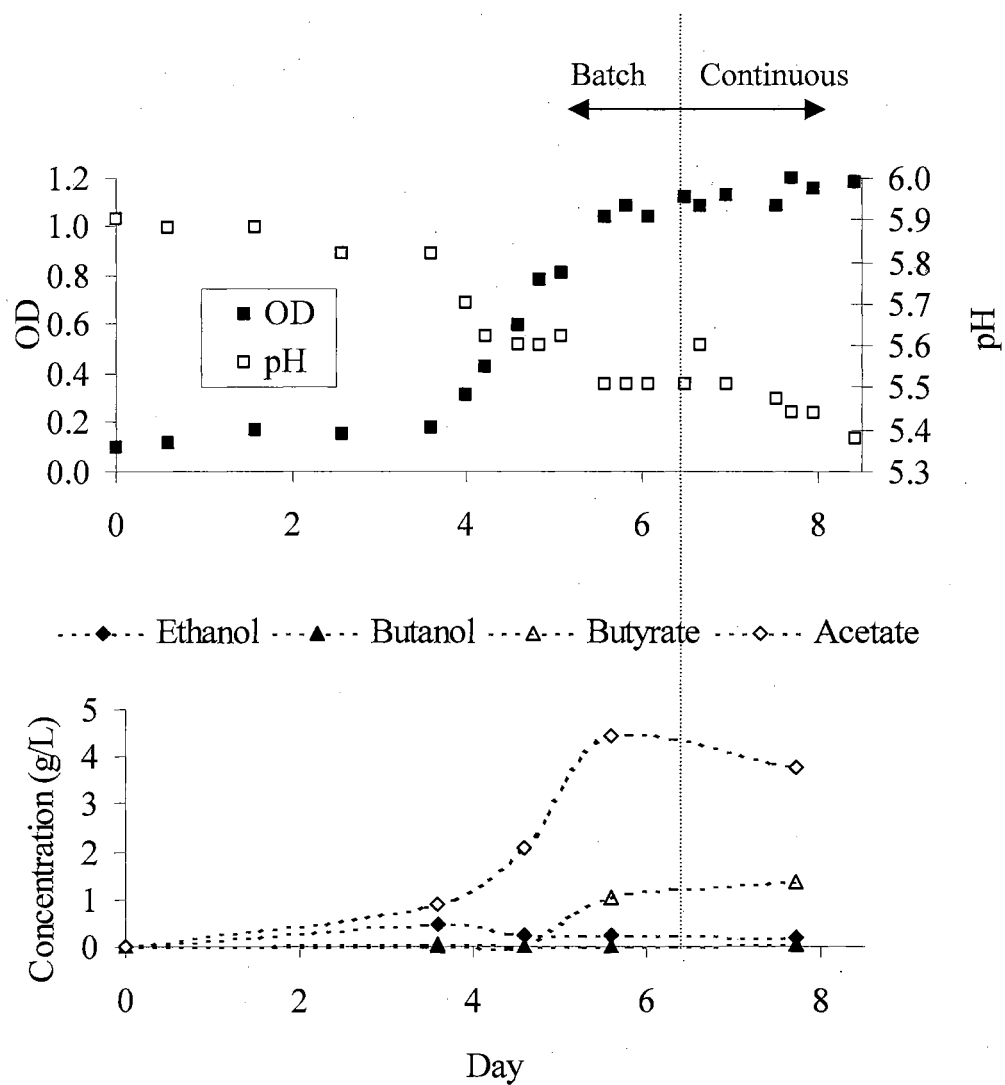


Figure 3.13. Cell OD, pH and product profiles for experiment 2 from Days 0 to 8. Clean bottled gas was used from Day 0 to 8

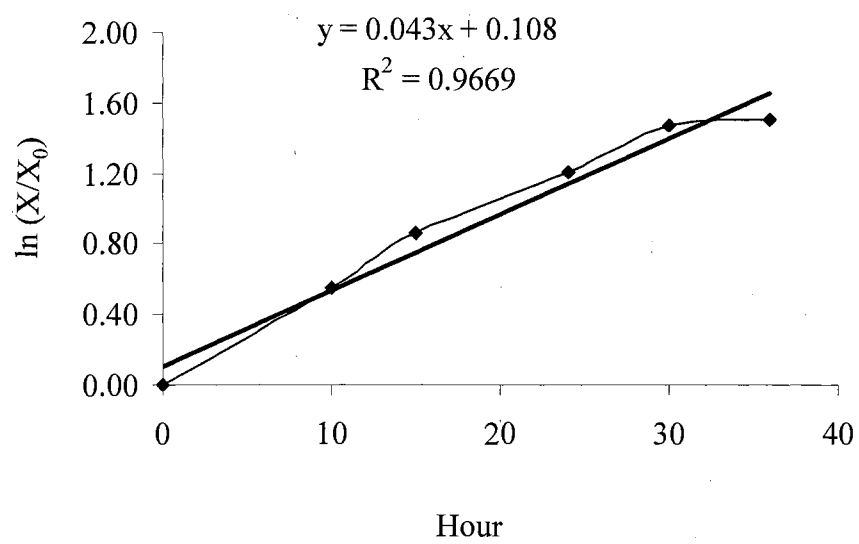


Figure 3.14. Batch growth curve for experiment 2.

X represents the OD, which is proportional to the cell concentration.

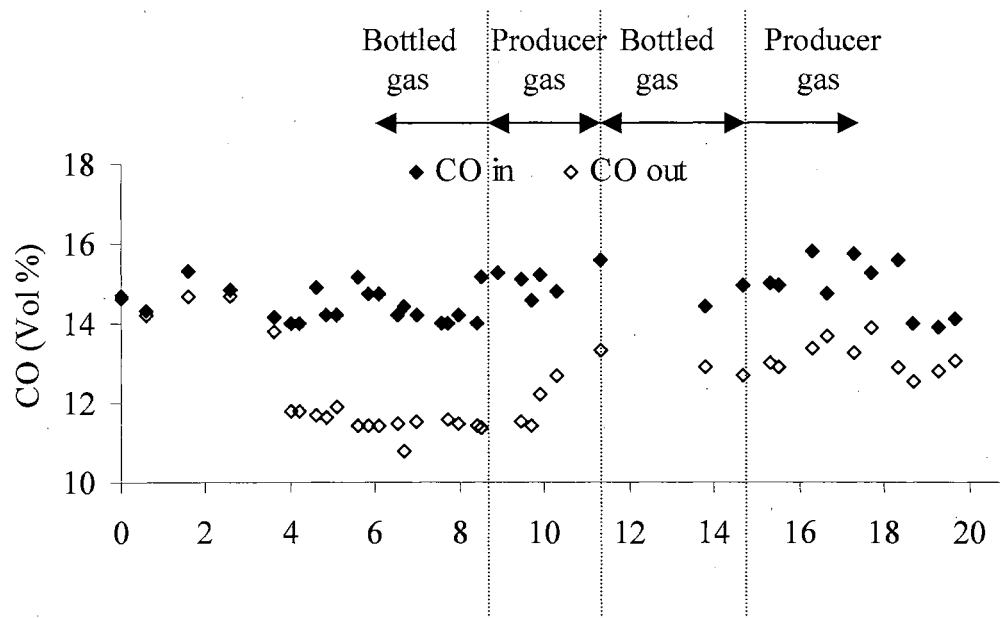


Figure 3.15. Inlet and outlet CO profiles for experiment 2

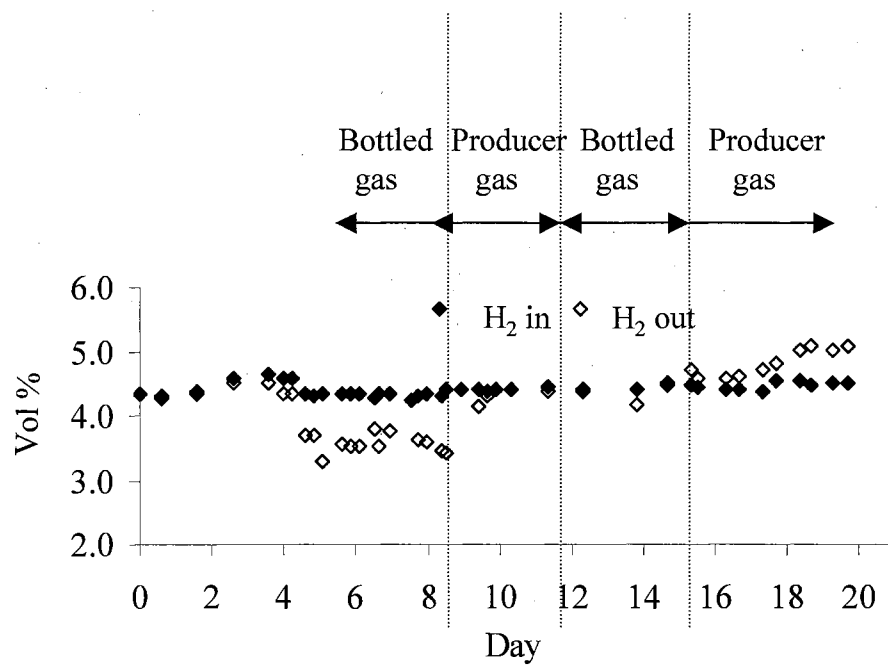


Figure 3.16. Inlet and outlet H<sub>2</sub> profiles for experiment 2

about 1.2 g/L. There was a small amount (about 0.23 g/L at steady state) of ethanol produced. The generation of CO<sub>2</sub> (shown in Figure 3.17) was consistent with the CO consumption profile for the entire experiment. The steady state inlet and outlet CO<sub>2</sub> concentrations were about 16.5 and 18.2 vol%, respectively.

*pH:* The pH was initially set and controlled at 5.9 during the batch mode for the first four days, after which the set point was gradually lowered and controlled at a lower limit of 5.4. The observed pH drop during this time is indicative of the acid formation.

#### **Days 8.5 to 11.5 (using biomass generated producer gas)**

*Cell concentration:* During this time, the reactor was operated with both liquid and gas in the continuous mode and the feed gas was changed from bottled gases to the stored producer gas on Day 8.5. As shown in Figure 3.18, the cell OD remained steady for 1.5 days at approximately 1.2 and then began decreasing on Day 10 to a value of 0.45 on Day 11.5. The trend was similar to that seen in experiment 1. Analysis of Equation 3.2 for cell OD (shown in Figure 3.18) beginning on Day 10 with an initial OD of 1.2 clearly indicated that the cell growth stopped (with negligible death) beginning on Day 10 and that the cell decrease was again due to washout.

*CO and H<sub>2</sub> utilization:* As shown in Figure 3.16, the H<sub>2</sub> utilization stopped shortly after Day 8.5 following the introduction of producer gas. The stop in H<sub>2</sub> utilization indicates that some component of the producer gas may be inhibiting the hydrogenase enzyme. CO utilization did not stop but was reduced to about 14% of the feed on Day 10 (shown in Figure 3.15) after the cells began to stop growing and began to washout. Thus at this point, CO utilization was used primarily for product formation (primarily the

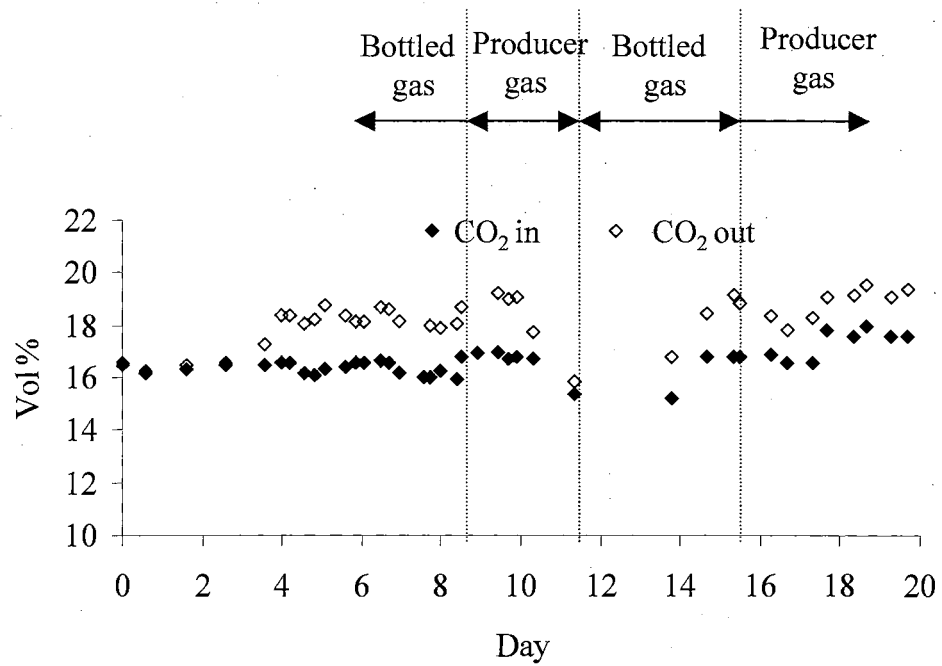


Figure 3.17. Inlet and outlet CO<sub>2</sub> profiles for experiment 2



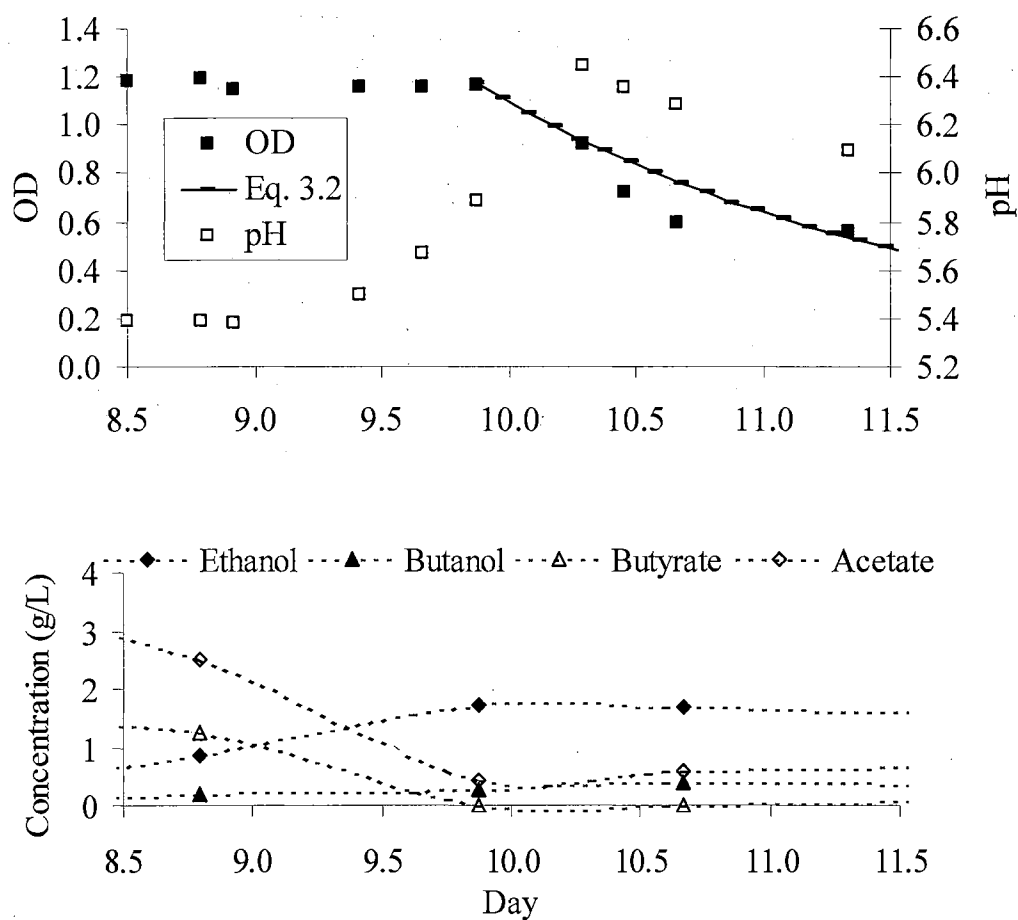


Figure 3.18. Cell OD, pH and product profiles for experiment 2 from Days 8.5 to 11.5. Biomass-generated producer gas was introduced on Day 8.5 and continued until Day 11.5. Liquid was in a continuous mode

alcohols) rather than cell growth and some of the utilization decrease was a result of fewer cells in the bioreactor.

*Product formation:* As seen in Figure 3.18, the ethanol concentration started to rise steadily following the introduction of producer gas, with a continual drop in acid production. After Day 10, the ethanol concentration remained steady at about 1.6 g/L, even though the cell concentration decreased steadily during this period. Thus, the ethanol production per unit mass of cell was increasing during this time and was likely not a result of acid conversion since the acid concentrations were very low at this point.

*pH:* A concurrent rise in pH from 5.4 to 6.5 (there was no upper pH control) was observed, likely a result of alcohol formation from the corresponding acid. Earlier studies have shown that introducing the producer gas into cell-free medium did not change the pH (details discussed in section 4.5.3 of Chapter 4). After the concentration of acids became very low, the pH began to drop back towards the liquid feed pH of 5.8-5.9. The pH decay rate was similar to the cell decay rate, giving credence that the pH change after Day 10 was likely due to replenishment of the media at the given dilution rate.

#### **Days 11.5 to 20 (liquid batch mode)**

*Cell concentration:* To avoid complete washout of the cells, the feed gas was switched back to bottled gas and the fresh feed/product removal was stopped such that the liquid was again in batch mode. As shown in Figure 3.19, the cells began to grow, again indicating that the cells were still viable although they had previously been exposed to producer gas. Cell viability was also demonstrated by using the cells as an inoculum for additional experiments in which cell growth was comparable to growth from cells that

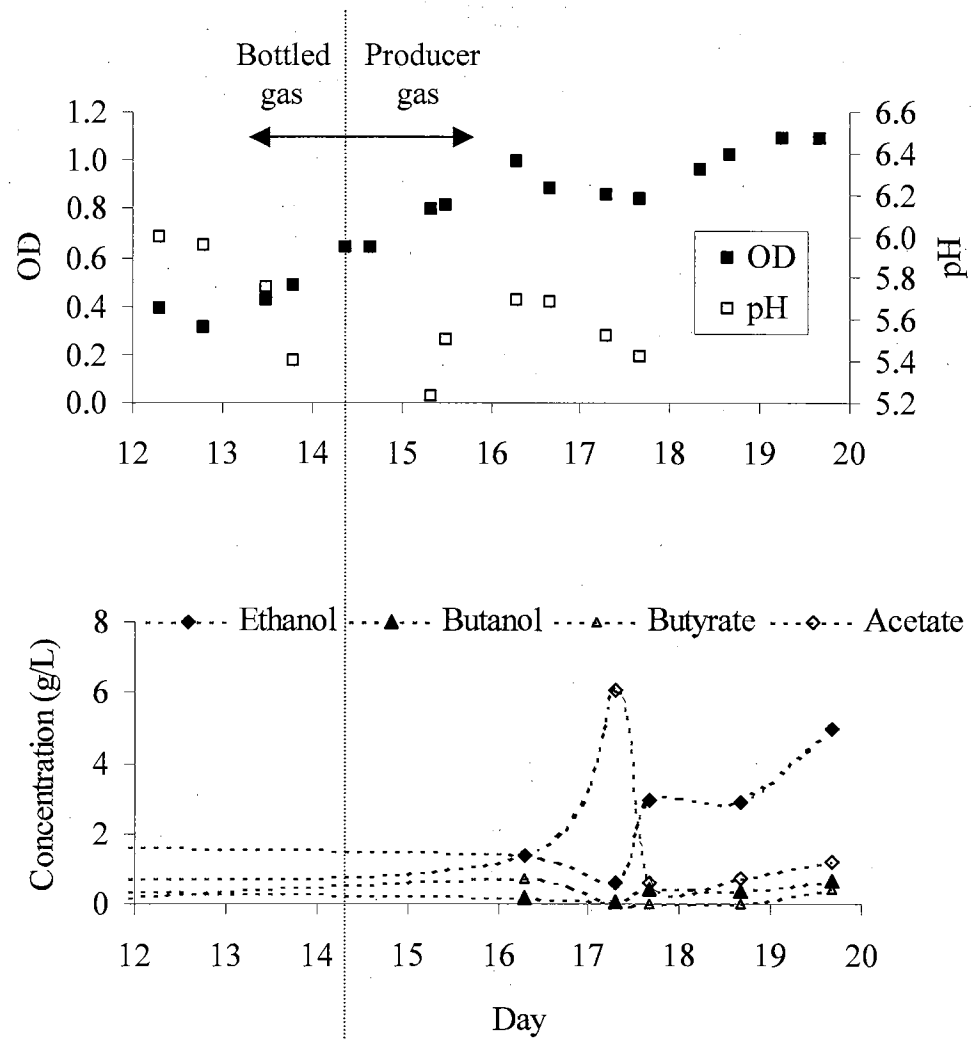


Figure 3.19. Cell OD, pH and product profiles for experiment 2 from Days 12 to 20. The liquid was in batch mode from Day 12 to 20

had not been previously exposed to producer gas (Shenkman, 2003). On Day 14.5, the gas source was switched back to producer gas. Cell growth was still observed for about 1.5 days after which the cell growth essentially stopped (but the cells did not die). These results agree with the results from Day 8.5 to 11.5 in which there was a 1.5 day delay following producer gas introduction before the cells stopped growing.

*CO and H<sub>2</sub> utilization:* During the batch mode, CO was utilized for both bottled and producer gas feeds (Figure 3.15). This is consistent with the findings previously described. However, the H<sub>2</sub> was not utilized and there may have been some H<sub>2</sub> production (shown in Figure 3.16). Hydrogenases are known to both generate and consume H<sub>2</sub> (Maness and Weaver, 2001 and 2002) and the reactor conditions may have favored the production of H<sub>2</sub>. The H<sub>2</sub> results need to be further explored.

*Product formation:* There was a rise in ethanol concentration from Day 17 to Day 20 with producer gas, even though there was no cell growth during this period. Thus, non-growth associated ethanol production was observed, which agrees with the previous findings with producer gas. The reasoning for the spike in acetate production on Day 17 is unknown and needs to be further explored.

*pH:* During the batch growth phase, the pH continued to decrease, likely a result of acid production. The pH decrease is in agreement with the findings from Day 0 to 6.5 in which the liquid was in batch mode with exposure to bottled gas. A pH rise was observed on Day 14.5, after the gas source was changed from bottled gas to biomass-generated producer gas.

### Specific production rate of ethanol

Since non-growth associated ethanol production was observed with producer gas in both continuous and batch liquid modes, a model was developed to estimate and compare the specific rate of production of ethanol for both liquid modes when exposed to producer gas. The concentration profile of ethanol in the continuous mode can be expressed as:

$$\frac{dP}{dt} = \alpha\mu X + \beta X - DP \quad (\text{Eq. 3.3})$$

where  $\alpha$  (growth associated) and  $\beta$  (non-growth associated) are constants denoting the specific production rate of ethanol;  $\mu$  is the specific cell growth rate;  $X$  is the cell concentration (in OD units) and  $D$  is the dilution rate. Integration of Equation 3.3, after substituting  $\alpha=0$  (since ethanol production is non-growth associated) and assuming  $X$  is constant (Days 8 to 10) yields,

$$P - P_i \exp(-Dt) = \frac{\beta X}{D} (1 - \exp(-Dt)) \quad (\text{Eq. 3.4})$$

The specific production rate ( $\beta$ ) for ethanol was calculated using the data points on Day 7.7 ( $P_i=0.19$  g/L) and Day 9.9 ( $P=1.74$  g/L with  $t=2.2$  days) and  $X$  and  $D$  of 1.2 and  $0.0225 \text{ hr}^{-1}$  respectively. Thus, the calculated specific rate of ethanol production ( $\beta$ ) was about  $1.07 \text{ g/L/day/OD}$ . In the batch mode ( $D=0$ ) and with  $\alpha=0$ , Equation 3.3 gives  $P = P_i + \beta X t$  for constant  $X$ . Using the fitted slope of ethanol concentration versus time

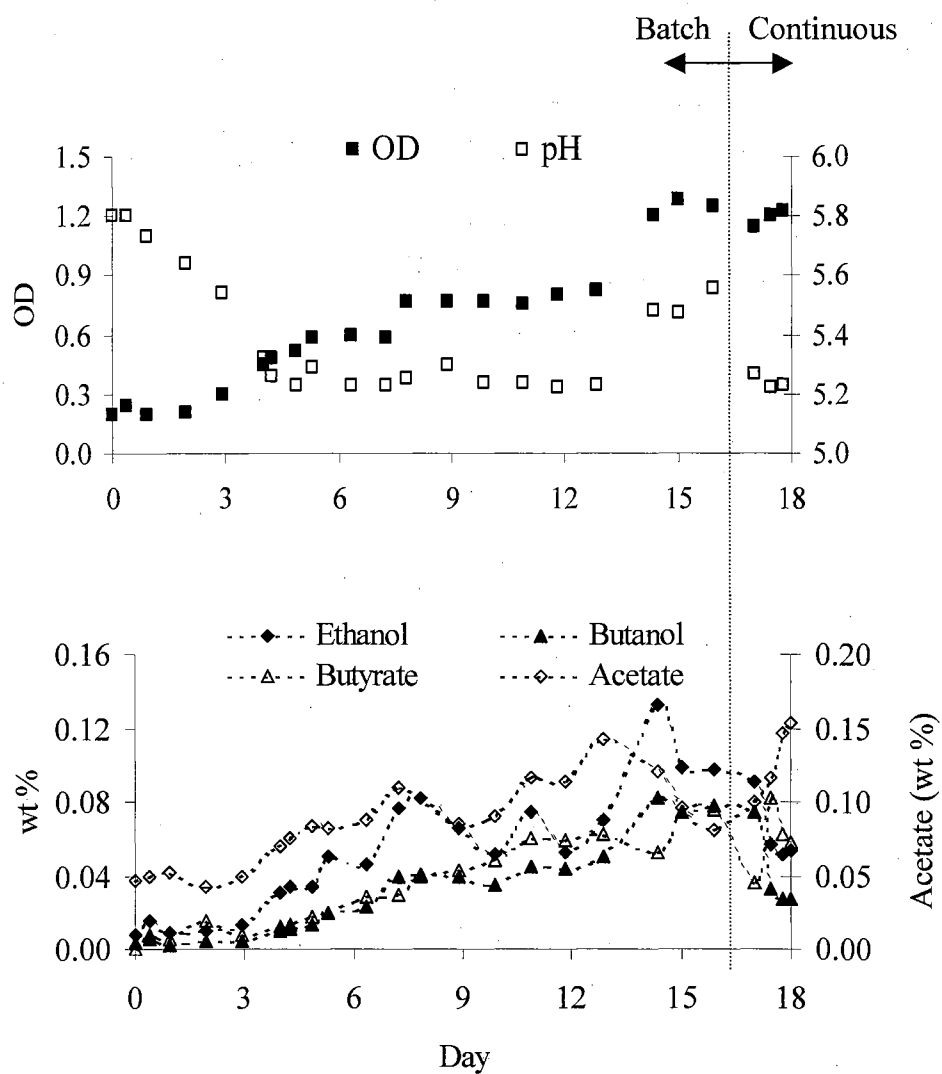


Figure 3.20. Cell OD, pH, and product profiles for experiment 3 from Days 0 to 18. Clean bottled gas was used from Day 0 to 18

(divided by the cell OD) would then yield  $\beta$  for the batch mode. Using the data from Days 17 to 20 (see Figure 3.19 with an OD of 1.0),  $\beta$  is about 1.53 g/L/day/OD. Thus, there is a reasonably good match between the two values for estimation of specific ethanol production rate with biomass-generated producer gas.

### **3.4.3 Experiment 3 (gas clean up using 10% acetone)**

#### **Day 0 to 18 (with bottled gas)**

*Cell concentration:* As shown in Figure 3.20, the cells started to grow after a lag phase of 2 days with clean bottled gas. The cells stopped growing after Day 6 and the cell OD remained stagnant at 0.75 for 7 days, until Day 13. Cell growth was observed again on Day 13 and the cell OD was 1.3 on Day 14.5. The liquid continuous mode was initiated on Day 17 at a cell OD of 1.2. The cause of cell OD stagnancy on Day 6 is uncertain, but it could be due to a bad inoculum source. The cell growth rate was not calculated because of the strange growth profile.

*CO and H<sub>2</sub> utilization:* The consumption of CO increased on Day 2, with cell growth (shown in Figure 3.21) until Day 6, but then decreased to almost negligible utilization until Day 12. The CO utilization increased again, to about 25% of the feed CO on Day 14 and was steady after initiation of the continuous liquid mode on Day 17. As seen in the Figure 3.22, no significant H<sub>2</sub> utilization was observed in the batch or continuous liquid mode.

*Product formation:* In addition to ethanol, butanol, butyrate, and acetate production, formation of propanol and propionate were also observed during the first 14 days of the

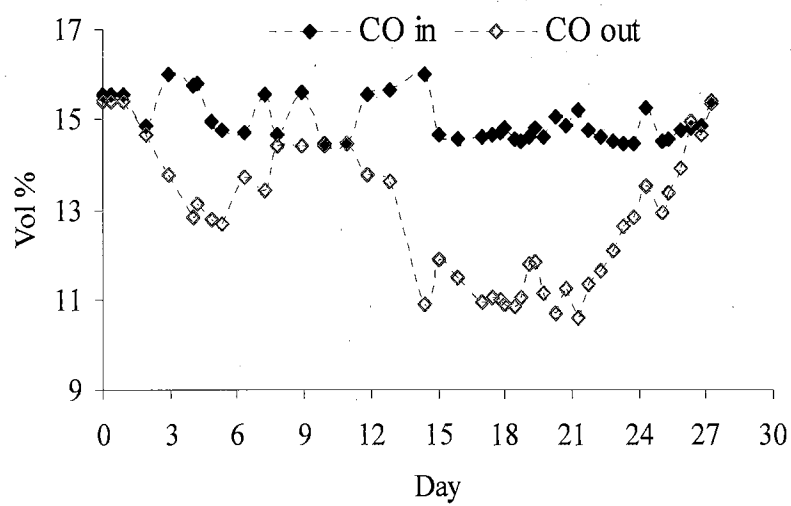


Figure 3.21. Inlet and outlet CO profiles for experiment 3.

Clean bottled gas was used from Day 0 to 18. Biomass-generated producer gas was used from Day 18 to 29



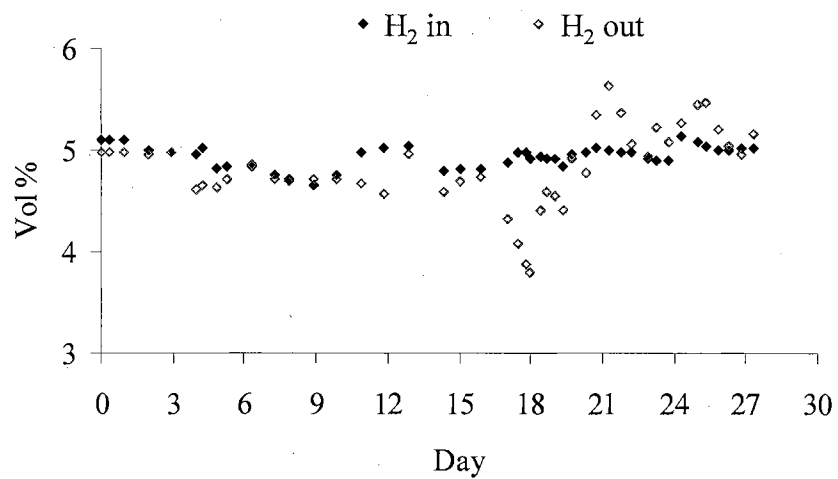


Figure 3.22. Inlet and outlet H<sub>2</sub> profiles for experiment 3.

Clean bottled gas was used from Day 0 to 18. Biomass-generated producer gas was used from Day 18 to 29

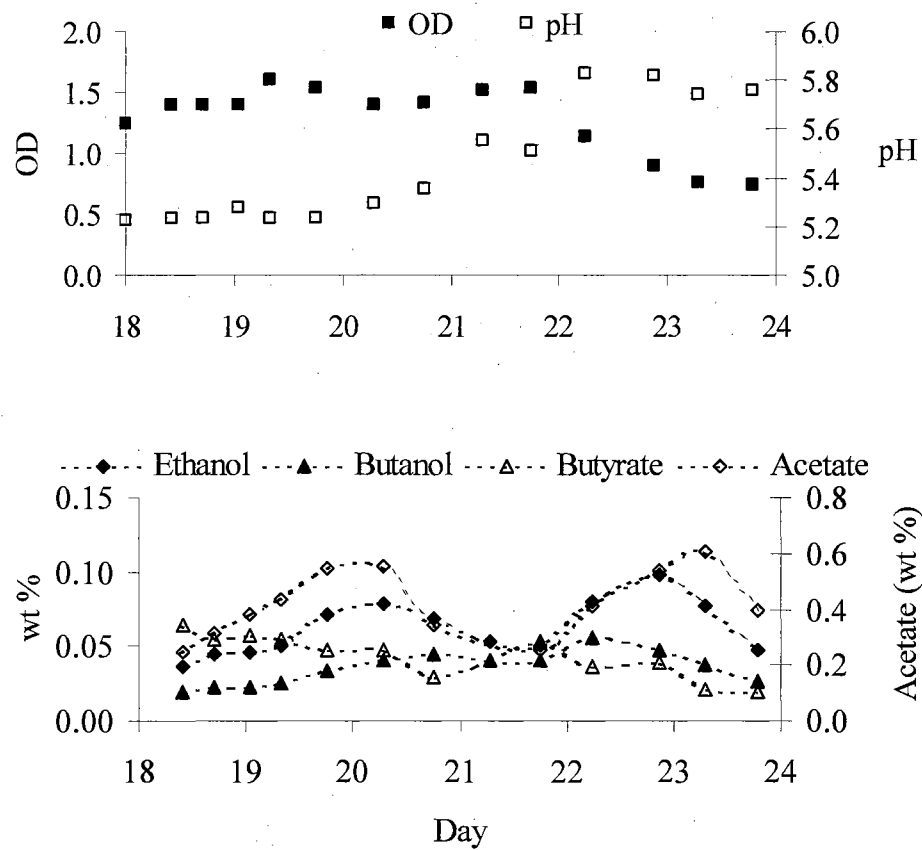


Figure 3.23. Cell OD, pH, and product profiles for experiment 3 from Days 18 to 24. Producer gas was used from Day 18 to 24

experiment, although the exact concentrations of propanol and propionate were not determined. Previous experiments did not assess propanol or propionate production. A steady accumulation of ethanol, butanol, butyrate, and acetate was observed during the batch mode to concentrations of about 0.1, 0.075, 0.04 and 0.1 wt% respectively on Day 17. After the continuous mode was initiated on Day 17, a drop in ethanol and butanol concentration was observed due to washout in the continuous mode.

*pH:* The pH dropped from an initial value of 5.8 to a value of 5.23 on Day 4. The pH was set and controlled at 5.23 (only lower control) during the batch mode, since acetate was the major product formed during this period.

#### **Day 18 to 24 (with biomass-generated producer gas)**

*Cell concentration:* The clean bottled gas was shifted to biomass-generated producer gas on Day 18, after the cell OD was stable at 1.25 in the continuous liquid mode. As seen from Figure 3.23, the cell OD remained steady for about four days (until Day 22). The cell OD then began diminishing on Day 22 and reached a value of 0.74 on Day 24. As seen from Figure 3.24, the data points for actual observed OD were above the curve for predicted OD using the cell washout model described in Equation 3.2. This suggested that the cells were not completely dormant but were indeed growing at a very slow rate (close to being dormant). The increased delay (before cell washout began) with better gas clean up could be due to a lower concentration of a toxic component in the producer gas that causes the cells to shift to a non-growth phase. Some of the possible contaminants are  $\text{NH}_3$ , HCN (Liu and Gibbs, 2003), phenols (Cummer and Brown, 2002), nitric oxide, and gaseous tar components (Devi et al., 2003).

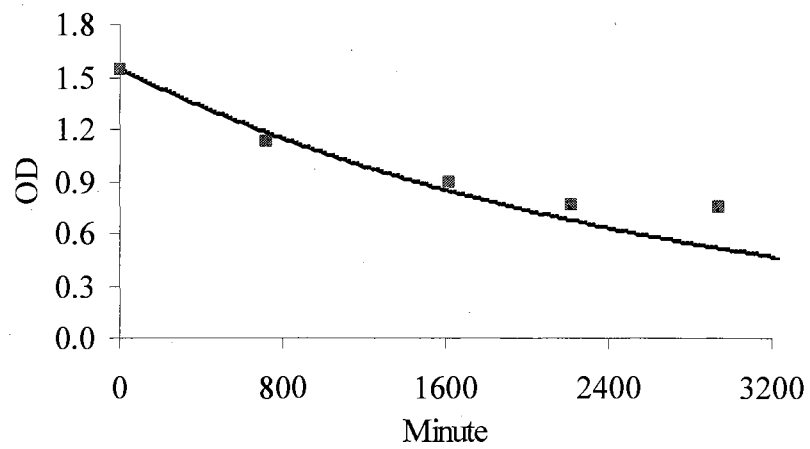


Figure 3.24. Observed and predicted cell OD assuming cell washout for experiment 3. Equation 3.2 was used to estimate the washout rate.

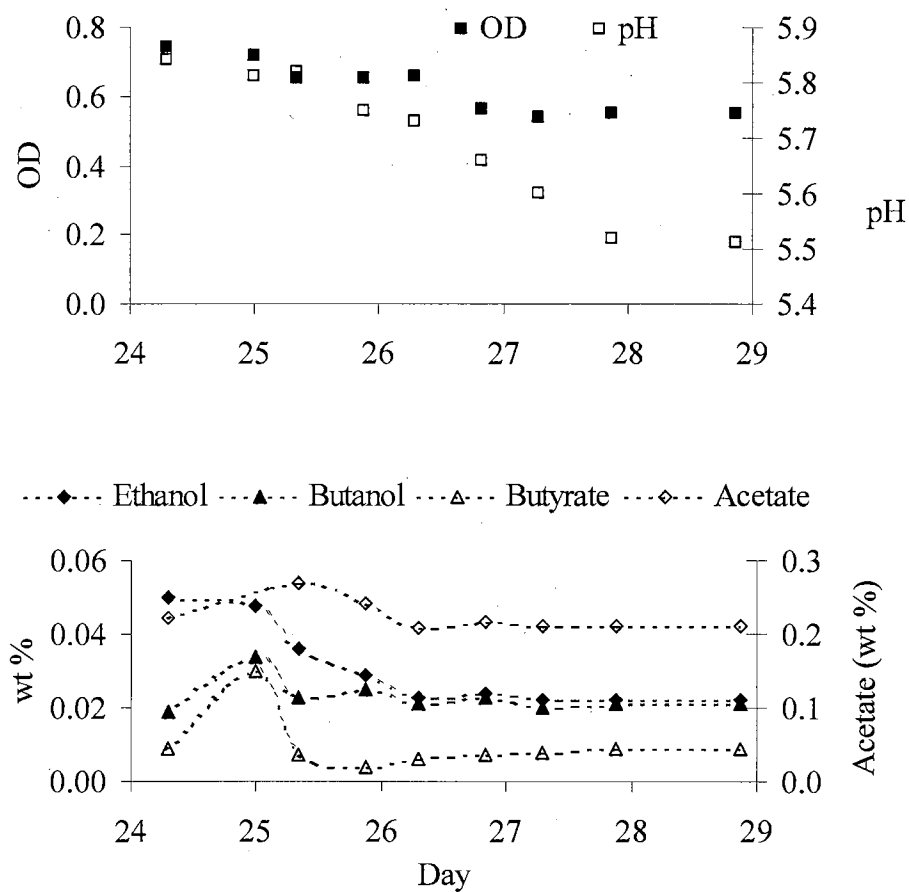


Figure 3.25. Cell OD, pH, and product profiles for experiment 3 from Days 24 to 29. Producer gas used from Day 24 to 29

*CO and H<sub>2</sub> utilization:* As seen from Figure 3.21, the utilization of CO was unaffected after the introduction of biomass-generated producer gas. The consumption of CO decreased steadily from Day 22 to about 15% of the feed CO on Day 24, likely due to cell washout. H<sub>2</sub> utilization stopped after a day following producer gas introduction. A slight production of H<sub>2</sub> was observed from Day 21 to Day 24 (shown in Figure 3.22), suggesting a possibly active evolution hydrogenase under the reactor conditions. These findings were consistent with results from previous studies.

*Product formation:* As shown in Figure 3.23, a rapid rise in acetate formation was observed from a value of 0.153 wt % on Day 18 to about 0.55 wt % on Day 20.5. The ethanol and butanol doubled from about 0.04 wt% to 0.08 wt % and 0.027 wt % to 0.058 wt % respectively during this period. The ethanol, acetate and butanol concentrations decreased from Day 20.5 to Day 22 and again increased until Day 23.5. The cause of this cyclical trend needs to be investigated further.

*pH:* Significant quantities of NaOH (120 ml) were consumed between Day 18 to Day 20 to maintain the pH at the lower set point of 5.22, due to acid formation during this period. Unlike in experiments described earlier, there was a 2-day delay (see Figure 3.23) before a rapid pH rise was observed after the introduction of producer gas. The increase in pH from Day 20 corresponds to the decrease in acetate concentration from Day 20. The pH control was changed to a upper limit of 5.82 on Day 21.5.

### **Day 24 to 29 (liquid batch mode)**

*Cell concentration:* The liquid was changed to batch mode on Day 24 to avoid complete washout in the continuous mode. As seen from Figure 3.25, the cell OD dropped slightly to 0.55 on Day 26 and remained steady until Day 29. The steady cell OD profile after Day 26 gives credence to the fact that cells don't die with producer gas, but shift to a non-growth phase.

*CO and H<sub>2</sub> utilization:* The CO utilization profile (seen in Figure 3.21) followed the cell OD profile. CO utilization decreased until Day 26 and was essentially negligible for the remainder of the experiment. Similarly, no detectable difference in the inlet and outlet H<sub>2</sub> concentration was observed. This suggested that the cells not only stopped growing, but also became metabolically inactive after Day 26.

*Product formation:* The concentration of ethanol, butanol, and acetate decreased until Day 26 to about 0.025, 0.02, and 0.2 wt % respectively and remained constant until Day 29. The butyrate concentration decreased to non-detectable levels. The flat profile for all the products also indicates the total metabolic inactivity of the cells. In experiment two, clean bottled gas was introduced during the continuous mode, following the exposure of the cells to biomass-generated producer gas (for 2 days). Unlike as in experiment two, the cells in were not again exposed to clean bottled gas and the liquid remained as a batch process. Hence, it is likely that the buildup of a metabolite in the medium, which was not observed in experiment two (since the liquid media was also replenished during exposure to clean gas), reached a critical concentration level, causing total inhibition of all enzymes responsible for cell growth, substrate utilization and product formation.

### 3.5 Conclusions

The successful implementation of generating producer gas from biomass and then fermenting the producer gas has been demonstrated. The key research findings following the introduction of producer gas are: 1) the cells stopped growing but did not die after a 1.5-day delay following the introduction of producer gas. The delay was extended by 2 more days with a better gas cleanup using a 10% acetone solution, 2) ethanol was primarily produced once the cells stopped growing (ethanol is non-growth associated), 3)  $H_2$  utilization stopped, and 4) cells began growing again if “clean” bottled gases were introduced following exposure to the producer gas. The possibility exists that following the introduction of producer gas, there is an alteration in the metabolic pathway(s) due to some trace species in the producer gas or the buildup of a metabolite in the medium. The decrease in hydrogen uptake after introduction of producer gas is likely explained by the inactivation or inhibition of hydrogenase. Previous studies have shown that nitric oxide (Hyman and Arp, 1988 and 1991), acetylene (Tibelius and Knowles, 1984, Sun et al., 1992) and oxygen (Maness et al., 2002) are strong inhibitors of hydrogenase, all of which have been identified as constituents in the biomass-generated producer gas.



## **CHAPTER 4**

### **EFFECTS OF INDIVIDUAL GAS IMPURITIES**

#### **4.1 Introduction**

The fermentation of producer gas to ethanol using anaerobic bacteria, such as P7, usually needs to be performed under oxygen-free conditions since the bacteria have a very low tolerance to oxygen. Enzymes like CODH and hydrogenase, which are responsible for utilization of gaseous substrates in producer gas for product formation, are extremely sensitive to oxygen (Drake, 1982, Maness et al., 2002) and could become inactive upon exposure to oxygen. Evidently, the maintenance of anoxic conditions in an integrated gasifier-bioreactor system is essential for maximum cell growth and product formation.

In an industrial scale operation of the fermentation process, there exists a possibility of oxygen entering the bioreactor due to a leak in the system. Maintaining an oxygen free environment during the production, cleaning and storage of producer gas obtained via biomass gasification could also be very challenging.

As described in the earlier chapter, the producer gas is composed of a large number of constituents (other than CO, CO<sub>2</sub>, N<sub>2</sub> and H<sub>2</sub>) like methane (CH<sub>4</sub>), ethane, ethylene, acetylene, NO<sub>x</sub> and in some cases oxygen (O<sub>2</sub>). These constituents may be toxic to the

cells and can cause the cells to change from a healthy to a dormant mode, or in some cases lead to cell death. Experimental verification with each individual impurity is necessary to assess the effect on cell growth and substrate utilization and to determine the probable cause of cell dormancy previously observed with biomass-derived producer gas (discussed in Chapter 3). The effects of  $O_2$  (likely the most harmful constituent) and  $CH_4$  (constituent with highest concentration) on cell growth, substrate utilization, and product formation are discussed in this chapter. As mentioned in the earlier chapter, a rise in pH was observed after the introduction of producer gas. The pH rise appeared to be due to the consumption of acetic acid following a change to biomass-generated producer gas. However, the possibility still exists that the pH rise could be a direct result of producer gas constituents. This latter possibility is assessed in this chapter.

#### **4.2 Objectives of the study**

The specific objectives of this study are aimed at investigating the effects of individual impurities identified in producer gas (namely  $O_2$  and  $CH_4$ ).

1. Determine the effect of  $O_2$  (1000 and 1900 ppm) on cell growth, pH, product formation and substrate utilization (specifically CO and  $H_2$ ).
2. Determine the effect of  $CH_4$  (at the concentration observed in producer gas) on the parameters mentioned above.
3. Assess the effect of producer gas on pH of liquid fermentation media without the presence of cells (P7) and ascertain whether the pH rise (observed in earlier experiments) was due to the dissolution of impurities in producer gas into liquid media.

## **4.3 Materials and Methods**

### **4.3.1 Biological catalyst**

The bacterium, P7 was provided by Dr. Ralph Tanner, University of Oklahoma, Norman. The organism was cultured and grown using strict anoxic techniques in a nutrient media described in Chapter 3. Fresh inoculum (100 ml) was used for the start of each experiment.

### **4.3.2 Culture medium**

A defined culture medium consisting of vitamins, trace metals and minerals was used to grow cells in the bioreactor. The composition of the stock solutions of vitamins, trace metals and minerals are described in section 3.3.4 of Chapter 3. The nutrient media contained (per liter) 30 ml of stock mineral solution, 10 ml of stock vitamin solution, 10 ml of stock trace metals solution, 0.5 g yeast extract, 5 g N-morpholinoethanesulfonic acid (MES), and 5 ml of 4% cysteine-sulfide (reducing agent) solution. Additionally, resazurin, a redox potential indicator was also added (0.1 ml of 0.1% solution) to indicate the presence of oxygen. Experiments were started with an initial pH of 6. The starting pH for the experiment conducted to assess the effect of producer gas on pH was 5.2. A pH of 5.2 was used to simulate the pH conditions present in the bioreactor before the introduction of producer gas.

### 4.3.3 Bioreactor operation

All the experiments were performed in a bubble column bioreactor as described in Chapter 3. The bioreactor was filled with 4.5 liters of sterile media and maintained under liquid batch conditions for initiating cell growth. Before shifting to a continuous mode, a 5-gallon glass tank was used to prepare anoxic and sterile liquid media. One tank was used during the entire experiment and the liquid media source was not changed during the course of the entire run. The startup and experimental run were similar to that described in section 3.3.5 of Chapter 3.

The composition of producer gas (made by mixing bottled gas) for the study with oxygen was N<sub>2</sub> (61.7%), CO (18%), CO<sub>2</sub> (15.5%) and H<sub>2</sub> (4.8%). O<sub>2</sub>, in the form of air (Air-Gas Co., Tulsa, OK), was mixed with the above gases using a mass flow meter (Porter Instruments, PA). Pure O<sub>2</sub> was not used because of safety concerns and operational limitation of the mass flow meter for O<sub>2</sub> concentrations required for the experiment. The composition of O<sub>2</sub> was chosen to represent the measured concentration found in the producer gas storage tank that was analyzed before the start of the experiment (to mimic the O<sub>2</sub> contribution to previous biomass-generated producer gas experiments). However, O<sub>2</sub> was not always detected in biomass-generated producer gas and thus would not always be a problem. The concentration of O<sub>2</sub> introduced was 1000 ppm or 1900 ppm. The O<sub>2</sub> concentration observed in the actual producer varied from 1000-1500 ppm. Similarly, the composition of “clean” bottled gas used for the CH<sub>4</sub> experiment was (prior to mixing) N<sub>2</sub> (65.1%), CO (14.6%), CO<sub>2</sub> (16.5%) and H<sub>2</sub> (3.8%). CH<sub>4</sub> was introduced using a mass flow meter to obtain a final concentration of 4.5 vol%

(typical concentration in biomass-generated producer gas). When CH<sub>4</sub> was added, the flow rate of N<sub>2</sub> was reduced to maintain a constant inlet gas feed rate.

For the pH experiment, biomass-generated producer gas was introduced at 180 ccm into an anoxic and sterile fermentation broth without any P7 bacteria. The starting pH of the fermentation broth was initially adjusted to 5.2 by adding a 1 N NaOH solution.

The analytical methods used for measuring the cell OD, products (ethanol, butanol, butyrate and acetate) and gaseous substrate (CO, CO<sub>2</sub>, N<sub>2</sub>, H<sub>2</sub>, CH<sub>4</sub>, O<sub>2</sub>) are described in section 3.3.6 of Chapter 3.

## **4.4 Results**

### **4.4.1 Effect of O<sub>2</sub> on bioreactor performance**

#### **Cell concentration and pH**

Cells were grown under batch phase for a period of 8 days (Figure 4.1). After a lag phase of 4 days, the cells started growing. The cell concentration reached a steady value of 1.2 OD on Day 7. Continuous product withdrawal and fresh nutrient feed at 1.5 ml/min was started on Day 8. Following a temporary increase in cell OD, due to fresh media, the cell concentration stabilized at around 1.2 OD units. 1000 ppm of O<sub>2</sub> was introduced on Day 11.5 and continued for a period of two days. No effect on the cell concentration was observed after the introduction of O<sub>2</sub>. The concentration of O<sub>2</sub> was increased to 1900 ppm (1500 ppm was the maximum O<sub>2</sub> concentration observed in producer gas stored in the tanks) on Day 13.5 and continued until the experiment was

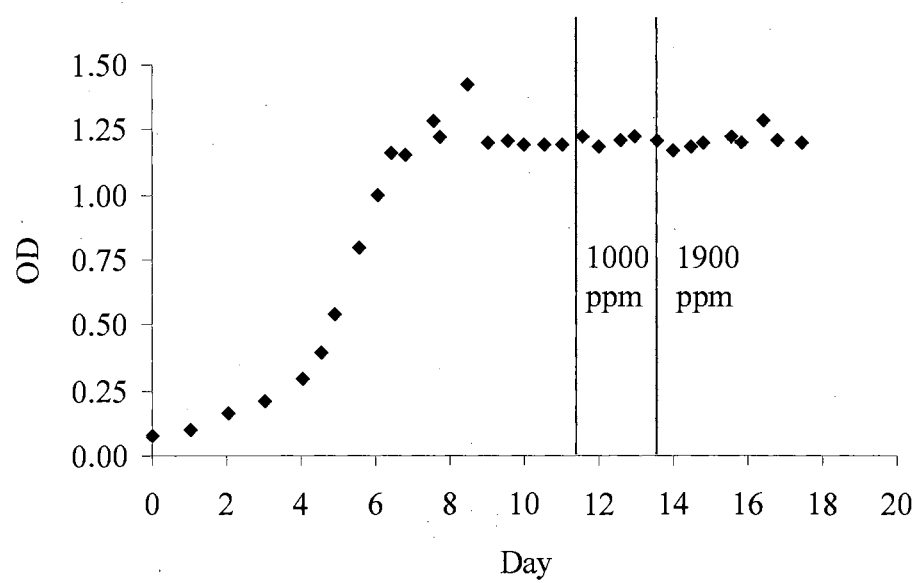


Figure 4.1. Cell OD profile at 1000 ppm and 1900 ppm O<sub>2</sub> concentrations

terminated. No detectable change in OD was observed even at the increased O<sub>2</sub> concentration and the OD remained steady at a value of 1.2 for four days, until Day 17.5. The experiment was terminated on Day 17.5.

The initial starting pH was 6 and was steadily lowered using a pH controller to 5.87 on Day 10. The pH was controlled at 5.87 from Day 10 until the end of the experiment (Figure 4.2). Previous studies have shown that cell growth and acetate formation are favored at a higher pH (between 5.8 to 6). Hence the pH was set at 5.87, to maximize cell OD and acetate formation, so that change (if any) in either, after introduction of O<sub>2</sub>, could be easily identified. The NaOH consumption profile during the experiment is shown in Figure 4.3. After the start of the continuous liquid mode on Day 8, about 137 ml/day of 1 N NaOH was required to maintain the pH in the bioreactor at the set point value of 5.87.

An additional experiment was conducted to mimic the addition of base (NaOH) and production of acids during the liquid batch phase. Fermentation media (composition was as described in section 4.3.2) was prepared (100 ml). Cysteine sulfide (0.5 ml) and resazurin (0.1 ml) were added to the media. The pH was adjusted to 6.0 by the addition of 1 ml, 1 N NaOH solution. NaOH was gradually added to this media. The total volume of NaOH added (11.1 ml) to the media was calculated based on the NaOH consumed in the 4.5-liter reactor. (500 ml of 1 N NaOH was consumed during the batch liquid phase). The final pH after the addition of NaOH was 11.8. Glacial acetic acid was then slowly added to the media until the pH of the media dropped down to 5.9. The total amount of acetic acid added was 0.6 ml, resulting in a final concentration of about 0.00933 moles/100 ml (calculated using a density of 1.05 g/L, total volume of 113.4 ml, and molecular weight

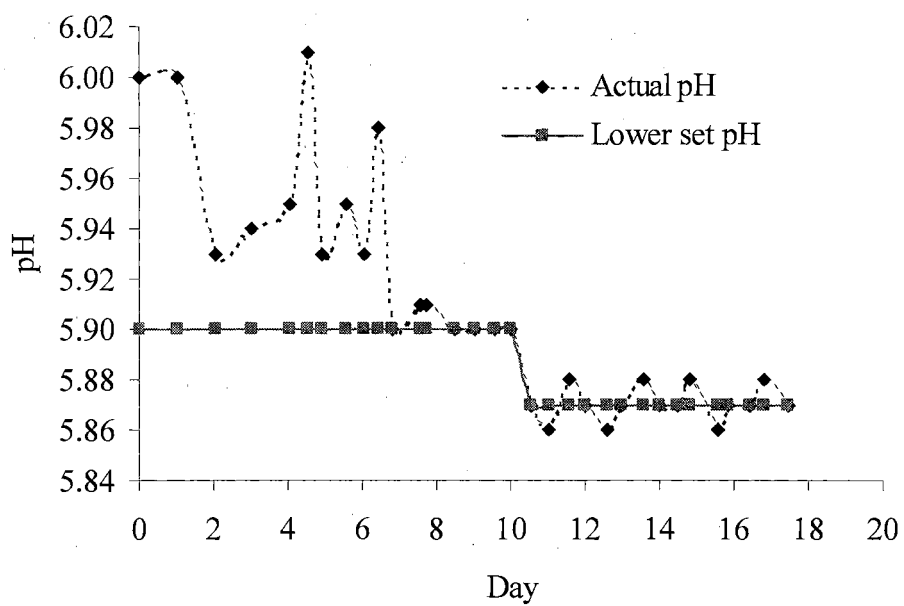


Figure 4.2. pH profiles for experiment with O<sub>2</sub> introduction  
 1000 ppm of O<sub>2</sub> was introduced on Day 11.5 and increased  
 to 1900 ppm on Day 13.5



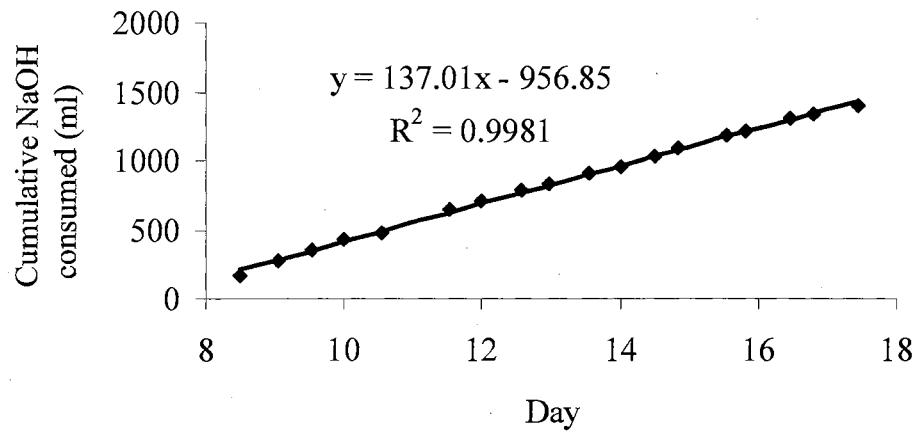
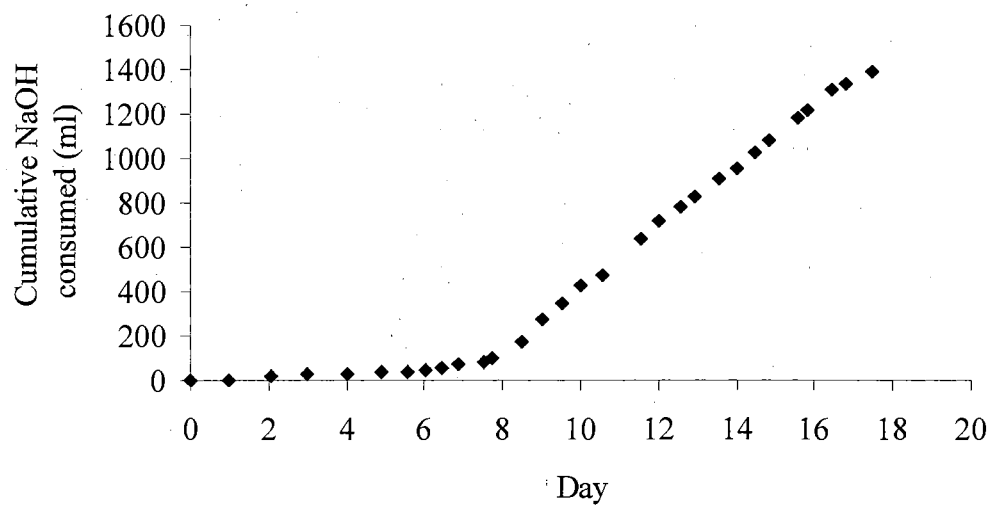


Figure 4.3. NaOH consumption profile for the experiment with O<sub>2</sub> introduction

of 60). The final concentrations of ethanol, butanol, acetate and butyrate in the batch phase were 0.08, 0.02, 0.3 and 0.03 wt%, respectively. Thus, the corresponding moles (per 100 ml) of ethanol, butanol, acetate and butyrate were about 0.0018, 0.00027, 0.005 and 0.00037 respectively. Hence, considering the stoichiometry for the conversion of acetate (1 mole acetate yields 1 mole ethanol, 2 moles acetate yield 1 mole butanol, and 2 moles acetate yield 1 mole butyrate), the total moles of acetate formed during the batch liquid phase were about 0.008 moles/100 ml. The observed value (of 0.008 moles/100 ml) is in close agreement with the calculated theoretical value (of 0.00933 moles/100ml). Also, the rise in pH during acetate consumption (details described in section 3.4.2 of Chapter 3) to 6.5 (higher than the initial pH of feed of 6) could be likely due to the extra NaOH solution added during the batch liquid phase.

### **CO and H<sub>2</sub> utilization**

A steady increase in CO utilization (shown in Figure 4.4) was observed with the increase in cell OD. The consumption of CO stabilized on Day 6. The inlet concentration of CO was around 18 vol%, while the steady state outlet concentration was about 10.5 vol%. Thus, the steady state CO utilization was about 41% of the feed CO. There was no significant change in the consumption of CO after the introduction of 1000 and 1900 ppm of O<sub>2</sub>. The experiment was terminated on Day 17.5.

No H<sub>2</sub> utilization was observed during the batch phase (Figure 4.5). The H<sub>2</sub> utilization increased following the change to continuous mode on Day 8 and stabilized on Day 10.5. The consumption of H<sub>2</sub> did not diminish after O<sub>2</sub> concentrations of

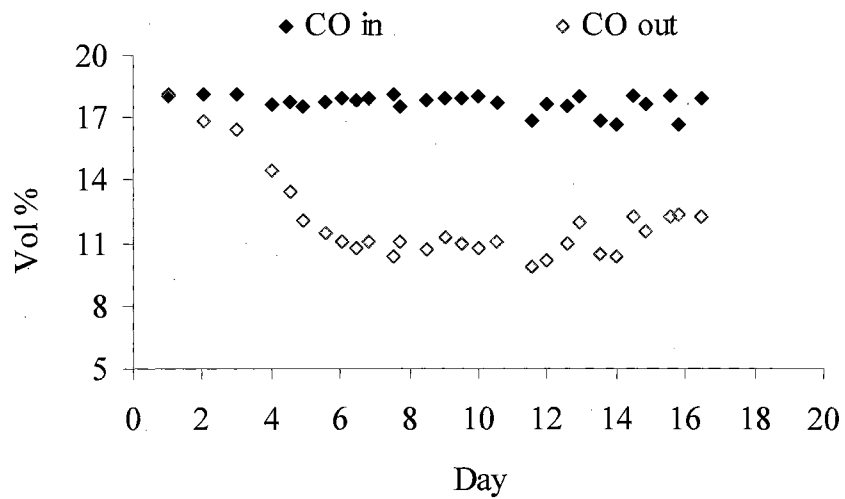


Figure 4.4. Inlet and outlet CO profiles for the experiment with O<sub>2</sub> introduction. 1000 ppm of O<sub>2</sub> was introduced on Day 11.5 and increased to 1900 ppm on Day 13.5.

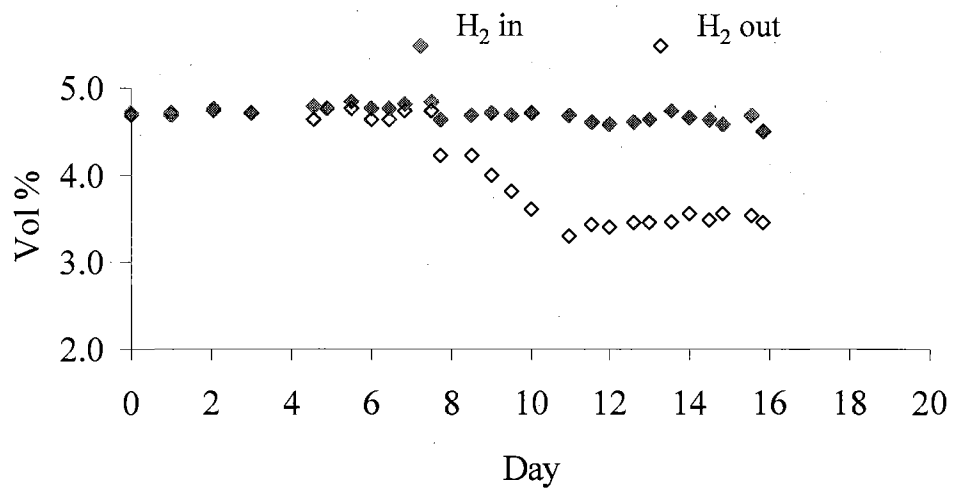


Figure 4.5. Inlet and outlet H<sub>2</sub> profiles for the experiment with O<sub>2</sub> introduction. 1000 ppm of O<sub>2</sub> was introduced on Day 11.5 and increased to 1900 ppm on Day 13.5.

1000 and 1900 ppm were introduced on Day 11.5 and Day 13.5, respectively. The inlet  $H_2$  concentration was maintained at about 4.8 vol% and the steady state  $H_2$  utilization was approximately 25% of the inlet  $H_2$ .

### **Product formation**

The inlet and outlet  $CO_2$  profiles, as shown in Figure 4.6, showed that the generation of  $CO_2$  also depended on the cell concentration in the bioreactor as expected. For an inlet concentration of about 15.6 vol%, the outlet concentration was steady at about 19.8 vol% from Day 5 to Day 17.5.

As shown in Figure 4.7, the ethanol and butanol concentration started to increase on Day 4. A rapid rise in the butanol concentration was observed beginning on Day 4 to a value of about 5 g/L on Day 8.5. During this period, the ethanol concentration went up to 0.8 g/L. Shortly after the change to continuous mode, the butanol concentration steadily decreased to 2.5 g/L on Day 10.5 and remained essentially unchanged even after the introduction of 1000 ppm of  $O_2$ . Similarly, a drop in ethanol concentration was observed after Day 8.5 to a concentration of about 0.5 g/L on Day 10. The ethanol concentration was steady at about 0.5 g/L from Day 10 to Day 13.5. However, the effect of  $O_2$  (1900 ppm) on the production of ethanol and butanol could not be assessed, since the liquid samples beyond Day 13.5 could not be analyzed.

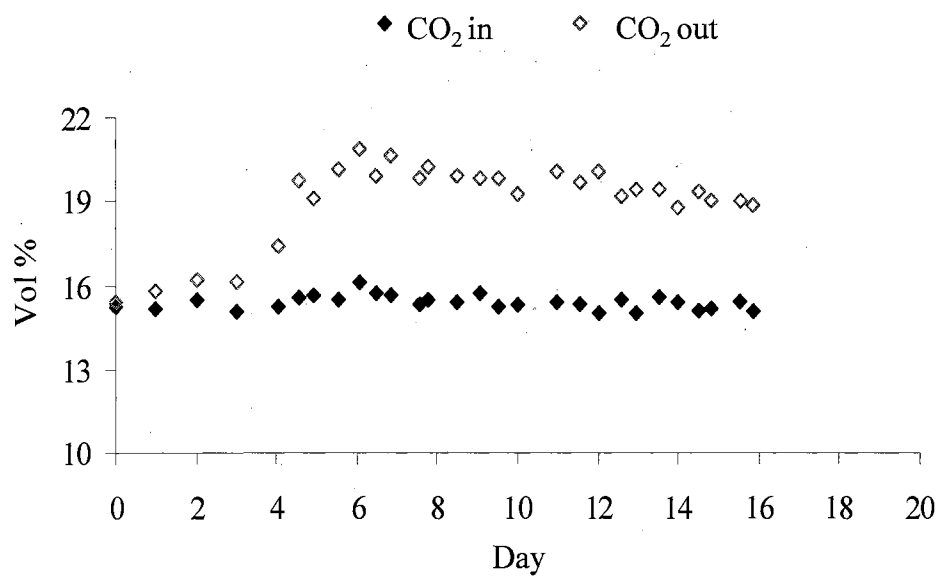


Figure 4.6. Inlet and outlet CO<sub>2</sub> profiles for the experiment with O<sub>2</sub> introduction. 1000 ppm of O<sub>2</sub> was introduced on Day 11.5 and increased to 1900 ppm on Day 13.5.

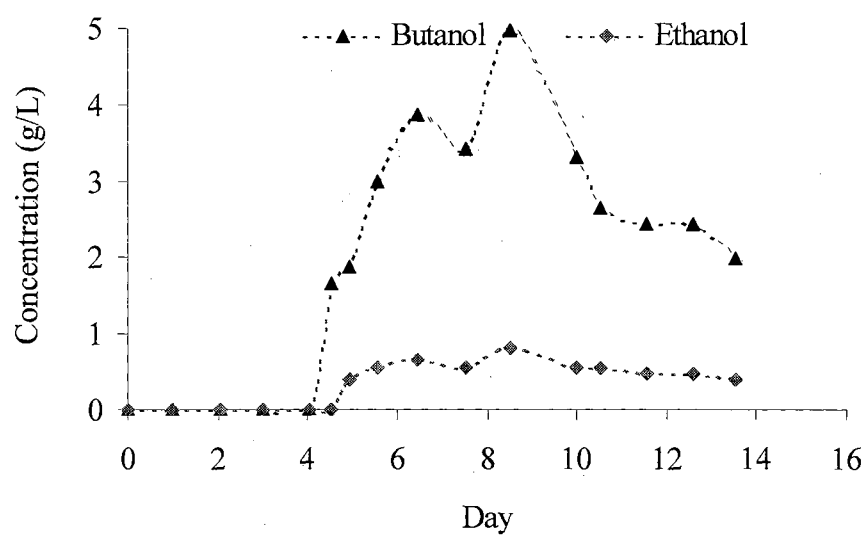


Figure 4.7. Ethanol and butanol profiles for the experiment with O<sub>2</sub> introduction.

1000 ppm of O<sub>2</sub> was introduced on Day 11.5 and increased to 1900 ppm on Day 13.5

#### 4.4.2 Effect of CH<sub>4</sub> on bioreactor performance

##### Cell concentration and pH

The reactor was operated with liquid in the batch mode until Day 8. As shown in Figure 4.8, cell growth was observed after an initial lag phase of 3.5 days. The cell OD started to level off on Day 7 to a value of 1.4 and remained steady until Day 11. After CH<sub>4</sub> was introduced on Day 11, the cell OD diminished slightly to a value of 1.1 and stayed constant until Day 14. The experiment was terminated on Day 14 since the liquid feed tank was exhausted.

The starting pH of the reactor was set at 5.94 and was controlled at a lower set point of 5.87 for the entire experiment. As seen in Figure 4.9, the pH increased to 6.7 on Day 2. The gas feed had stopped sometime between Day 1.5 and 2 due to a power failure. The rise in pH was observed due to the unintentional stoppage in the flow of CO<sub>2</sub>. The pH dropped instantly to 6.5 after gas flow was initiated and continued dropping steadily to a value of 5.87 on Day 5. The pH remained steady at 5.87 for the remainder of the experiment (Day 14). The amount of NaOH required to maintain the pH in the continuous mode (Day 8 to Day 14) was about 330 ml/day (shown in Figure 4.10). Although the optimal pH range of P7 for growth and product formation is between 5 and 6, the cells survived and recovered from a pH shock of 6.7. This demonstrates that P7 is an extremely robust organism, and is capable of tolerating process shocks that are likely in industrial bioreactors.



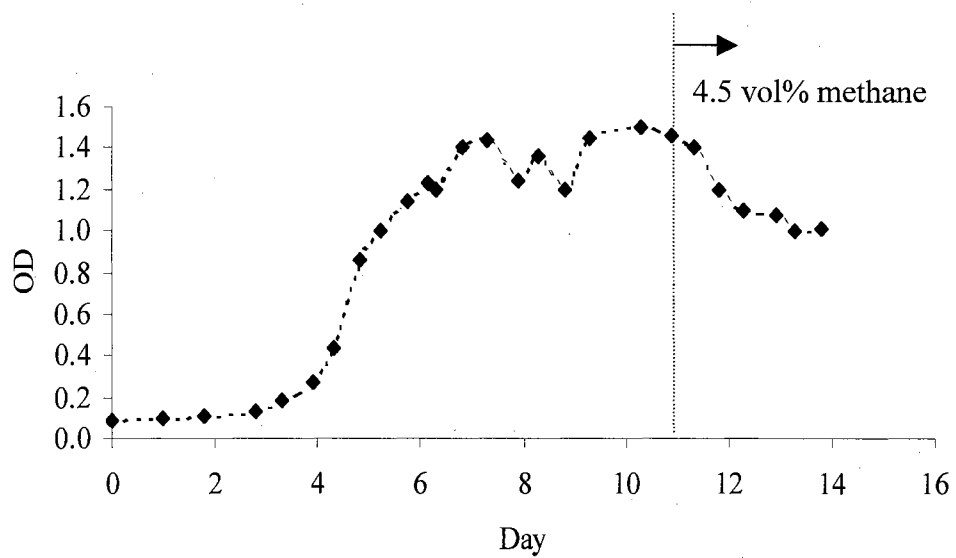


Figure 4.8. Cell OD profile for the experiment with  $\text{CH}_4$  introduction. 4.5 vol% of methane was introduced on Day 10.9

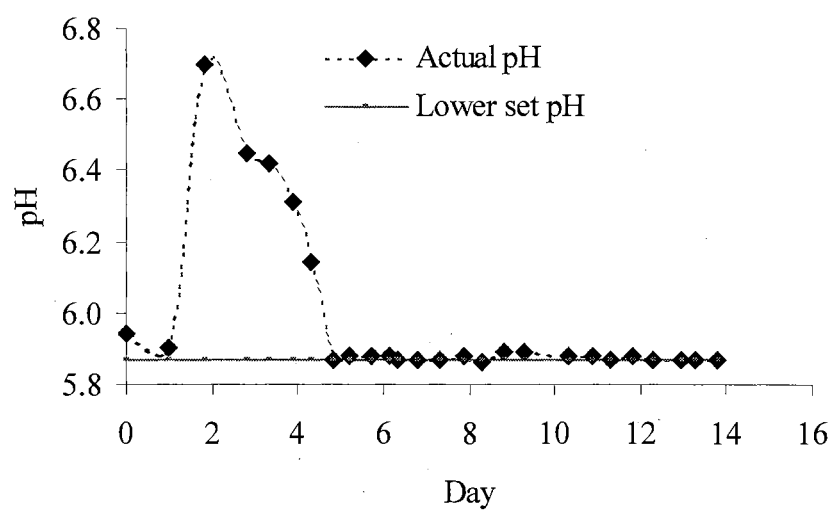


Figure 4.9. pH profile for the experiment with  $\text{CH}_4$   
4.5 vol% of methane was introduced on Day 10.9

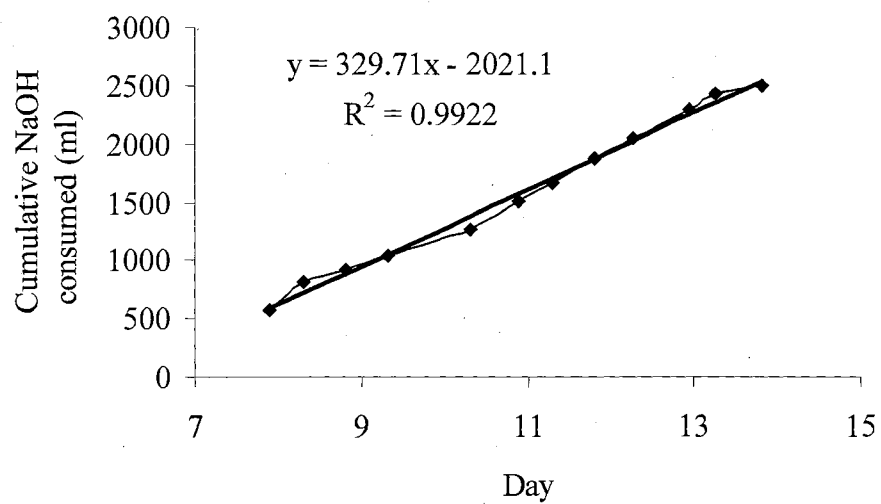
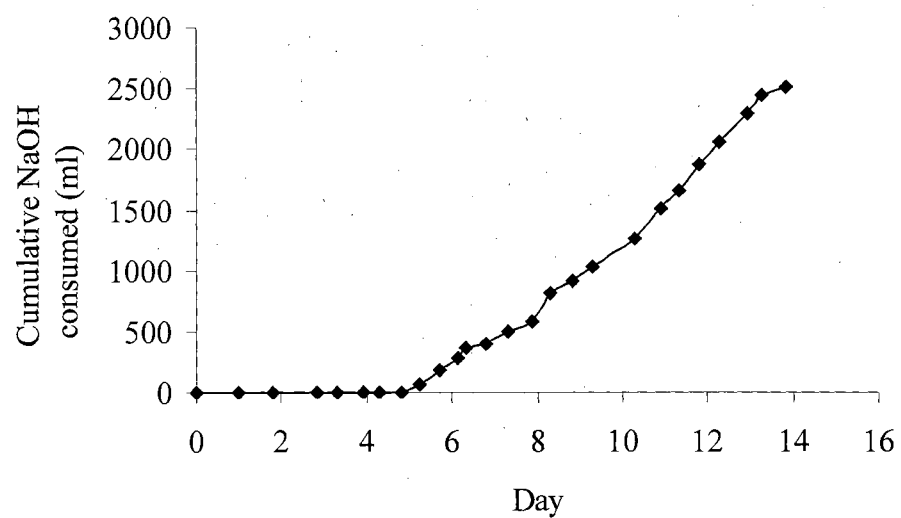


Figure 4.10. NaOH consumption profile for the experiment with CH<sub>4</sub>  
4.5 vol% of methane was introduced on Day 10.9

## **CO and H<sub>2</sub> utilization**

The utilization of CO increased steadily (with increase in cell OD) until Day 5 (shown in Figure 4.11). The steady state inlet and outlet concentrations were about 14.5 and 9 vol% respectively, corresponding to a 37% utilization of the feed CO. No significant changes in CO utilization were observed after CH<sub>4</sub> was introduced on Day 11.

As seen in Figure 4.12, negligible H<sub>2</sub> utilization was observed until Day 5. H<sub>2</sub> consumption increased steadily from Day 5 to Day 7.5 to approximately 30% of the feed H<sub>2</sub>. The H<sub>2</sub> consumption remained steady until Day 12, not long after the introduction of CH<sub>4</sub>. Eventually, the H<sub>2</sub> utilization dropped to about 20% of the feed H<sub>2</sub>.

## **Product formation**

The production of CO<sub>2</sub> (which is proportional to cell OD and CO utilization) increased gradually until Day 6 (shown in Figure 4.13) and remained constant for the remainder of the experiment. The steady state inlet and outlet CO<sub>2</sub> concentrations were about 16.5 and 20 vol%, respectively.

As shown in Figure 4.14, the concentrations of ethanol, butanol, butyrate and acetate increased in the batch mode to about 0.08, 0.02, 0.03, and 0.3 wt.% respectively on Day 8. After a drop in concentrations was observed following initiation of the continuous mode on Day 8, the ethanol, butanol, butyrate and acetate concentrations steadied on Day 9 and stayed constant until Day 14 at approximately 0.03, 0.015, 0.06, and 0.28 wt. % respectively. CH<sub>4</sub> did not seem to have any effect on the product formation.

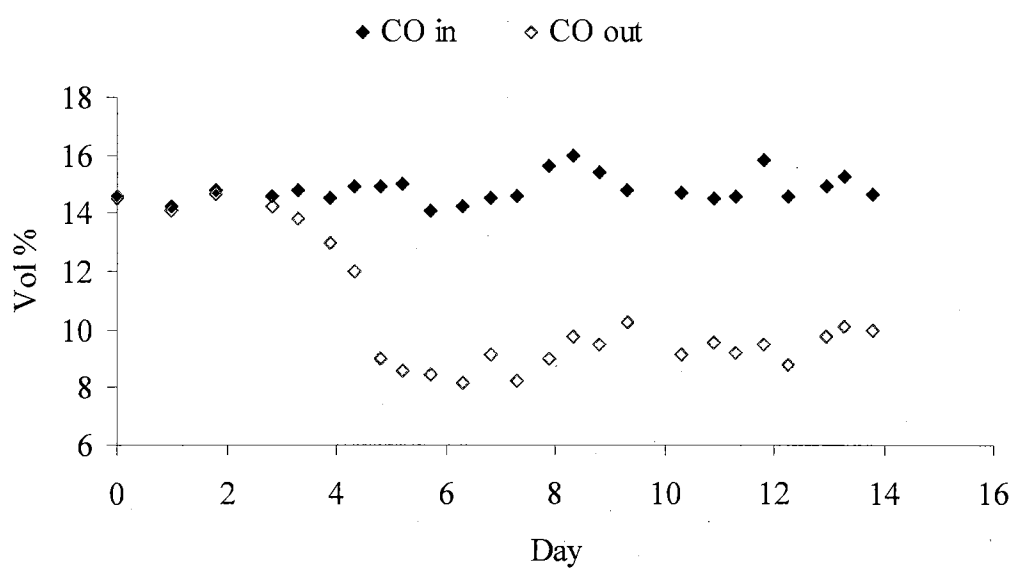


Figure 4.11. Inlet and outlet CO profiles for the experiment with  $\text{CH}_4$   
4.5 vol% of methane was introduced on Day 10.9

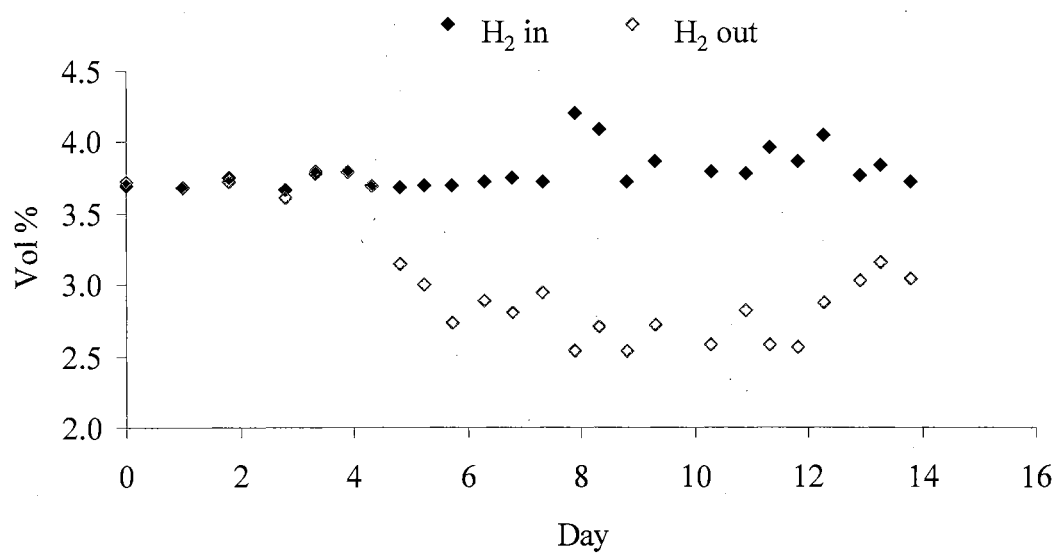


Figure 4.12. Inlet and outlet  $H_2$  profiles for the experiment with  $CH_4$   
4.5 vol% of methane was introduced on Day 10.9

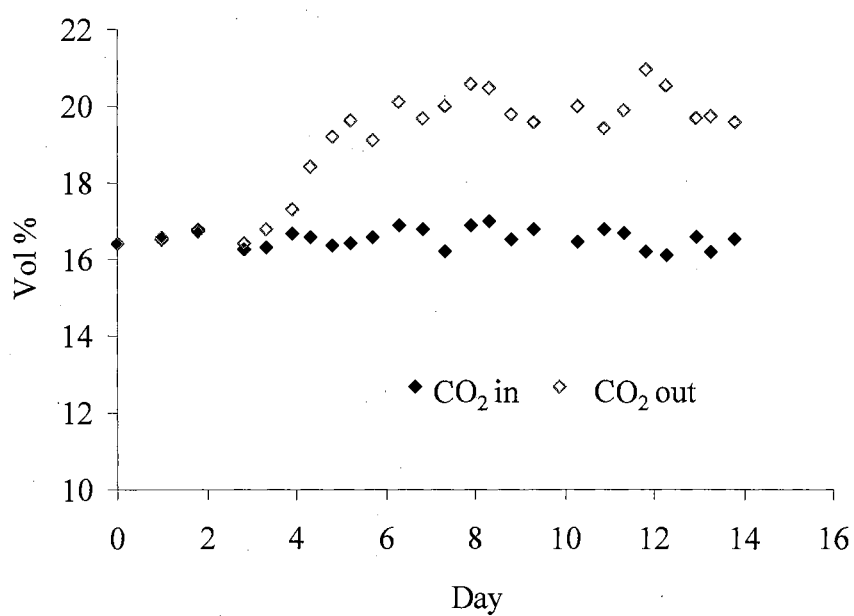


Figure 4.13. Inlet and outlet CO<sub>2</sub> profiles for the experiment with CH<sub>4</sub>  
4.5 vol% of methane was introduced on Day 10.9

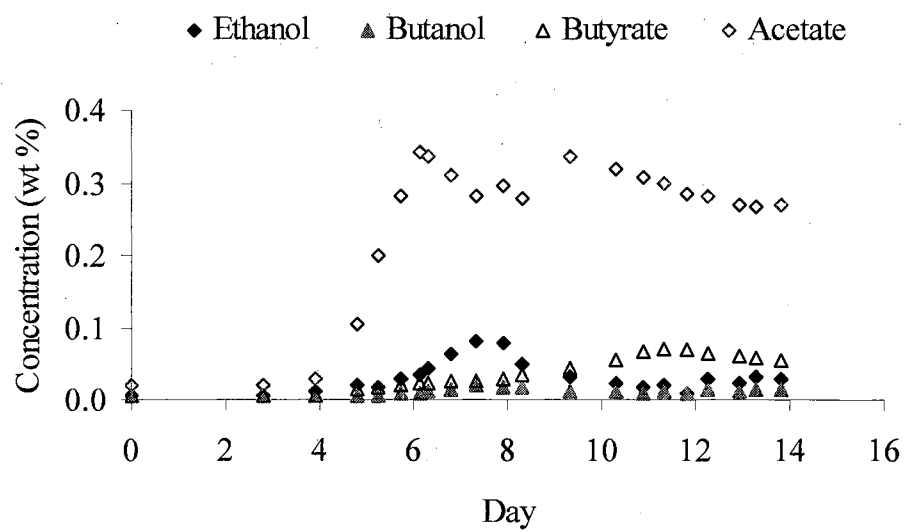


Figure 4.14. Product profiles for the experiment with CH<sub>4</sub>  
 4.5 vol% of methane was introduced on Day 10.9



#### **4.4.3 Effect of biomass-derived producer gas on pH of fermentation media**

The pH decreased from 5.21 to 5.13 after 1 day of producer gas was introduced into cell-free media, and then reached a steady value of 5.16 on Day 2 (shown in Figure 4.15). No further change in pH was observed for the remainder of the experiment.

### **4.5 Discussion**

#### **4.5.1 Effect of O<sub>2</sub> introduction**

It is evident from the cell OD profile described in section 4.4, that O<sub>2</sub> did not affect the cell OD at concentrations up to 1900 ppm. A constant cell OD during the continuous mode also indicated that the cells were active after the introduction of O<sub>2</sub> and continued to grow at a rate of 0.023 hr<sup>-1</sup> ( $\mu = D$  at steady state in the continuous mode). Here,  $\mu$  represents the net cell growth rate and  $D$  is the dilution rate (liquid feed rate/liquid volume).

Enzymes such as CODH and hydrogenase, which are responsible for the uptake of CO and H<sub>2</sub> are extremely sensitive to O<sub>2</sub>. A loss in enzyme activity can result in a drop in substrate utilization and even cell death. The utilization of CO and H<sub>2</sub> was unaffected after the introduction of O<sub>2</sub>, suggesting that CODH and hydrogenase found in clostridial P7 can tolerate O<sub>2</sub> up to 1900 ppm.

The diminished concentration of butanol and ethanol shortly after Day 8 was likely due to the washout of products during the continuous mode. The steady butanol and ethanol profiles shortly after the introduction of O<sub>2</sub> indicate that O<sub>2</sub> did not affect the rate of product formation and the ethanol to butanol ratio.

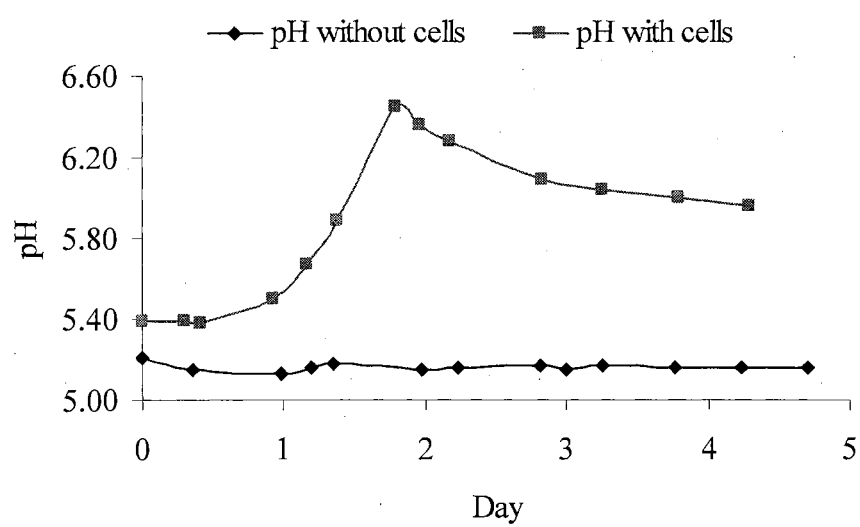


Figure 4.15. pH profiles following the introduction of producer gas on Day 0.

The pH was always controlled at 5.87 using a lower pH control. No rise in pH was observed after O<sub>2</sub> was introduced and the consumption of NaOH remained steady during the continuous liquid phase. This suggests that the cells produced acids at a constant rate (indicated by constant NaOH consumption) after exposure to O<sub>2</sub>.

#### 4.5.2 Effect of CH<sub>4</sub>

In previous studies on fermentation of CO, CO<sub>2</sub> and H<sub>2</sub> with *Peptostreptococcus productus*, CH<sub>4</sub> was used as an inert component for producer gas fermentations (Vega et al., 1989). The effects of CH<sub>4</sub> on fermentation of producer gas using P7 were not investigated earlier and hence were a part of this study. The cell OD diminished slightly after the introduction of CH<sub>4</sub>, but stabilized after a day. The cell OD remained constant during the continuous mode, indicating that the cells did not go in the dormant mode, but were active and growing for the entire period. Thus, CH<sub>4</sub> is not a toxic component of producer gas at the concentration studied in this study.

Also, no significant change in CO utilization following the introduction of CH<sub>4</sub>, was observed. This suggests that CH<sub>4</sub> (4.5 vol%) did not inhibit the enzyme CODH. However, the diminished H<sub>2</sub> utilization from Day 12 was likely due to a lower cell OD during this period. Acetate was the principal product during the entire course of the experiment and this explains the continuous consumption of NaOH to maintain the pH. Also, the steady acetate profile and constant NaOH consumption from Day 11 to 14 suggests that the rate of acetate formation remained unchanged after the introduction of CH<sub>4</sub> on Day 11. Also, the acetate to ethanol ratio was unaffected after the introduction of CH<sub>4</sub>.

### **4.5.3 Effect of producer gas on pH**

No change in pH was observed following producer gas introduction in the bioreactor containing bacteria-free (P7) fermentation broth, giving credence to the hypothesis that pH rise following introduction of producer gas was most likely due to the conversion of acetate to ethanol (see section 3.4.2 of Chapter 3) and not due to the dissolution of constituents of actual producer gas in the fermentation broth.

## **4.6 Conclusions**

The response of P7 to O<sub>2</sub> and CH<sub>4</sub> (impurities identified in actual producer gas) with regards to cell OD, pH, product formation, and CO and H<sub>2</sub> utilization has been experimentally investigated in this study.

O<sub>2</sub> and CH<sub>4</sub> (at concentrations identified in actual producer gas) had no or negligible effect on cell OD, pH, CO and H<sub>2</sub> utilization, and product formation. Thus, cell dormancy, rapid pH rise, and the rapid decrease in H<sub>2</sub> utilization, observed shortly after the introduction of biomass-generated producer gas into the bioreactor studies described in Chapter 3, were not a result of the introduction of O<sub>2</sub> or CH<sub>4</sub>. In addition, constituents of biomass-generated producer gas do not directly influence the pH of the fermentation broth in the bioreactor. However, further studies would need to be pursued to determine if CH<sub>4</sub> generates a media component (via metabolism by P7) that leads to cell dormancy initiated by exposure to producer gas.

## **CHAPTER 5**

### **MEDIA OPTIMIZATION**

#### **5.1 Introduction**

The productivity of a fermentation process can be increased by optimization of the nutritional and physical conditions to which the organism is exposed. The fermentation of producer gas to ethanol and other liquid products by P7 is a very complex process that currently involves about 30 different nutrients in the form of minerals, vitamins and metals. The level of nutrients present in the fermentation media significantly influences the bacterial growth and metabolic activities.

Development of a successful commercial fermentation process is significantly influenced by the culture medium used for cell growth. The formulation of the media should be such that the nutrients maximize the cell growth and yields of desired products at the lowest possible cost. Previous studies on producer gas fermentations using P7 (described in Chapters 3 and 4) have shown that the maximum cell concentration only increases to 1.5-1.7 OD. It is likely that the cell concentration can be increased further by optimization of the nutrients in the liquid media. The determination of optimal nutrient levels is a complex multivariable problem and requires initial screening of factors prior to a more rigorous analysis. In the present work, an initial screening of nutrients present in

the fermentation media (minerals, vitamins and trace metals) for P7 is discussed with regards to maximizing cell growth and minimizing nutrient cost.

Media optimization by the classical method (changing one independent variable while fixing the others at a certain level) or by the full factorial design (examining all possible combinations at appropriate levels) is feasible for only a small number of variables. Specific to fermentation of producer gas by P7, the process currently requires 30 different nutrients in the liquid phase for growth. Evaluation of the optimal concentration of each nutrient by a full factorial design at two levels would require  $2^{30}$  (1073741824) experimental trials. Although this seems almost impossible and extremely formidable, the optimization task can be reduced to practical levels by the use of appropriate statistical techniques.

An initial screening for a large number of factors can be performed by using the Plackett-Burman, fractional factorial, or the Taguchi designs (Schmidt and Launsby, 1994). Reportedly, Plackett-Burman and Taguchi designs require fewer experimental trials than the fractional factorial designs (Kalil et al., 2000, Idris et al., 2002, Houngh et al., 2003). A Taguchi  $L_{12}$  design is used, since it is best suited for optimization of factors ranging from 4 to 11.

## **5.2 Objectives of the study**

- Identify the specific nutrients that affect the cell concentration for conversion of synthetic (bottled gas mixture) producer gas using P7.
- Reduce/eliminate the nutrients that do not affect the cell OD and hence lower media cost.

## **5.3 Materials and Methods**

### **5.3.1 Biological catalyst**

The microorganism used in this study was initially provided by Dr. Ralph Tanner, University of Oklahoma, Norman. Although, the bacterium used for all experiments was the same, different inoculum was used to inoculate each set of experiments. Usually, the control bottle from the previous set of experiments was used as a source of inoculum for the following experiment.

### **5.3.2 Culture Media**

A defined media consisting of Pfennig's minerals, and vitamins, and trace metals was used to cultivate cells in the bottles. The compositions of each stock solution are described in section 3.3.4 of Chapter 3. Individual experiments described in this chapter were performed with different compositions of minerals, vitamins, and trace metals. The compositions used are mentioned in the respective studies. The control bottles in each experimental set contained (per liter), 15 ml of stock mineral solution, 10 ml of stock vitamin solution and 10 ml of stock trace metal solution. In addition to the minerals, vitamins, and trace metals, the media contained (per liter), 10 g MES (N-Morpholinoethane sulfonic acid), 1 g yeast extract, 5 ml of 4% cysteine-sulfide solution, and 0.1 ml of 0.1% resazurin solution.

### 5.3.3 Experimental layout and operation

All experimental trials were conducted in triplicates in 250-ml serum bottles (Wheaton, Millville, NJ), with a working liquid volume of 100 ml. The experimental design for the mineral optimization study is shown in Table 5.1. Although, only 300 ml (3 bottles of 100 ml each) was used for each trial run, 500 ml of media (to facilitate easy calculations) was prepared by adding 5 ml of stock vitamin solution, 5 ml of stock trace metal solution, 490 ml of DI water and appropriate quantities of each mineral nutrient. The final concentration of each mineral in the media is shown in Table 5.2. After mixing the minerals, vitamins and trace metals, 200 ml of media was discarded, and MES, yeast and resazurin were added to the remaining 300 ml.

The pH was measured by an Oakton (pH 10 series) meter and an Accumet<sup>®</sup> electrode (both from Cole Parmer, Vernon Hills, IL) and adjusted to 6 by adding a 50% NaOH solution. The media was equally divided into 3 bottles. The bottles were transferred to a 3.1 kW thermolyne hot plate (Barnstead International, Dubuque, IA) and the solution was boiled. After the solution in each bottle started to boil, N<sub>2</sub> gas was introduced in each bottle through a 22-gauge, six-inch long needle (Popper and Sons Inc., New Hyde park, NY). A needle was also inserted to allow N<sub>2</sub> to exit the bottle. The N<sub>2</sub> (Air-Gas CO., Tulsa, OK) flow was controlled using a rotameter (Cole Parmer, Vernon Hills, IL). Each bottle was boiled and purged simultaneously for 3 minutes to deoxygenate the media and sealed with a butyl rubber stopper (Size 1). Additionally the bottles were crimped using a 30-mm aluminum seal (Wheaton, Millville, NJ).

After each bottle was sealed and crimped, all the bottles were steam autoclaved at 121 °C for 30 minutes. Following sterilization, the bottles were allowed to cool to room



<b>Factor</b>	<b>A</b>	<b>B</b>	<b>C</b>	<b>D</b>	<b>E</b>	<b>F</b>
<b>Trial #</b>						
<b>1</b>	-1	-1	-1	-1	-1	-1
<b>2</b>	-1	-1	-1	-1	-1	1
<b>3</b>	-1	-1	1	1	1	-1
<b>4</b>	-1	1	-1	1	1	-1
<b>5</b>	-1	1	1	-1	1	1
<b>6</b>	-1	1	1	1	-1	1
<b>7</b>	1	-1	1	1	-1	-1
<b>8</b>	1	-1	1	-1	1	1
<b>9</b>	1	-1	-1	1	1	1
<b>10</b>	1	1	1	-1	-1	-1
<b>11</b>	1	1	-1	1	-1	1
<b>12</b>	1	1	-1	-1	1	-1

Table 5.1. Taguchi L<sub>12</sub> design for optimization of minerals. Factors A through F and associated concentrations are indicated in Table 5.2

<b>Factor</b>	<b>Nutrient (Minerals)</b>	<b>Level (-1)</b>	<b>Level (1)</b>
A	Sodium chloride	0.3 g/L	1.2 g/L
B	Ammonium chloride	0.6 g/L	1.5 g/L
C	Potassium chloride	0.06 g/L	0.15 g/L
D	Potassium monophosphate	0.06 g/L	0.15 g/L
E	Magnesium sulfate	0.12 g/L	0.3 g/L
F	Calcium chloride	0.03 g/L	0.06 g/L

Table 5.2. Factors and levels selected for various minerals.

The amounts denote the final concentration of each nutrient in the media. Level (1) is half the original composition used in

Chapter 3

temperature. A specially designed gassing manifold (shown in Figure 5.1) was used to pressurize the bottles. The needle (with all valves open) was inserted into the bottle to pressurize each bottle. The bottles were then pressurized to a positive (slightly above atmospheric) pressure (usually the pressure in each bottle after sterilization was about – 10 psig) with N<sub>2</sub>. The pressure inside each bottle was monitored by the pressure gauge. Each bottle was then purged for 2 minutes with N<sub>2</sub> (another needle was inserted into the bottle to serve as a gas outlet). After the bottles were purged with N<sub>2</sub>, both (inlet and outlet) needles were pulled out from the bottle (the outlet needle was pulled out first). 0.5 ml of 4% cysteine-sulfide was added to each bottle and then the bottles were pressurized with an 80/20, CO/CO<sub>2</sub> gas mixture (Aeriform, Pasadena, TX) to 10 psig in a fume hood, (Model # H05, Kewanunee Scientific Corporation, Statesville, NC) to avoid exposure to CO. During pressurization with the CO/CO<sub>2</sub> mixture, the needle (with all valves open and gas flowing) was inserted into the bottle. The needle (with gas flowing) was withdrawn from the bottle when the pressure inside the bottle reached 10 psig. All the bottles were then transferred to a warm room maintained at 37 °C. Following one day after sterilization and prior to inoculation, the bottles were checked for contamination by a visual inspection, i.e. liquid should be clear and not turbid. The bottles were then inoculated with 1 ml of inoculum using sterile 1-ml luer-lok syringes under sterile and anoxic conditions. A microscope (Nikon Eclipse, Model # TE2000-U) with an attached camera (Hamamatsu, Model # ORCA-ER) was also used occasionally to inspect the solution. The bottles were then transferred to a shaker (Barnstead Lab-Line, Melrose Park, IL) rotating at 100 rpm. The shaker was used for uniform mixing of liquid and gas transfer enhancement. During the first experimental set, 3 ml of inoculum was withdrawn

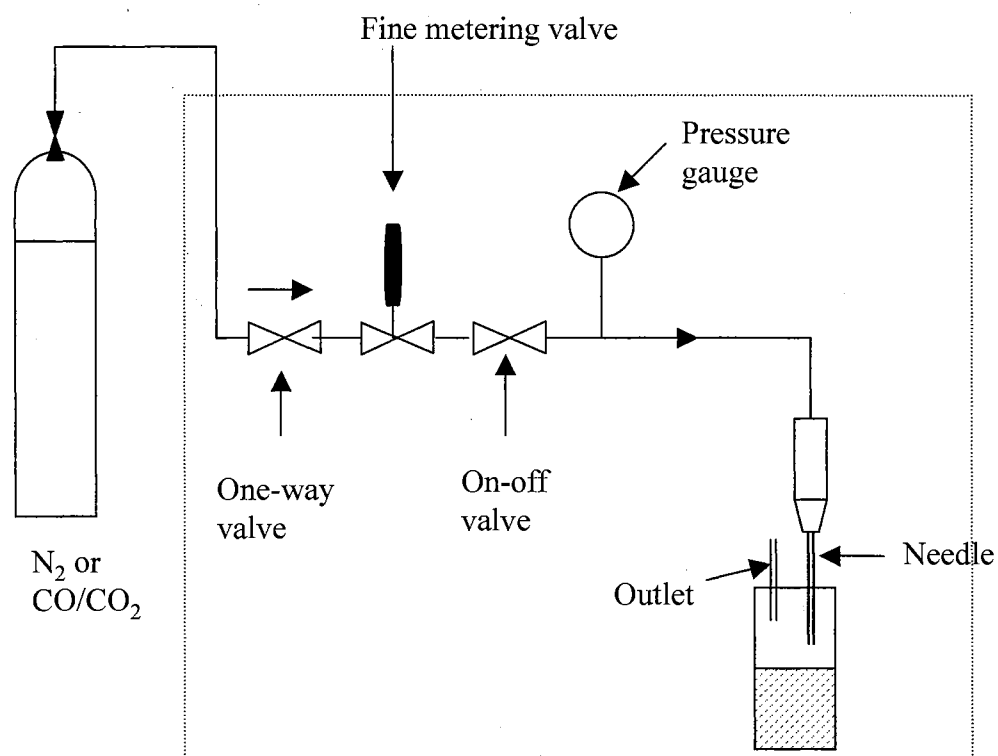


Figure 5.1. Design of gassing manifold

from the inoculum bottle to inoculate the 3 bottles (each bottle with 1 ml). Better repeatability between the triplicates was observed when each bottle was inoculated with 1 ml of inoculum withdrawn each time rather than withdrawing 3 ml and portioning the inoculum into each of the bottles. The schematic for the experimental set-up is shown in Figure 5.2. The bottles were pressurized to 10 psig (with CO/CO<sub>2</sub>) every two days following inoculation to avoid substrate (CO/CO<sub>2</sub>) limitation.

A similar protocol was followed for optimization of the vitamins and trace metals. The experimental design for the vitamin optimization is shown in Table 5.3. The final concentration of each vitamin in the media is shown in Table 5.4. The amounts of stock mineral and trace metals solutions were (per liter), 15 ml and 10 ml, respectively. Similarly, the experimental design for trace metal optimization is shown in Table 5.5. The final concentration of each trace metal in the media is shown in Table 5.6. The amounts of stock mineral and vitamin solutions were (per liter), 15 ml and 10 ml, respectively. For the experiments without d-biotin and/or vitamin B<sub>12</sub>, a separate vitamin stock solution was prepared without these two components. Each of these two components was added individually as per the design of the specific experiment. The amount of minerals and trace metals were (per liter) 15 and 10 ml, respectively.

A control run was selected for each experimental set to account for variations during different trials. The control run should give similar results for all sets and provides a good measure of the process variations during different experimental sets. Each set of experiments lasted 7-10 days following inoculation.

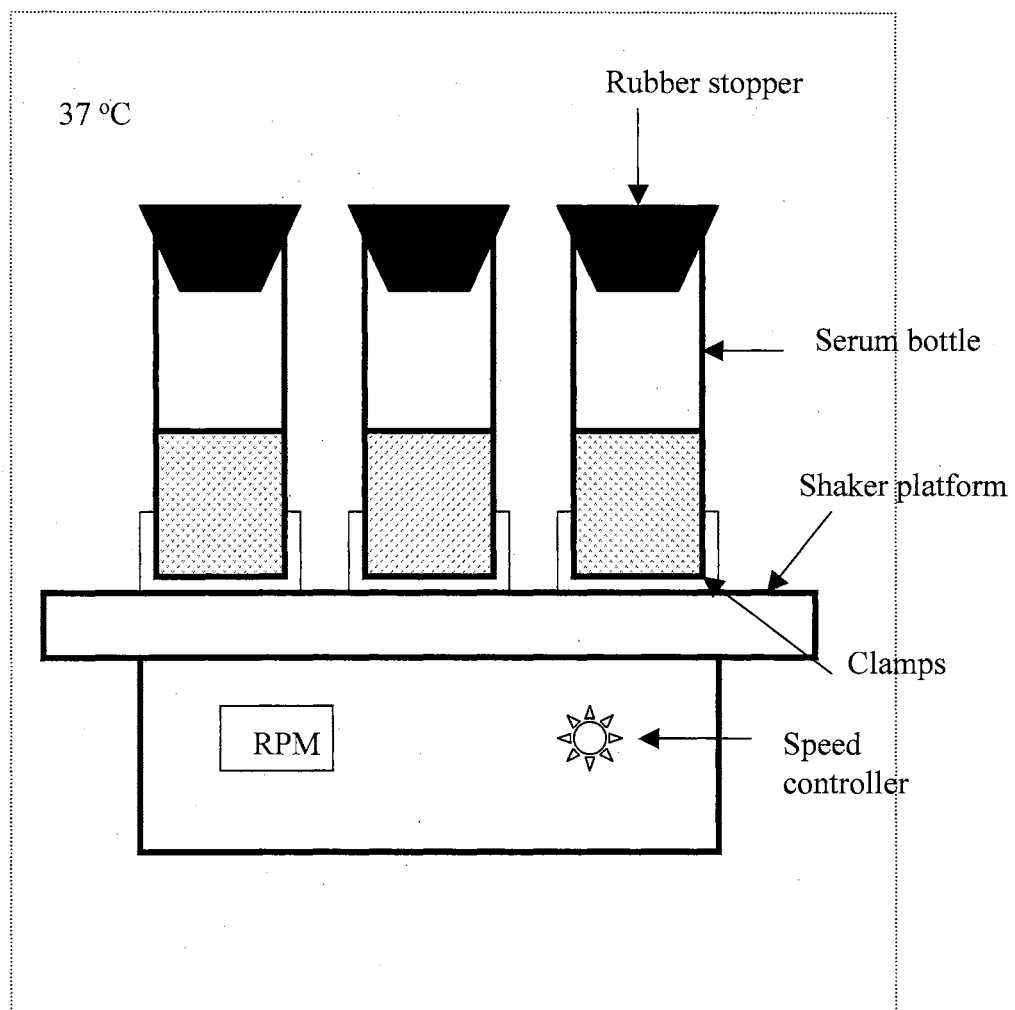


Figure 5.2. Experimental layout for nutrient optimization

Factor	A	B	C	D	E	F	G	H	I	J	K
Trial #											
1	-1	-1	-1	-1	-1	-1	-1	-1	-1	-1	-1
2	-1	-1	-1	-1	-1	1	1	1	1	1	1
3	-1	-1	1	1	1	-1	-1	-1	1	1	1
4	-1	1	-1	1	1	-1	1	1	-1	-1	1
5	-1	1	1	-1	1	1	-1	1	-1	1	-1
6	-1	1	1	1	-1	1	1	-1	1	-1	-1
7	1	-1	1	1	-1	-1	1	1	-1	1	-1
8	1	-1	1	-1	1	1	1	-1	-1	-1	1
9	1	-1	-1	1	1	1	-1	1	1	-1	-1
10	1	1	1	-1	-1	-1	-1	1	1	-1	1
11	1	1	-1	1	-1	1	-1	-1	-1	1	1
12	1	1	-1	-1	1	-1	1	-1	1	1	-1

Table 5.3. Taguchi L<sub>12</sub> design for optimization of vitamins. Factors A through K and associated concentrations are indicated in Table 5.4

Factor	Nutrient (Vitamins)	Level (-1)	Level (1)
A	Pyridoxine	0.05 mg/L	0.1 mg/L
B	Thiamine	0.025 mg/L	0.05 mg/L
C	Riboflavin	0.025 mg/L	0.05 mg/L
D	Calcium pantothenate	0.025 mg/L	0.05 mg/L
E	Thioctic acid	0.025 mg/L	0.05 mg/L
F	Amino benzoic acid	0.025 mg/L	0.05 mg/L
G	Nicotinic acid	0.025 mg/L	0.05 mg/L
H	Vitamin B <sub>12</sub>	0 mg/L	0.025 mg/L
I	d-Biotin	0 mg/L	0.01 mg/L
J	Folic acid	0.01 mg/L	0.02 mg/L
K	Mercaptoethanesulfonic acid (MESNA)	0.05 mg/L	0.1 mg/L

Table 5.4. Factors and levels selected for various vitamins.

The amounts denote the final concentration of each nutrient in the media. Level (1) is the original composition used in Chapter 3



Factor	A	B	C	D	E	F	G	H	I	J
Trial #										
1	-1	-1	-1	-1	-1	-1	-1	-1	-1	-1
2	-1	-1	-1	-1	-1	1	1	1	1	1
3	-1	-1	1	1	1	-1	-1	-1	1	1
4	-1	1	-1	1	1	-1	1	1	-1	-1
5	-1	1	1	-1	1	1	-1	1	-1	1
6	-1	1	1	1	-1	1	1	-1	1	-1
7	1	-1	1	1	-1	-1	1	1	-1	1
8	1	-1	1	-1	1	1	1	-1	-1	-1
9	1	-1	-1	1	1	1	-1	1	1	-1
10	1	1	1	-1	-1	-1	-1	1	1	-1
11	1	1	-1	1	-1	1	-1	-1	-1	1
12	1	1	-1	-1	1	-1	1	-1	1	1

Table 5.5. Taguchi L<sub>12</sub> design for optimization of trace metals. Factors A through J and associated concentrations are indicated in Table 5.6.

Factor	Nutrient (Trace metals)	Level (-1)	Level (1)
A	Nitrilotriacetic acid	10 mg/L	20 mg/L
B	Manganese sulfate	5 mg/L	1 mg/L
C	Ferrous ammonium sulfate	4 mg/L	8 mg/L
D	Cobalt chloride	1 mg/L	2 mg/L
E	Zinc sulfate	1 mg/L	2 mg/L
F	Cupric chloride	0.1 mg/L	0.2 mg/L
G	Nickel chloride	0.1 mg/L	0.2 mg/L
H	Sodium molybdate	0.1 mg/L	0.2 mg/L
I	Sodium selenate	0.1 mg/L	0.2 mg/L
J	Sodium tungstate	0.1 mg/L	0.2 mg/L

Table 5.6. Factors and levels selected for various trace metals.

The amounts denote the final concentration of each nutrient in the media. Level (1) is the original composition used in Chapter 3

### 5.3.4 Analytical procedures

*Cell concentration and pH:* The bottles were sampled for cell OD and pH every 1-2 days. Samples (about 1.5 ml) were withdrawn from each bottle using sterile 3-ml luer-lok syringes and needles (20 gauge, 1.5 inch) and collected in 2-ml centrifuge tubes. Precautionary measures were employed to avoid contamination of the bottles. 1 ml of the fermentation broth was transferred to a 2 ml cuvette using a digital micropipette (Model 5000 DG, Nichiryo Corporation, Tokyo, Japan). The pH of the sample (in the centrifuge tube) was measured. The cell OD was measured using a UV-visible spectrophotometer (UV-1601, Shimadzu Corporation, Japan). Each cuvette was gently tapped before OD measurement to avoid erratic results due to bubble formation. The spectrophotometer was blanked against DI water before measurement of cell OD. DI water was substituted for fresh liquid media (without cells) since the OD value of fresh liquid media (when blanked against DI water) was only about 0.02-0.03 (in OD units). Also, preparation of fresh liquid media during each sampling was impractical because of the time constraints.

### 5.3.5 Experimental design

The optimization of minerals (6 factors), vitamins (11 factors), and trace metals (10 factors) was based on the standard Taguchi  $L_{12}$  design (Schmidt and Launsby, 1994). The Taguchi  $L_{12}$  design is a fraction of the two-factorial design, allowing screening of up to  $N-1$  factors from  $N$  experimental trials. The variables were investigated at two different concentration levels, upper level (indicated by 1) and lower level (indicated by -1). The concentration range for each variable was chosen based on the original media composition for cell culture. A level of +1 indicates the concentration of each nutrient in

the stock solution of the original media recipe before optimization. However, for the mineral optimization study, a level of +1 denotes the halved concentration (as compared to the original recipe) of each nutrient in the stock solution. Each experimental trial was performed in triplicate, and three responses Y1, Y2, and Y3, represent the cell concentration (OD units) for each of the three bottles, respectively. Multiple regression analysis was performed on the data set using the software, DOE-KISS (Design of Experiments-Keep it Statistically Simple).

## **5.4 Results**

### **5.4.1 Mineral optimization**

A preliminary mineral optimization study was initially conducted in which the concentration of all the minerals was half of the original composition. The average final cell OD values after seven days and the cell OD profile for the preliminary mineral optimization experiment are shown in Figure 5.3. As shown in Figure 5.3, no significant change in cell OD was observed after the reduction. Hence, for future optimization mineral optimization studies, the reduced amount was selected as the upper higher limit for each individual mineral.

The cell OD for all the experimental trials using the Taguchi L<sub>12</sub> design for mineral optimization is shown in Table 5.7. Y1, Y2, and Y3 indicate the final cell OD for the same experimental trial after a period of eight days. The average cell OD for all 12 trials for mineral optimization is shown in Figure 5.4. Results from the first regression analysis

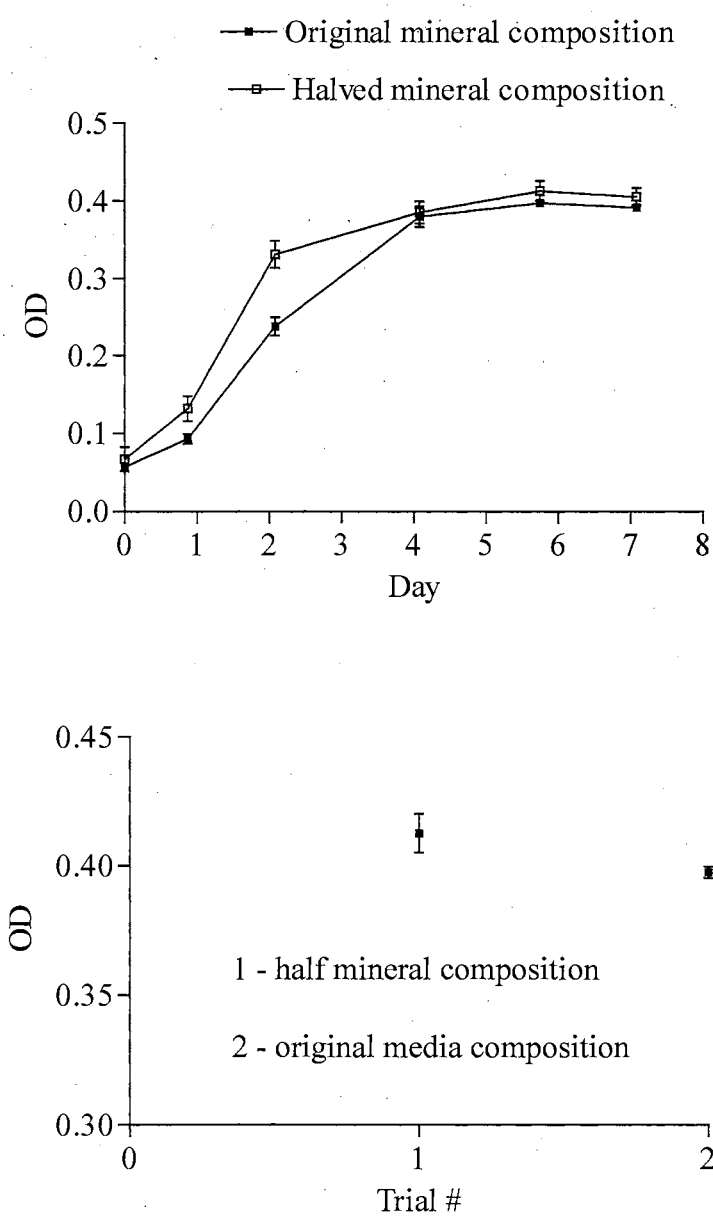


Figure 5.3. Cell OD profile and final cell OD for preliminary mineral optimization. Each data point is the average of 3 points and denotes the OD value after a period of 7 days

<b>Trial #</b>	<b>Y1</b>	<b>Y2</b>	<b>Y3</b>	<b>Average Y</b>	<b>Std. Dev.</b>
<b>1</b>	0.446	0.432	0.366	0.415	0.043
<b>2</b>	0.53	0.446	0.42	0.465	0.057
<b>3</b>	0.504	0.416	0.4	0.440	0.056
<b>4</b>	0.465	0.441	0.453	0.453	0.012
<b>5</b>	0.387	0.378	0.405	0.390	0.014
<b>6</b>	0.08	0.09	0.085	0.085	0.005
<b>7</b>	0.415	0.405	0.405	0.408	0.006
<b>8</b>	0.435	0.405	0.441	0.427	0.019
<b>9</b>	0.39	0.388	0.422	0.400	0.019
<b>10</b>	0.107	0.1	0.12	0.109	0.010
<b>11</b>	0.156	0.11	0.142	0.136	0.024
<b>12</b>	0.389	0.414	0.4	0.401	0.013

Table 5.7. Cell concentrations (OD) for different mineral compositions.

Y1, Y2 and Y3 are the triplicate responses for cell concentration (OD) for the same mineral composition after 8 days.

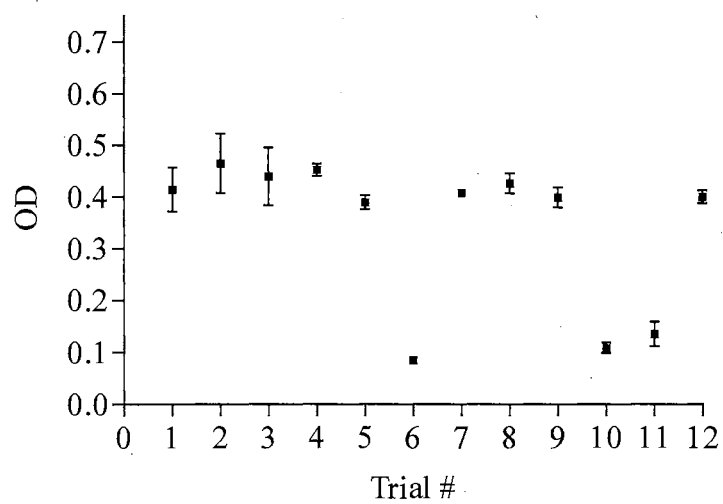


Figure 5.4. Average OD and standard deviation plot for mineral optimization. Each data point is the average of 3 points and denotes the OD value after a period of 8 days

					Active
Factor		Coeff	P (2 Tail)	Tol	
Constant		0.34411	<b>0.0000</b>		
A		-0.03056	<b>0.0121</b>	1	X
B		-0.08178	<b>0.0000</b>	1	X
C		-0.03422	<b>0.0055</b>	1	X
D		-0.02372	<b>0.0467</b>	1	X
E		0.07439	<b>0.0000</b>	1	X
F		-0.02689	<b>0.0255</b>	1	X
Rsq            0.8050 Adj Rsq       0.7647 Std Error     0.0685 F               19.9555 Sig F           0.0000					
<b>Source</b>	<b>SS</b>	<b>df</b>	<b>MS</b>		
<b>Regression</b>	0.6	6	0.1		
<b>Error</b>	0.1	29	0.0		
<b>Total</b>	0.7	35			

Table 5.8. Y-hat model from first regression for mineral optimization



are shown in Table 5.8. The “p (2 Tail)” column in the table represents the probability of placing an insignificant factor in the model described below. According to the rule of thumb, a factor is significant and should be included in the model if the p (2 Tail) for the factor is less than 0.05 (Schimdt and Launsby, 1994). If the p (2 Tail) lies between 0.05 and 0.1, the factor may or may not be included in the model depending on the type of experimental design. The p (2 Tail) is less than 0.1 for all the factors shown in Table 5.8, and hence all the factors are significant and are included in the model (indicated by X in the Active column). The tolerance (indicated by Tol in the regression table) is the proportion of orthogonality for each factor. Orthogonality means that the factor can be evaluated independently of other factors in the model. The tolerance value for each factor in the regression table is 1. The F-value for the model is 19.955. The absolute coefficients of each significant factor are shown in Figure 5.5 in the form of a Pareto chart. The lower the coefficient, the lower the effect the component has on the cell OD. Factor B has the highest coefficient (-0.0817), stating that B has a high effect on cell OD, followed by Factor E (coefficient is 0.074). Thus, from the regression table, the cell OD (Y) can be described by the linear model given below:

$$Y = 0.34411 - 0.03056 A - 0.08178 B - 0.03422 C - 0.02372 D + 0.07439 E - 0.02689 F \quad (\text{Eq. 5.1})$$

where Y is the cell concentration (in OD units), A is the concentration of sodium chloride, B is the concentration of ammonium chloride, C is the concentration of

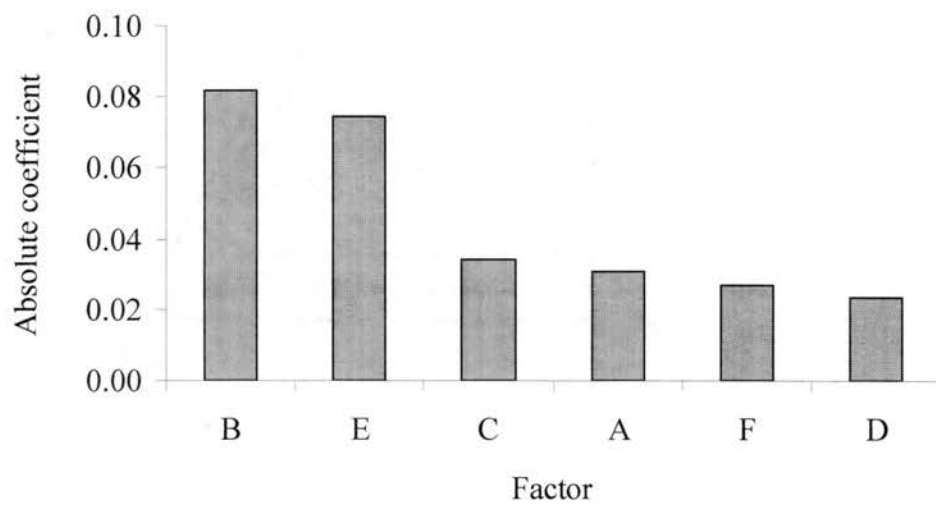


Figure 5.5 Y-hat pareto of coefficients for minerals

potassium chloride, D is the concentration of potassium monophosphate, E is the concentration of magnesium sulfate, and F is the concentration of calcium chloride. The concentration of each nutrient in the model is represented in coded values and varies between  $-1$  (minimum concentration) to  $+1$  (maximum concentration). See Table 5.2 for the final concentration of each mineral corresponding to a coded value of  $-1$  and  $+1$ . The predictions for cell OD, using the model described by Eq. 5.1, are compared to the actual observations and the residuals (difference between the observed value and predicted value) were determined (Table 5.9 and Figure 5.6). The marginal means plot for each factor is shown in Figure 5.7. The marginal means plot shows the variation in cell OD for each factor at the two concentration levels tested in the study. Factors B (ammonium chloride) and E (magnesium sulfate) affect the cell OD significantly at the lower and higher tested levels, while the other factors (A, C, D, F) had a negligible effect on the cell OD.

#### **5.4.2 Vitamin optimization**

The final cell OD (after a period of 8.5 days) values for the vitamin optimization experiments are as shown in Table 5.10 and Figure 5.8. Table 5.11, indicates the results obtained after the first regression analysis. As seen from the table, the  $p$  (2 Tail) values for Factors A and F were 0.0001 and 0.0314, respectively. All other factors had a  $p$  (2 Tail) of greater than 0.1. The  $F$ -value after the first regression was 2.60. The pareto chart denoting the absolute value of coefficients of all factors is shown in Figure 5.9. It is clear from the pareto chart that Factors A and F are the most dominant factors, while the effect of all other factors was almost negligible. Since, the  $p$  (2 Tail) of only two factors was

<b>Trial #</b>	<b>Response</b>	<b>Observed</b>	<b>Predicted</b>	<b>Residual</b>
<b>1</b>	Y1	0.446	0.4668	-0.0208
	Y2	0.432	0.4668	-0.0348
	Y3	0.366	0.4668	-0.1008
<b>2</b>	Y1	0.53	0.4131	0.1169
	Y2	0.446	0.4134	0.0326
	Y3	0.42	0.4134	0.0066
<b>3</b>	Y1	0.504	0.4998	0.0042
	Y2	0.416	0.4998	-0.0838
	Y3	0.4	0.4998	-0.0998
<b>4</b>	Y1	0.465	0.4047	0.0603
	Y2	0.441	0.4047	0.0363
	Y3	0.453	0.4047	0.0483
<b>5</b>	Y1	0.387	0.3299	0.0571
	Y2	0.378	0.3299	0.0481
	Y3	0.405	0.3299	0.0751
<b>6</b>	Y1	0.08	0.1337	-0.0537
	Y2	0.09	0.1337	-0.0437
	Y3	0.085	0.1337	-0.0487
<b>7</b>	Y1	0.415	0.2899	0.1251
	Y2	0.405	0.2899	0.1151
	Y3	0.405	0.2899	0.1151
<b>8</b>	Y1	0.435	0.4323	0.0027
	Y2	0.405	0.4323	-0.0273
	Y3	0.441	0.4323	0.0087
<b>9</b>	Y1	0.39	0.4533	-0.0633
	Y2	0.388	0.4533	-0.0653
	Y3	0.422	0.4533	-0.0313
<b>10</b>	Y1	0.107	0.1738	-0.0668
	Y2	0.1	0.1738	-0.0738
	Y3	0.12	0.1738	-0.0538
<b>11</b>	Y1	0.156	0.1410	0.0150
	Y2	0.11	0.1410	-0.0310
	Y3	0.142	0.1410	0.0010
<b>12</b>	Y1	0.389	0.3910	-0.0020
	Y2	0.414	0.3910	0.0230
	Y3	0.4	0.3910	0.0090

Table 5.9. Residuals using regression analysis for mineral optimization.

Experimentally observed values are compared to the predicted values

obtained from the linear model described by Eq. 5.1

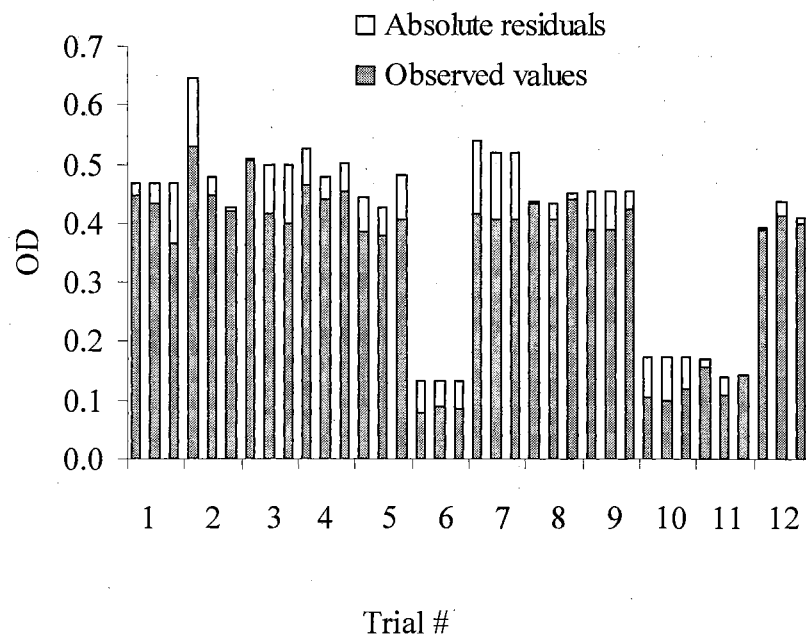


Figure 5.6. Observed cell concentrations (OD) and absolute residuals from regression analysis for minerals

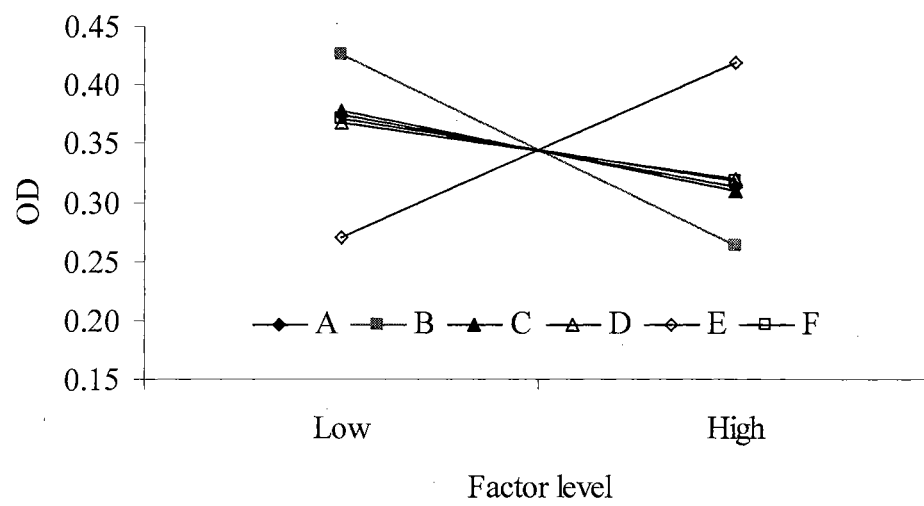


Figure 5.7. Y-hat marginal means plot for minerals

<b>Trial #</b>	<b>Y1</b>	<b>Y2</b>	<b>Y3</b>	<b>Average Y</b>	<b>Std. Dev</b>
<b>1</b>	0.423	0.39	0.405	0.406	0.0165
<b>2</b>	0.393	0.411	0.417	0.407	0.0125
<b>3</b>	0.393	0.387	0.39	0.390	0.0030
<b>4</b>	0.384	0.405	0.375	0.388	0.0154
<b>5</b>	0.396	0.417	0.402	0.405	0.0108
<b>6</b>	0.396	0.414	0.417	0.409	0.0114
<b>7</b>	0.344	0.37	0.25	0.321	0.0631
<b>8</b>	0.288	0.396	0.406	0.363	0.0654
<b>9</b>	0.356	0.416	0.344	0.372	0.0386
<b>10</b>	0.328	0.314	0.4	0.347	0.0461
<b>11</b>	0.373	0.374	0.378	0.375	0.0026
<b>12</b>	0.306	0.336	0.34	0.327	0.0186

Table 5.10. Cell concentrations (OD) for different vitamin compositions.

Y1, Y2 and Y3 are the triplicate responses for cell concentration (OD) for the same vitamin composition after 8.5 days.

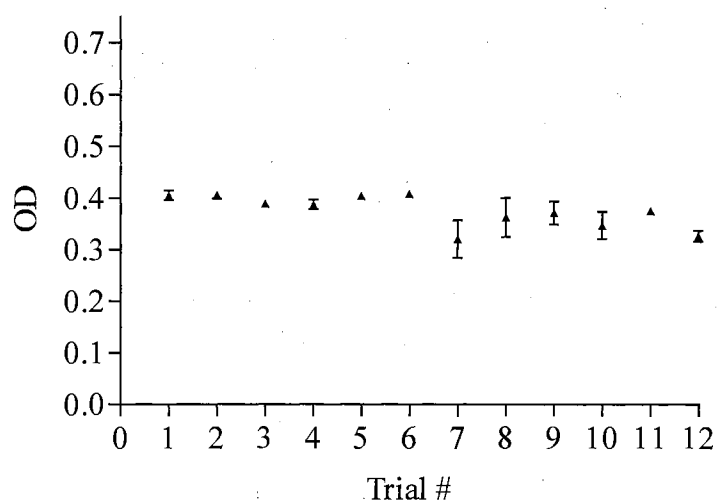


Figure 5.8. Average OD and standard deviation plot for vitamin optimization. Each data point is the average of 3 points and denotes the OD value after a period of 8.5 days



					Active
Factor	Coeff	P(2 Tail)	Tol		
Constant	0.37594	0.0000			
A	-0.02489	0.0001	1	X	
B	-0.000666667	0.9049	1		
C	-0.00328	0.5581	1		
D	-5.55556E-05	0.9921	1		
E	-0.00167	0.7653	1		
F	0.01261	0.0314	1	X	
G	-0.00661	0.2426	1		
H	-0.00250	0.6546	1		
I	-0.0005	0.9286	1		
J	-0.00500	0.3739	1		
K	0.00250	0.6546	1		
Rsq 0.5445					
Adj Rsq 0.3358					
Std Error 0.0331					
F 2.6085					
Sig F 0.0240					
Source	SS	df	MS		
Regression	0.0	11	0.0		
Error	0.0	24	0.0		
Total	0.1	35			

Table 5.11. Y-hat model from first regression for vitamin optimization

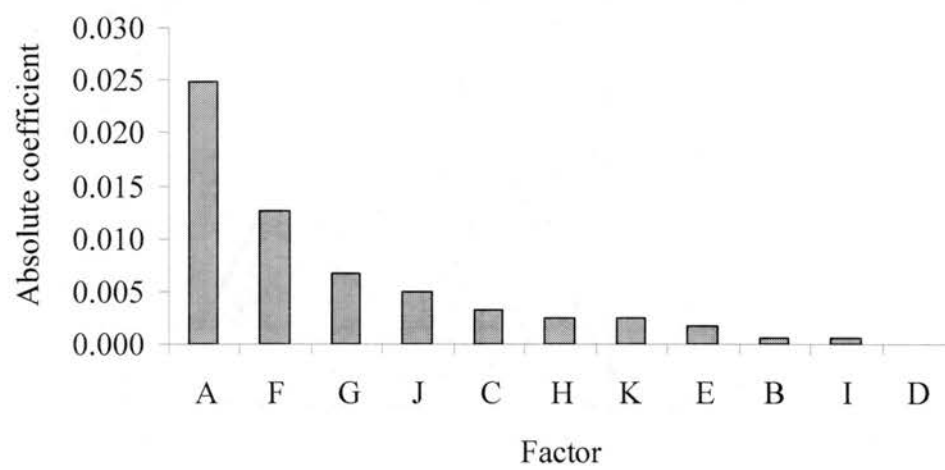


Figure 5.9. Y-hat pareto of coefficients for vitamins from first regression

				Active
Factor	Coeff	P(2 Tail)	Tol	
Constant	0.37594	0.0000		
A	-0.02489	0.0000	1	X
F	0.01261	0.0168	1	X
Rsq 0.4851 Adj Rsq 0.4539 Std Error 0.0300 F 15.5438 Sig F 0.0000				
Source	SS	df	MS	
Regression	0.0	2	0.0	
Error	0.0	33	0.0	
Total	0.1	35		

Table 5.12. Y-hat model from second regression for vitamin optimization

less than 0.1, a second regression analysis (Table 5.12) was performed by keeping Factors A and F as active factors, and changing the status of all other factors to non-active (X from the active column was deleted). An improvement in the F-value was observed from an initial value of 2.6 to 15.54. Thus, from the second regression table, a linear model for predicting the cell OD is described below:

$$Y = 0.37594 - 0.02489 A + 0.01261 F \quad (\text{Eq. 5.2})$$

where Y is cell concentration (in OD units), A is the concentration of pyridoxine, and F is concentration of amino benzoic acid. The concentration of each nutrient in the model is represented in coded values and varies between -1 (minimum concentration) to +1 (maximum concentration). See Table 5.4 for the final concentration of each vitamin corresponding to a coded value of -1 and +1. The cell OD was predicted using Eq. 5.2, and compared to the observed values and the residuals were calculated (Table 5.13 and Figure 5.10). As seen from the marginal means plot (Figure 5.11), none of the factors, other than Factors A (pyridoxine) and F (amino benzoic acid) significantly influenced the cell OD at the high and low concentration levels.

Thus, from the results discussed so far, it is obvious that the cell OD was not affected even after complete elimination of vitamin B<sub>12</sub> and d-biotin from the nutrient media. Additional experiments were conducted without vitamin B<sub>12</sub> and/or d-biotin as confirmation runs. The final cell OD from these experimental trials is shown in Figure 5.12. As seen from the figure, the average cell OD of the bottles 1) without d-biotin,

<b>Trial #</b>	<b>Response</b>	<b>Observed</b>	<b>Predicted</b>	<b>Residual</b>
<b>1</b>	Y1	0.423	0.3882	0.0348
	Y2	0.39	0.3882	0.0018
	Y3	0.405	0.3882	0.0168
<b>2</b>	Y1	0.393	0.4134	-0.0204
	Y2	0.411	0.4134	-0.0024
	Y3	0.417	0.4134	0.0036
<b>3</b>	Y1	0.393	0.3882	0.0048
	Y2	0.387	0.3882	-0.0012
	Y3	0.39	0.3882	0.0018
<b>4</b>	Y1	0.384	0.3882	-0.0042
	Y2	0.405	0.3882	0.0168
	Y3	0.375	0.3882	-0.0132
<b>5</b>	Y1	0.396	0.4134	-0.0174
	Y2	0.417	0.4134	0.0036
	Y3	0.402	0.4134	-0.0114
<b>6</b>	Y1	0.396	0.4134	-0.0174
	Y2	0.414	0.4134	0.0006
	Y3	0.417	0.4134	0.0036
<b>7</b>	Y1	0.344	0.3384	0.0056
	Y2	0.37	0.3384	0.0316
	Y3	0.25	0.3384	-0.0884
<b>8</b>	Y1	0.288	0.3637	-0.0757
	Y2	0.396	0.3637	0.0323
	Y3	0.406	0.3637	0.0423
<b>9</b>	Y1	0.356	0.3637	-0.0077
	Y2	0.416	0.3637	0.0523
	Y3	0.344	0.3637	-0.0197
<b>10</b>	Y1	0.328	0.3384	-0.0104
	Y2	0.314	0.3384	-0.0244
	Y3	0.4	0.3384	0.0616
<b>11</b>	Y1	0.373	0.3637	0.0093
	Y2	0.374	0.3637	0.0103
	Y3	0.378	0.3637	0.0143
<b>12</b>	Y1	0.306	0.3384	-0.0324
	Y2	0.336	0.3384	-0.0024
	Y3	0.34	0.3384	0.0016

Table 5.13. Residuals using second regression analysis for vitamin optimization. Experimentally observed values are compared to the predicted values given by the linear model described by Eq. 5.2

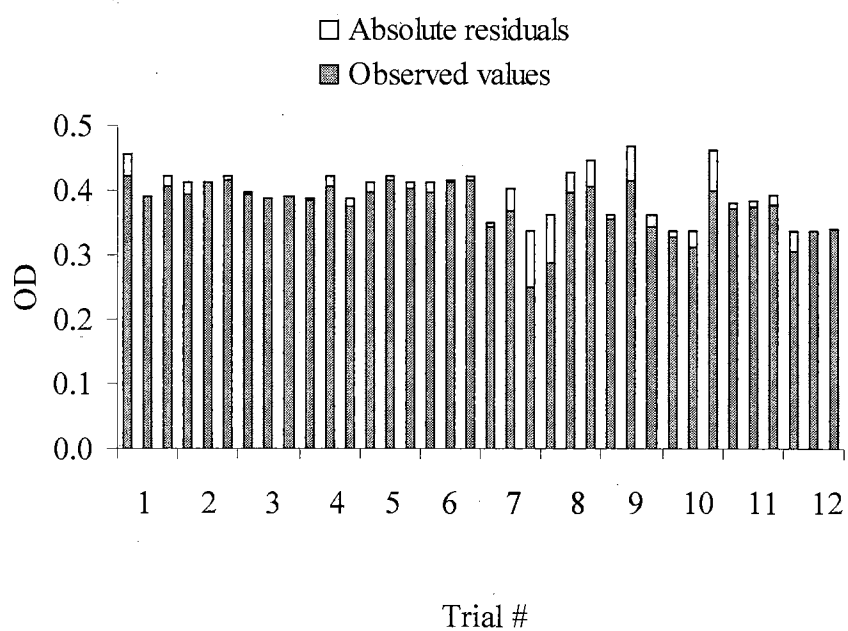


Figure 5.10. Observed cell concentrations (OD) and absolute residuals from regression analysis for vitamins

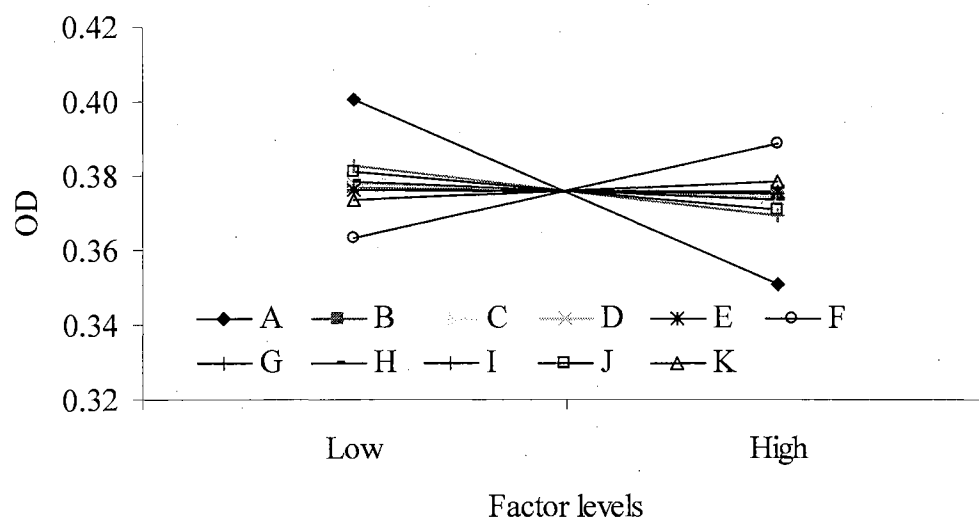


Figure 5.11. Y-hat marginal means plot for vitamins

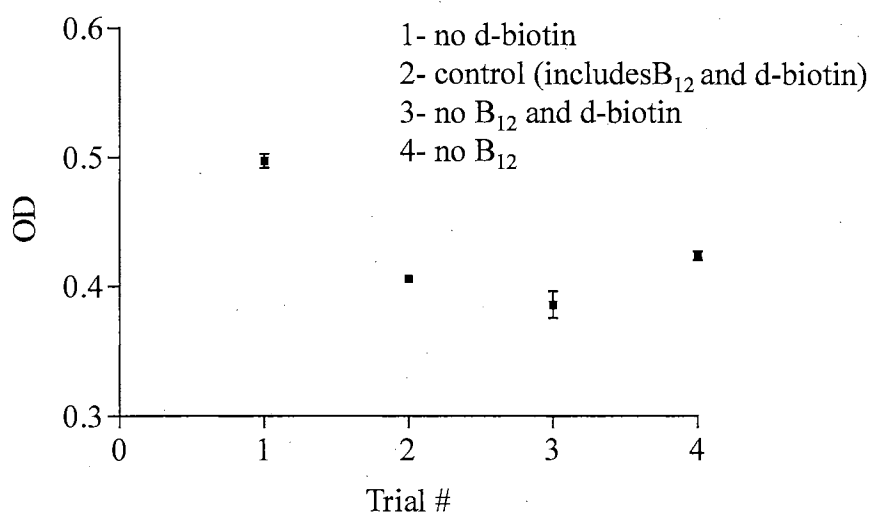


Figure 5.12. Final cell OD for vitamin confirmation experiments.

Each data point was the average of 3 points and denotes the

OD value after a period of 9 days



2) control (includes B<sub>12</sub> and d-biotin), 3) without both (no B<sub>12</sub> and d-biotin), and 4) without vitamin B<sub>12</sub> are about 0.5, 0.4, 0.39, and 0.42 respectively.

### 5.4.3 Trace metal optimization

As seen from Table 5.14 and Figure 5.13, the average cell OD for all the experimental runs (after 8 days) for trace metals optimization is between 0.33 and 0.41. The cell OD for trials 10, 11 and 12 showed the highest value of about 0.41. A visual analysis of Table 5.5 indicates that all three trials had higher levels of nutrients A and B. The results from the first regression analysis are shown in Table 5.15. As seen from the table, the F-value for the model is 5.92 and the tolerance for all factors is 1. The p (2 Tail) for Factors A, B, and E is less than 0.05, while the Factors G and H have a p (2 Tail) of 0.0838 and 0.0528 respectively. Since, this is a screening experiment, Factors G and H (along with A, B and E) are included in the model as active factors. The results from the second regression analysis are shown in Table 5.16. The F-value after the second regression is 10.71. A linear model was developed using the coefficients for each factor and is described below:

$$Y = 0.38084 + 0.00728 A + 0.01546 B + 0.00902 E - 0.00510 G - 0.00575 H \quad (\text{Eq. 5.3})$$

where Y is the cell concentration (in OD units), A is the concentration of nitrilotriacetic acid, B is the concentration of manganese sulfate, E is the concentration of zinc sulfate, G is the concentration of nickel chloride, and H is the concentration of sodium molybdate.

<b>Trial #</b>	<b>Y1</b>	<b>Y2</b>	<b>Y3</b>	<b>Average Y</b>	<b>Std. Dev.</b>
<b>1</b>	0.3698	0.3462	0.3536	0.3565	0.012
<b>2</b>	0.332	0.34	0.326	0.3326	0.007
<b>3</b>	0.4002	0.3622	0.3992	0.3872	0.021
<b>4</b>	0.3778	0.4234	0.3996	0.3992	0.022
<b>5</b>	0.3892	0.3916	0.372	0.3822	0.009
<b>6</b>	0.3892	0.3954	0.3656	0.3834	0.015
<b>7</b>	0.354	0.3502	0.3439	0.3493	0.005
<b>8</b>	0.376	0.3874	.394	0.3858	0.009
<b>9</b>	0.384	0.378	0.38	0.3806	0.003
<b>10</b>	0.3878	0.3924	0.4386	0.4062	0.028
<b>11</b>	0.386	0.404	0.418	0.4026	0.016
<b>12</b>	0.4176	0.3784	0.4158	0.4039	0.0221

Table 5.14. Cell concentrations (OD) for different trace metal compositions. Y1, Y2 and Y3 are the triplicate responses for cell concentration (OD) for the same trace metal composition after 8 days

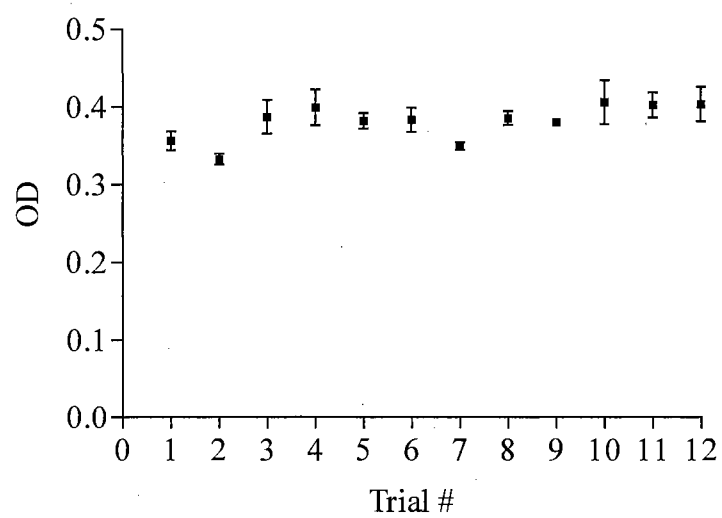


Figure 5.13. Average OD and standard deviation plot for trace metal optimization. Each data point is the average of 3 points and denotes the OD value after a period of 8 days

				Active
Factor	Coeff	P(2 Tail)	Tol	
Constant	0.38084	<b>0.0000</b>		
A	0.00728	<b>0.0164</b>	1	X
B	0.01546	<b>0.0000</b>	1	X
C	0.00155	0.5894	1	
D	0.00293	0.3112	1	
E	0.00902	<b>0.0038</b>	1	X
F	-0.00293	0.3112	1	
G	-0.00510	<b>0.0838</b>	1	X
H	-0.00575	<b>0.0528</b>	1	X
I	0.00152	0.5961	1	
J	-0.00449	0.1255	1	
Rsq            0.7033 Adj Rsq       0.5846 Std Error      0.0170 F        5.9246 Sig F     0.0001				
Source	SS	df	MS	
<b>Regression</b>	0.0	10	0.0	
<b>Error</b>	0.0	25	0.0	
<b>Total</b>	0.0	35		

Table 5.15. Y-hat model from first regression for trace metal optimization

Factor	Coeff	P(2 Tail)	Tol	Active
Constant	0.38084	<b>0.0000</b>		
A	0.00728	<b>0.0157</b>	1	X
B	0.01546	<b>0.0000</b>	1	X
E	0.00902	<b>0.0035</b>	1	X
G	-0.00510	<b>0.0829</b>	1	X
H	-0.00575	<b>0.0519</b>	1	X
Rsq            0.6411 Adj Rsq       0.5813 Std Error      0.0170 F               10.7175 Sig F           0.0000				
Source	SS	df	MS	
<b>Regression</b>	0.0	11	0.0	
<b>Error</b>	0.0	24	0.0	
<b>Total</b>	0.1	35		

Table 5.16. Y-hat model from second regression for trace metal optimization

The concentration of each nutrient in the model is represented in coded values and varies between  $-1$  (minimum concentration) to  $+1$  (maximum concentration). See Table 5.6 for the final concentration of each trace metal corresponding to a coded value of  $-1$  and  $+1$ . The predictions for cell OD, using the model described by Eq. 5.3 are compared to the actual observations and the residuals were determined (Table 5.17 and Figure 5.14). The pareto of coefficients for all factors, shown in Figure 5.15, suggests that Factors B and E are the dominant factors. The marginal means plot (shown in Figure 5.16) indicates that all factors except Factors A, B, E, G and H have an insignificant effect (difference in OD  $< 0.01$  units) on cell OD at the two concentration levels under investigation in this study.

## 5.5 Discussion

The Taguchi  $L_{12}$  design is very useful for screening a large number of factors and to reduce the large set to a smaller set of important factors for subsequent rigorous experimentation. However, the design is based on the assumption that interactions (if any) are not strong enough to mask the main effects. Hence, a more extensive experimental design is required to identify and account for possible interactions between individual factors.

The F-value in the regression table determines the statistical significance of the model developed. The observed F-value is compared to the critical F-value ( $F_c$ ).  $F_c = F(a, v_1, v_2)$  where,  $a$  is the confidence level,  $v_1 = 1$  (for a 2-level design), and  $v_2 = \sum(n_r - 1)$ .  $n_r$  denotes the number of replications and equals 3 for this study. The F-values for the models developed for mineral, vitamin and trace metal optimization are 19.95, 15.54, and 10.71 respectively. These F-values are greater than the listed F-value of 7.82 for 99% of

<b>Trial #</b>	<b>Response</b>	<b>Observed</b>	<b>Predicted</b>	<b>Residual</b>
<b>1</b>	Y1	0.3698	0.3599	0.0348
	Y2	0.3462	0.3599	0.0018
	Y3	0.3536	0.3599	0.0168
<b>2</b>	Y1	0.332	0.3382	-0.0062
	Y2	0.34	0.3382	0.0018
	Y3	0.326	0.3382	-0.0122
<b>3</b>	Y1	0.4002	0.3780	0.0222
	Y2	0.3622	0.3780	-0.0158
	Y3	0.3992	0.3780	0.0212
<b>4</b>	Y1	0.3778	0.3872	-0.0094
	Y2	0.4234	0.3872	0.0362
	Y3	0.3966	0.3872	0.0094
<b>5</b>	Y1	0.3892	0.3974	-0.0082
	Y2	0.3916	0.3974	-0.0058
	Y3	0.372	0.3974	-0.0254
<b>6</b>	Y1	0.3892	0.3807	0.0085
	Y2	0.3954	0.3807	0.0147
	Y3	0.3656	0.3807	-0.0151
<b>7</b>	Y1	0.354	0.3528	0.0012
	Y2	0.3502	0.3528	-0.0026
	Y3	0.3439	0.3528	-0.0089
<b>8</b>	Y1	0.376	0.3823	-0.0063
	Y2	0.3874	0.3823	0.0051
	Y3	0.394	0.3823	0.0117
<b>9</b>	Y1	0.384	0.3810	0.0030
	Y2	0.378	0.3810	-0.0030
	Y3	0.38	0.3810	-0.0010
<b>10</b>	Y1	0.3878	0.3939	-0.0061
	Y2	0.3924	0.3939	-0.0015
	Y3	0.4386	0.3939	0.0447
<b>11</b>	Y1	0.386	0.4054	-0.0194
	Y2	0.404	0.4054	-0.0014
	Y3	0.418	0.4054	0.0126
<b>12</b>	Y1	0.4176	0.4133	0.0043
	Y2	0.3784	0.4133	-0.0349
	Y3	0.4158	0.4133	0.0025

Table 5.17. Residuals using second regression analysis for trace metal optimization. Experimentally observed values are compared to the predicted values obtained from the linear model described by Eq. 5.3

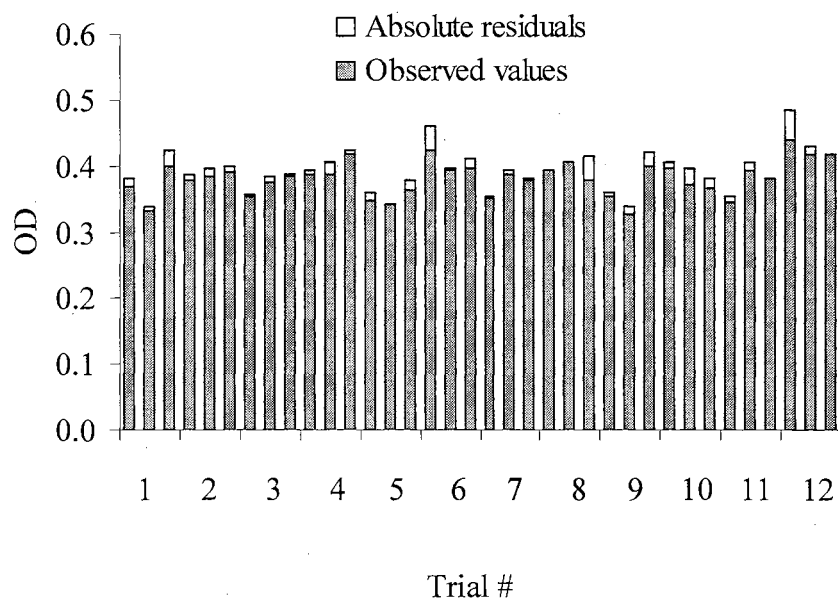


Figure 5.14. Observed cell concentrations (OD) and absolute residuals from regression analysis for trace metals



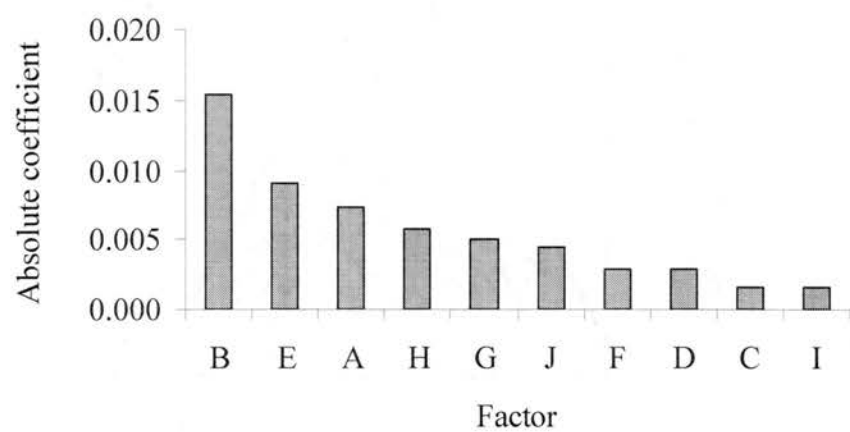


Figure 5.15. Y-hat pareto of coefficients for trace metals  
from first regression

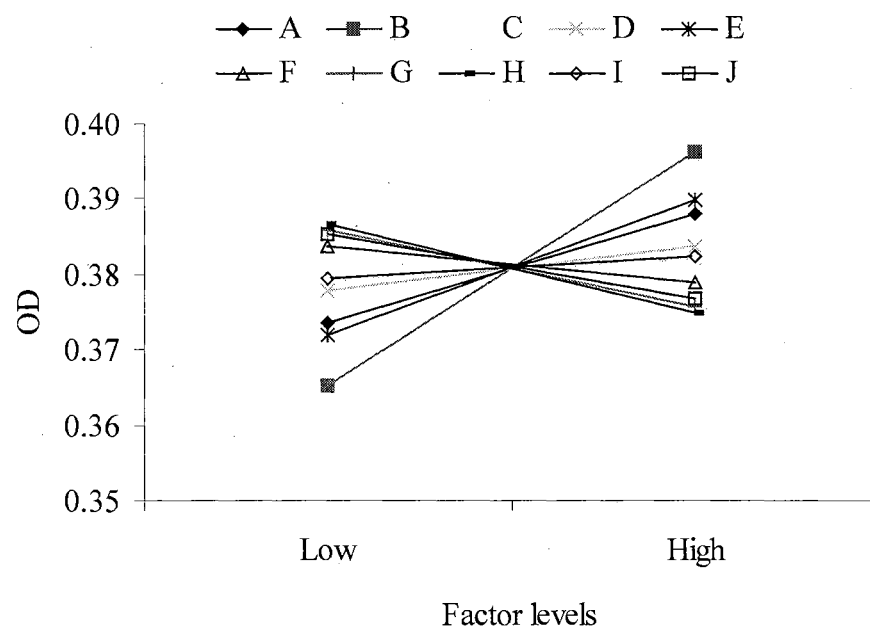


Figure 5.16. Y-hat marginal means plot for trace metals

confidence (Schmidt and Launsby, 1994). Thus, there is a 99% confidence that the models developed are reliable. The tolerance values should be greater than 0.5 for meaningful coefficients of the factors included in the model. The tolerance values are 1 for all factors in all models, further demonstrating the reliability of the models.

The coefficients of Factors A (sodium chloride), B (ammonium chloride), C (potassium chloride), D (potassium monophosphate) and F (calcium chloride) were negative in the mineral model described by Eq. 5.1. The fact that the cell concentration was higher at lower levels of these nutrients suggested the possibility of substrate inhibition on cell growth. Factor E (magnesium sulfate) had a positive coefficient, thus suggesting a positive effect on cell growth. However, the studies on mineral optimization need to be further expanded to include potential interaction effects and to determine the optimal nutrient levels.

The vitamin optimization studies indicated that only Factors A (pyridoxine) and F (p-amino benzoic acid) influenced the cell OD at the tested levels. Lowering the concentration of pyridoxine favored cell growth, while the reduction in p-amino benzoic acid negatively affected the cell OD. Vitamin B<sub>12</sub> and d-biotin can be eliminated from the media without affecting the cell OD. Previous studies showed that strain P7 required d-biotin, pantothenate, p-amino benzoic acid, isoleucine and proline for growth on CO (Liou et al., 2002), while the required B-vitamins for growth of *Clostridium ljungdahlii* are biotin, thiamine-HCl, and pantothenate (Phillips et al., 1993). The findings from the vitamin optimization study are in agreement with the previously reported results, except for d-biotin. However, yeast extract present in the nutrient media, of which the composition is undetermined, could be a source of d-biotin.

The key nutrients identified after the screening experiments for trace metals are nitrilotriacetic acid, manganese sulfate, zinc sulfate, nickel chloride, and sodium molybdate. The first three nutrients enhanced cell OD, while the latter two inhibited cell growth at higher levels as compared to lower levels. Since, the other trace metals had a negligible effect on the cell OD while lowering their concentrations, further reduction in the concentration of these nutrients must be explored in the future.

Using the optimized concentrations obtained from the above experiments, a cost analysis for minerals (Table 5.18), vitamins (Table 5.19), and trace metals (Table 5.20) show a reduction of 78%, 87% and 0.5% in the final cost of the optimized fermentation media as compared to the original media.

Although, the work discussed in this chapter was aimed at optimization of nutrient media to maximize cell OD and minimize costs, additional studies must be performed with regards to maximizing final concentrations of ethanol and other liquid products. Obviously to reduce the media costs, the nutrients contribute to a majority of the cost and the nutrient optimization should be further explored.

## 5.6 Conclusions

The nutrients affecting the cell OD (positively and negatively) were identified after a rigorous screening exercise. Significant reductions in the final concentrations of minerals were successfully targeted. Biotin and vitamin B<sub>12</sub> can be completely eliminated from the nutrient media. The final optimized media cost was about 75% lower than the original media cost. Full factorial experiments must be performed to determine the interactions between the selected nutrients, since only the main effects were considered during this study.

Original Media			Optimized Media	
Nutrient	Amount (g/L)	Cost (₹/L) of broth	Amount (g/L)	Cost (₹/L) of broth
Sodium chloride	80	1.24	10	0.15
Ammonium chloride	100	4.11	20	0.82
Potassium chloride	10	0.34	2	0.06
Potassium monophosphate	10	0.85	2	0.17
Magnesium sulfate	20	0.93	10	0.46
Calcium chloride	80	0.15	1	0.03
Total		<b>7.64</b>		<b>1.72</b>

Table 5.18. Cost analysis for original and optimized mineral composition

Original Media			Optimized Media	
Nutrient	Amount (g/L)	Cost (¢/L) of broth	Amount (g/L)	Cost (¢/L) of broth
Nitrilotriacetic acid	2	0.132	2	0.132
Manganese sulfate	1	0.109	1	0.109
Ferrous ammonium sulfate	0.8	0.027	0.8	0.027
Cobalt chloride	0.2	0.045	0.2	0.045
Zinc sulfate	0.2	0.008	0.2	0.008
Cupric chloride	0.02	0.003	0.02	0.003
Nickel chloride	0.02	0.001	0.01	0.0007
Sodium molybdate	0.02	0.003	0.01	0.0016
Sodium selenate	0.02	0.019	0.02	0.019
Sodium tungstate	0.02	0.005	0.02	0.005
Total cost		<b>0.356</b>		<b>0.354</b>

Table 5.20. Cost analysis for original and optimized trace metal composition

Original Media			Optimized Media	
Nutrient	Amount (g/L)	Cost (¢/L) of broth	Amount (g/L)	Cost (¢/L) of broth
Pyridoxine	0.01	0.0099	0.005	0.0049
Thiamine	0.005	0.0074	0.005	0.0074
Riboflavin	0.005	0.0061	0.005	0.0061
Calcium pantothenate	0.005	0.0037	0.005	0.0037
Thioctic acid	0.005	0.0313	0.005	0.0313
Amino benzoic acid	0.005	0.0150	0.005	0.01505
Nicotinic acid	0.005	0.0004	0.005	0.0004
Vitamin B <sub>12</sub>	0.005	0.7	0	0
d-Biotin	0.002	0.113	0	0
Folic acid	0.002	0.0041	0.002	0.0041
MESNA	0.01	0.0519	0.01	0.0519
Total		<b>0.943</b>		<b>0.1250</b>

Table 5.19. Cost analysis for original and optimized vitamin composition



## CHAPTER 6

### DESIGN OF A CONTINUOUS MICROBUBBLE GENERATION SYSTEM

#### 6.1 Introduction

The transport of a gaseous substrate to active sites on the microbial catalyst is a very complex process. The constituents of producer gas, such as  $H_2$  and CO, have aqueous solubilities of 60% and 4% respectively as compared to oxygen on a mass basis (Bredwell et al., 1999). These low solubilities result in low concentration gradients, leading to low volumetric mass transfer rates of the gaseous substrate. The constituents of producer gas must pass through a series of transport resistances before they are utilized and converted to useful products by the microorganisms. Similarly, the transport of gaseous products out of the microbial cell is also very important to prevent retardation of cell growth due to product inhibition. The magnitude of the resistances encountered depends on various factors. Some of the factors include bubble size, temperature, liquid density and viscosity, and diffusivity of gas. Figure 6.1 is a schematic diagram indicating the individual steps involved in the transport of gas from the bulk gas phase to within the cell. The mass transfer coefficient is dependent on the combination of the following resistances (Bailey and Ollis, 1986, Blanch and Clark, 1997).

- Resistance 1: Transport of the gas from the bulk gas phase to the gas liquid interface.

- Resistance 2: Movement of the gas across the gas-liquid interface, which is a function of the gas solubility.
- Resistance 3: Transport of the gas through the stagnant and relatively unmixed liquid film surrounding the gas-liquid interface.
- Resistance 4: Transport of gas through the bulk liquid phase.
- Resistance 5: Transport of gas from the bulk liquid phase through a second relatively unmixed liquid film surrounding the cells.
- Resistance 6: Transport across the cell membrane into the cell.
- Resistance 7: Transport from the inner cell membrane to the intracellular active reaction site.

These resistances appear in series and the rate limiting step is controlled by the largest resistance(s). Since the gas phase diffusivities are much higher than the liquid phase diffusivities, Resistance 1 can be neglected. Typically, in well-mixed reactor systems for fermentation of constituents of producer gas, Resistances 4 and 5 can be eliminated since these are much smaller than the other resistances. Due to the structural characteristics of a microbial cell (enormous surface area and minute size as compared to the gas bubble), the transport of gas through the liquid cell interface is much faster as compared to the bulk liquid phase, and therefore Resistance 6 can also be ignored (Klasson et al., 1992).

Thus, if the primary resistance for the transfer of sparingly soluble gases (contributing to Resistance 2) lies in the liquid film surrounding the gas-liquid interface (Resistance 3 > Resistance 7), then the transport of gas is said to be mass transfer limited. On the other hand, if the microbial kinetic activity governs the reaction rate (Resistance 7 > Resistance 3), then the transport of gas is limited by the cellular gas uptake kinetics. In previous

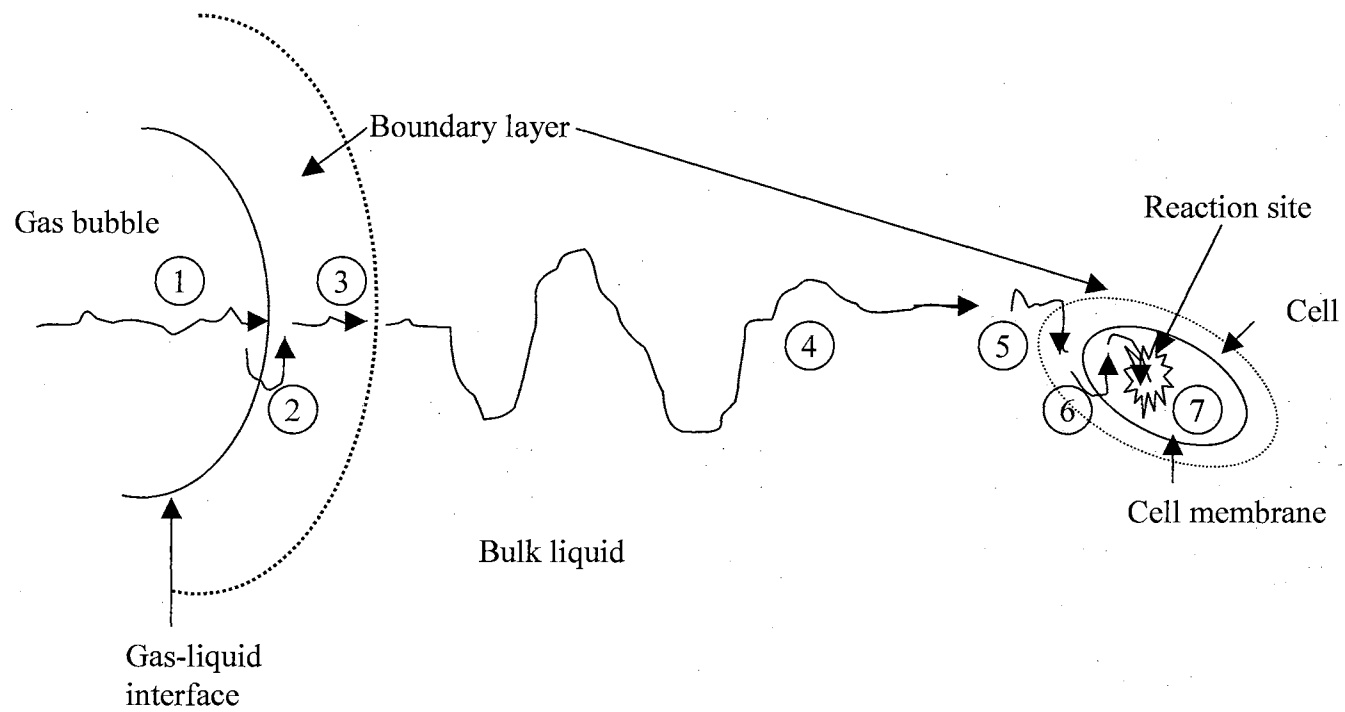


Figure 6.1. Resistances involved in gas transport from bulk gas to reaction site in a cell.

(Bailey and Ollis, 1986)

studies conducted with the bubble column bioreactor, where the gas was dispersed through a fritted disc at the bottom of the reactor, the transport of gas was governed by the gas uptake kinetics (Rajagopalan, 2001). However, it is expected that at higher cell concentrations and on a larger scale, mass transfer would be the controlling step, since the rate of consumption of the gaseous substrate by the cells will be higher than the mass transfer rate of the gaseous substrate to the cells.

The traditional approach of increasing the mass transfer by increasing the agitation rate in continuous stirred tank reactors can be expensive in large reactors, since the power consumption is proportional to the impeller speed to the third power and the impeller diameter to the fifth power (Shuler and Kargi, 1992). The gas transfer rate is also inversely proportional to the radius of the gas bubbles, thus, smaller the bubbles, the greater the gas transfer rate. Microbubble dispersions offer an excellent alternative by providing a high interfacial area, and thus enhancing the mass transfer. Microbubbles are surfactant-stabilized gas bubbles with radii in the order of 50-100 microns. The structure of a microbubble is as shown in Figure 6.2. The surfactant-stabilized shell of water lies between the gas bubble and the bulk liquid phase.

Hence, it is essential to develop a continuous, reliable and an inexpensive system for potential scale-up delivery of producer gas in the form of microbubbles, to minimize the resistance of mass transfer affecting the gas uptake rate.

The quality of microbubbles, which is defined as the percentage of gas in the microbubbles, and the percentage of total inlet producer gas incorporated into microbubbles are very important from an economic aspect of fermenting producer gas. The formation and use of microbubbles with a higher gas fraction (thus a lower liquid

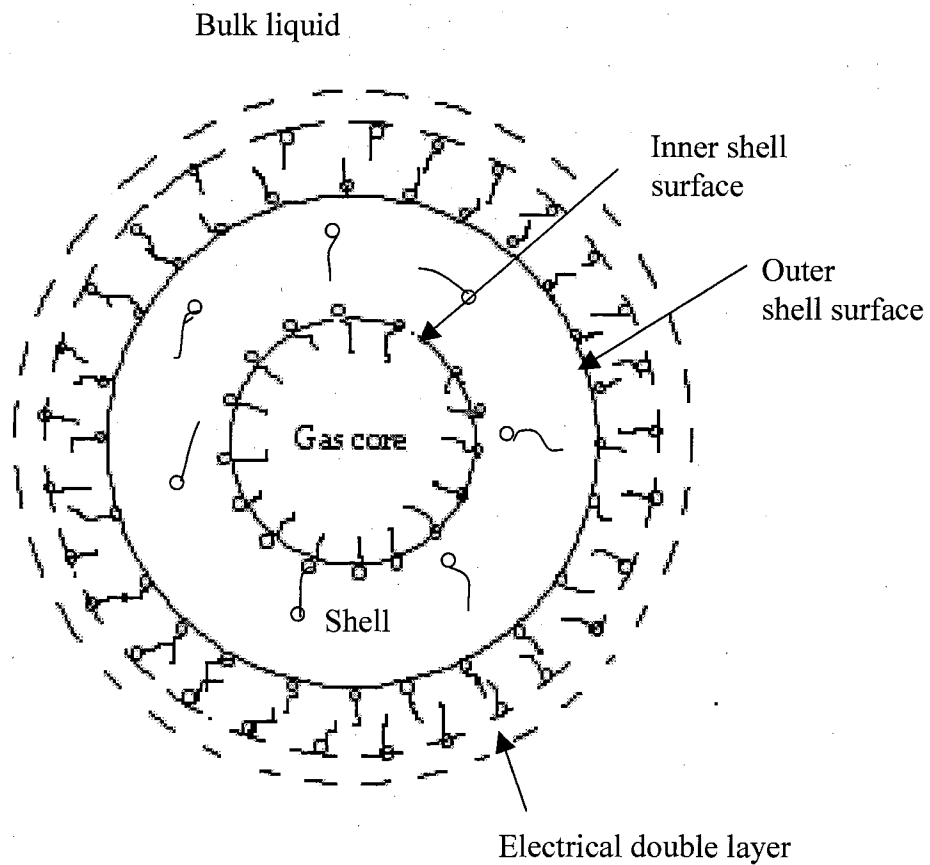


Figure 6.2 Structure of a microbubble (colloidal gas aphron).

The surfactant molecule is represented by the head-tail structure where the head (circular portion) denotes the hydrophilic part of the surfactant while the tail denotes the hydrophobic part of the surfactant

fraction) will result in lower liquid feed rates for delivering the same amount of gas. The fraction of total inlet gas incorporated into microbubbles is also critical because higher gas incorporation will result in better utilization and delivery of gas as microbubbles and minimize the amount of unincorporated gas being wasted from the generator. Thus, a microbubble generation system, capable of producing microbubbles with a high gas fraction and with maximum producer gas incorporation and minimum gas wastage (in the form of unincorporated gas) will obviously be economically favorable.

As stated previously, producer gas can be mass transfer limited and hence there is a need to develop reliable and inexpensive techniques for mass transfer enhancement. In this study, the development of a stable and efficient microbubble generation system for potential scale-up delivery of the producer gas is discussed. This study will be helpful in determining the optimal parameters for maximizing the gas fraction in the microbubbles and the gas incorporation and in future scale up studies on the microbubble generator.

## **6.2 Objectives of the study**

This chapter focuses on the following specific objectives:

- Design and evaluate a steady microbubble generation system, aimed at maximizing the microbubble gas fraction (quality) and percentage of gas incorporated into microbubbles.
- Assess the effect of salt addition, surfactant concentration, disc speed, gas and liquid flow rates on the quality of microbubbles and gas incorporation.

## **6.3 Materials and Methods**

### **6.3.1 Design of Microbubble generator**

The microbubble generator (see Figure 6.3 and Table 6.1) was designed based on the high speed spinning disc design described by Sebba (1985) and Bredwell et al. (1998). The generator is made of plexiglass and has a height of 21 cm and an inside diameter of 16 cm. The total volume of the microbubble generator is 4.2 liters, although the working volume of the liquid is only one liter. Four stationary baffles made of plexiglass are symmetrically attached to the sides of the cylinder. The four-baffle design was a modification of the two-baffle design described by Sebba (1985) and Bredwell et al. (1998), aimed at increasing the efficiency of the microbubble generator. A thin disc made of stainless steel is attached to a vertical shaft connected to a high speed, low torque electric motor (1/10 hp, 150-6000 rpm, 17 oz-in torque, Cole Parmer, Chicago, IL). The motor is controlled by a mixer controller with digital speed control (Cole Parmer, Chicago, IL). Two square plexiglass plates are attached to the top and bottom of the cylinder. A flexible rubber gasket is inserted in between the cylinder and each plate to prevent gas leaks. Four metal screws connect the top and the bottom plate and can be tightened as necessary to avoid gas and liquid leaks from the generator. The motor is attached to the shaft and supported by the headplate. The shaft is supported by bearings to avoid vibrations and ensure stability during high rotational speeds. The shaft is capable of moving vertically so that the distance 'A' (shown in Figure 6.3) can be adjusted. The baffles are positioned very close to the spinning disc (5 mm from the top and side) to create a high shear zone and to reduce vortex formation. Gas was introduced into the

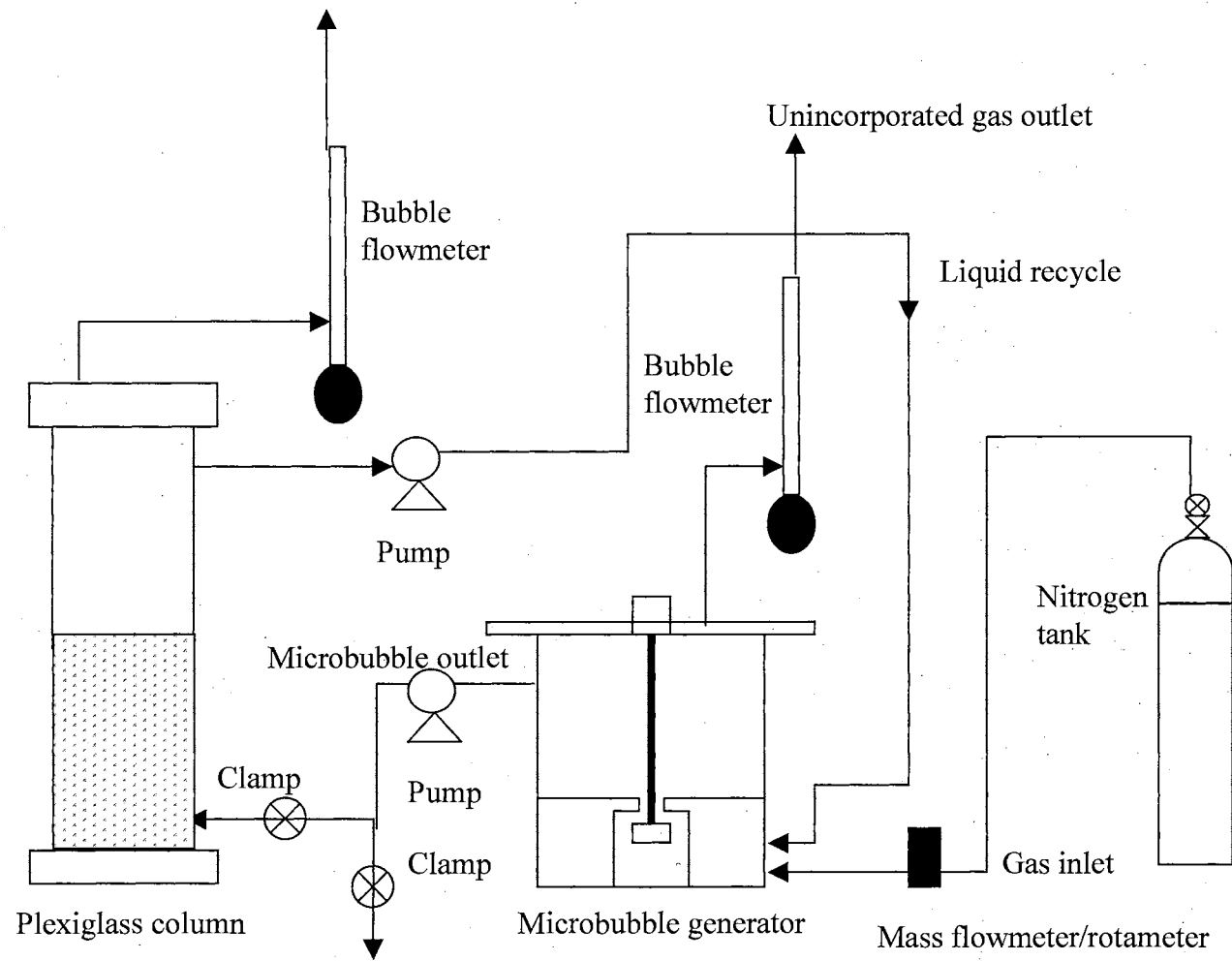


Figure 6.3. Experimental layout for microbubble generation system



<b>Microbubble generator</b>	<b>Specifications</b>
Material of construction	Plexiglass (poly methyl methacrylate)
Height	21 cm
Inside diameter	16 cm
Wall thickness	1 cm
Head and bottom plate	20 X 20 X 1.2 cm (plexiglass)
Total volume	4.2 liters
Liquid volume	1 liter
<b>Baffles</b>	<b>Specifications</b>
Number of baffles	4 (Inverted L shaped)
Material of construction	Plexiglass
Thickness	1.8 cm
Height	10 cm
Width	6 cm
<b>Spinning disc</b>	<b>Specifications</b>
Material of construction	Stainless steel
Diameter	5 cm
Thickness	0.9 cm

Table 6.1 Design specifications for microbubble generator

generator just below the spinning disc with a 1/8-inch flexible plastic tubing. Liquid was introduced through from the bottom of the cylinder. Microbubbles were withdrawn from an outlet at the top of the cylinder. Additional outlets are provided on the head plate to release pressure if necessary and vent the unincorporated gas.

### **6.3.2 Experimental layout and operation**

The experimental set-up used for all experiments is shown in Figure 6.4. Nitrogen was used as the model gas because of its low cost and ease of handling. Gas was introduced into the microbubble generator by using a rotameter (Cole Parmer, Vernon Hills, IL). The rotameter was initially calibrated for nitrogen using a bubble flow meter. The use of a rotameter facilitated easy control of the gas flow rate. In later experiments, the rotameter was replaced with a mass flow controller (Porter Instruments, Hatfield, PA) for a more accurate and steady gas flow. The range of the inlet gas flow rates was between 180 and 900 ccm. The lower rate of 180 ccm was chosen based on the inlet gas flow rate used in experiments described earlier (Chapters 3 and 4), while the upper rate of 900 ccm was based on the operational limitations of the experimental apparatus. The microbubble generator was filled with one liter of distilled water with 120 ppm of surfactant (unless stated otherwise) and the gas flow was initiated. The surfactant used in these studies was Tween 20 (Sigma Chemicals, St. Louis, MO). This non-ionic surfactant was chosen because it is nontoxic and inexpensive and had little or no inhibitory effect on bacterial growth for fermentations using *Butyribacterium methylotrophicum* (Worden et al., 1997, Bredwell et al., 1997).

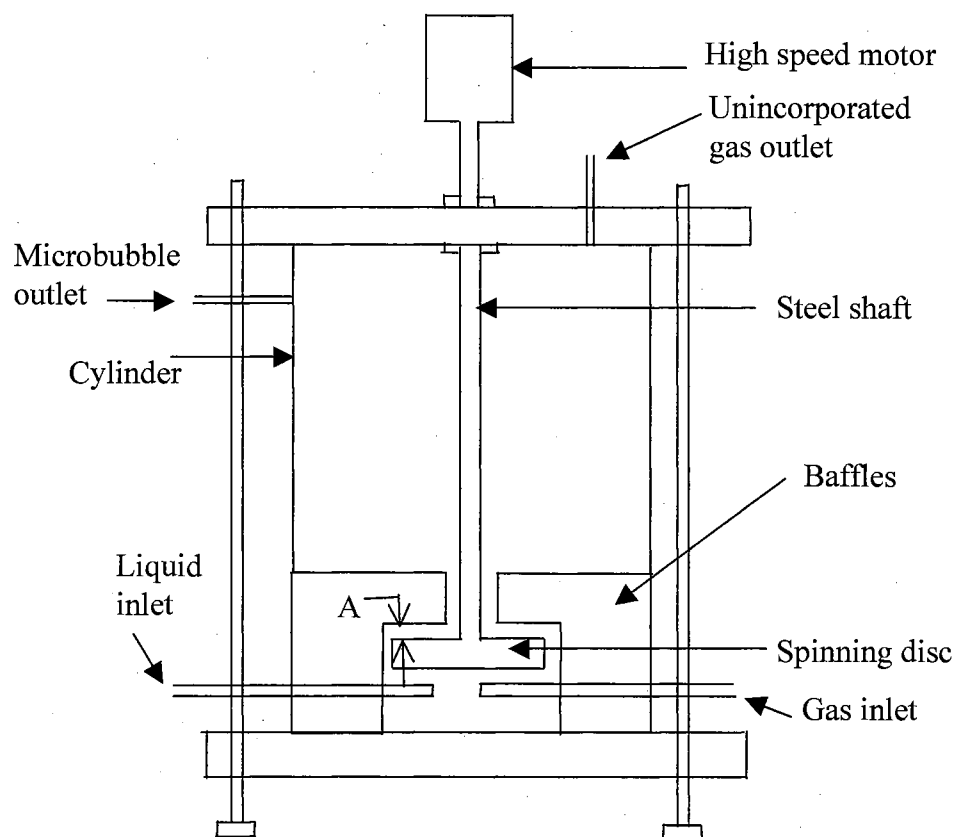


Figure 6.4 Design of the microbubble generator

The generator was slightly pressurized initially by closing all outlets and checked for gas leaks at the start of each experiment. Necessary remedial measures were adopted to fix the leaks, if any. The gas outlet on the headplate of the generator was then opened. The disc speed was gradually increased from 150 rpm to 5950 rpm (unless stated otherwise) to ensure smooth start-up and stability. Continuous liquid flow was initiated using a peristaltic pump after microbubble generation was observed. The inlet liquid flow rate depended on the inlet gas flow rate used during the experiment. The liquid flow in the recycle loop was calibrated at different pump settings using a graduated cylinder and stopwatch to obtain the volumetric inlet flow rate of liquid entering the microbubble generator. The microbubbles were withdrawn from the top of the generator via plastic tubing attached to a pump. The withdrawal rate for the microbubbles varied for different experiments, and was such that there was no accumulation of microbubbles in the generator. The microbubbles were either collected in a tall graduated cylinder (to measure microbubble quality) or pumped into an empty plexiglass column (the column mimicked the bioreactor described in previous chapters). The plexiglass column has a height of 75 cm with an inside diameter of 15 cm and a total volume of six liters. Gas flow out of the plexiglass column was measured using a bubble flow meter to facilitate volumetric material balance calculations. The unincorporated gas exiting from the top of the generator was also measured using a bubble flow meter.

Several process variables such as surfactant concentration, salt addition, disc speed and gas and liquid flow rates were adjusted one at a time to assess the effect of these parameters on fractional incorporation of gas and on microbubble quality. The process variables such as surfactant concentration and disc speed were chosen on the

basis of their likely importance for development of a stable and efficient microbubble generation system for subsequent use in producer gas fermentations. The effect of salt was important to evaluate the formation of microbubbles with fermentation media. Information on the range of gas and liquid flow rates is needed to estimate the volume of the microbubble generator for future potential delivery of producer gas to large fermenters. The range of each variable, i.e. surfactant concentration (80-200 ppm), disc speed (4750-5950 rpm), salt (2.8 g/L), and gas flow rate (180-900 ccm) was chosen based on previously reported work (Bredwell et al., 1995, Bredwell and Worden, 1998, Jauregi et al., 1997, Sebba, 1985) and on the operational limitation of the experimental apparatus used for the study.

### **6.3.3 Analytical procedures**

The inlet gas flow rate was measured at the start of the experiment using a bubble flowmeter. It was assumed that the inlet gas flow rate remained constant during the course of the experiment. The inlet gas was assumed to be at atmospheric pressure. This assumption was based on the downstream delivery pressure information provided for the mass flowmeter. Similarly, the inlet liquid flow rate was measured using the calibrated pump settings. Gas exiting from the top plate of the generator (unincorporated gas) and from the plexiglass column (incorporated gas) was measured using a bubble flowmeter. The outlet gas was at atmospheric pressure, since the outlet was open to the atmosphere. Also, the inlet and outlet gas temperature was assumed to be constant at 25 °C, since the entire experimental apparatus was kept in the same room.

### **Volumetric flow rate of microbubbles**

The volumetric flow rate ( $Q_a$ ) of microbubbles pumped out of the generator was estimated by collecting a fixed volume of microbubbles (usually 100 ml) and dividing by the time required to collect the microbubbles. The volume of microbubbles collected to measure the quality and flow rate was not constant for every experiment and was dependant on the experimental conditions.

### **Gas fraction and quality of microbubbles**

To calculate the gas fraction of microbubbles, microbubbles were pumped into a graduated cylinder for a short time and the volume ( $V$ ) was noted. The microbubbles were then untouched until they all collapsed and only the liquid fraction remained in the cylinder. The volume of the remaining liquid ( $V_L$ ) was measured and the liquid fraction ( $f_L$ ) =  $V_L/V$  was calculated. Thus, the gas fraction is  $f_G = 1 - f_L$ , since the microbubbles consist of only gas and liquid. The quality, which denotes the percentage of gas incorporation in the microbubbles, is  $f_G * 100$ .

### **Volumetric gas balance**

The volumetric gas balance around the microbubble generator was calculated assuming that the gas temperature and pressure was the same for the inlet and outlet. The inlet gas flow rate ( $G_{in}$ ) was measured using a bubble flow meter and verified against the calibrated rotameter/mass flowmeter. Gas exiting from the microbubble generator occurred in two places. Unincorporated gas exited from the top of the generator and the flow rate ( $G_u$ ) was measured using a bubble flowmeter. The incorporated gas exited in

the form of microbubbles from the side of the generator and the flow rate ( $G_i$ ) was estimated by using equation  $G_i = Q_a * f_G$ . The flowrate of gas exiting from the plexiglass column was independently measured using a bubble flow meter and verified against  $G_i$ .

In theory,  $\frac{G_i + G_u}{G_m} = 1$

### **Volumetric liquid balance**

The total inlet liquid flow rate into the microbubble generator was measured using a measuring cylinder and stopwatch at the start of each experiment and verified with the calibrated pump. It was assumed that the liquid inlet flow rate remained constant throughout the experiment for establishing the volumetric liquid balance. Liquid exited the generator in the form of microbubbles. The total outlet liquid flow rate ( $L_{out}$ ) was estimated using from  $L_{out} = Q_a * f_L$ . At steady state conditions,  $L_{in}/L_{out}$  should be unity.

## **6.4 Results**

### **6.4.1 Microbubble quality and fractional incorporation**

Over a hundred data points were collected under different experimental conditions and analyzed for estimating the microbubble quality using the microbubble generator. The highest microbubble quality and fractional gas incorporation was about 89% and 99%, respectively, while the lowest was about 75% and 62.5%, respectively. The range was observed under different experimental conditions, with the highest values (for both quality and fractional incorporation) observed at inlet gas and liquid flow rates of 180 ccm and 25.4 ml/min respectively and surfactant concentration of 180 ppm, while the

lowest values for both were at inlet gas and liquid flow rates of 900 ccm and 190 ml/min and surfactant and salt concentration of 120 ppm and 2.8 g/L respectively. The details of the specific experimental results (at different conditions) for the estimation of microbubble quality are discussed below.

#### **6.4.2 Volumetric material balance**

Several continuous experiments were conducted at different liquid and gas flow rates for sixty minutes to evaluate the material balance for gas and liquid. Results for the gas balance from a representative run are shown in Figure 6.5. Since the temperature and pressure were assumed constant throughout the process, the volumetric flow was proportional to the molar flow for ideal gas assumptions. Thus, a volumetric balance was used for evaluation. The inlet gas flow rate was set at 190 ccm (at temperature of 25 °C and atmospheric pressure) using a rotameter and was assumed to be constant throughout the experiment. The average outlet gas flow rate over the course of the experiment was 175 ccm. Similarly, the average inlet and outlet liquid flow rates were 25.4 and 25.0 ml/min respectively (Figure 6.6). The maximum deviation was 18% (for gas) and 4% (for liquid). The average microbubble flow rate was 200 ccm, while the combined inlet flow rate (gas and liquid) was 215.4 ccm (Figure 6.7). Thus there was a 7.5 % difference observed between the combined inlet and outlet flow rates.

However, the gas balance (Figure 6.8) and combined material balance (Figure 6.9) was much more accurate when the rotameter was replaced with a mass flowmeter. The difference in the average inlet and outlet gas flow rates was less than 1% after 60 minutes as compared to about 8.5% using a rotameter for the same experimental



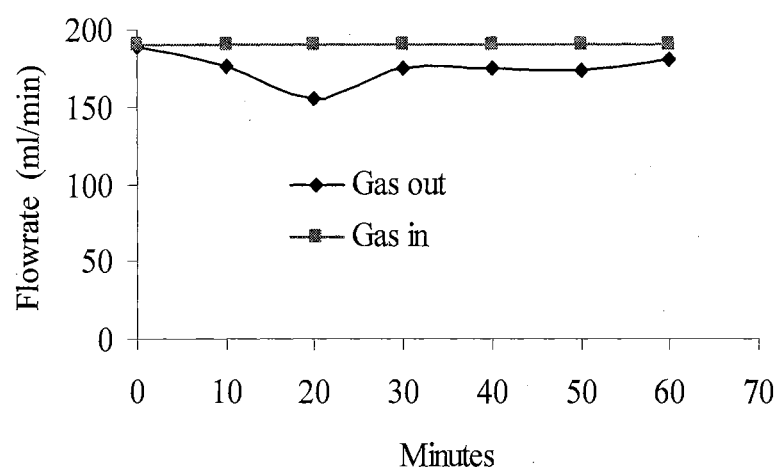


Figure 6.5. Total volumetric gas balance around the microbubble generator.

The inlet gas was controlled using a rotameter.

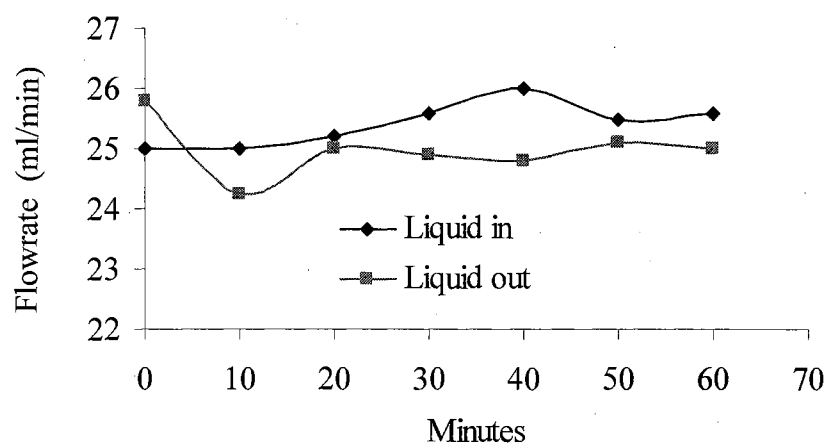


Figure 6.6. Total volumetric liquid balance around the microbubble generator

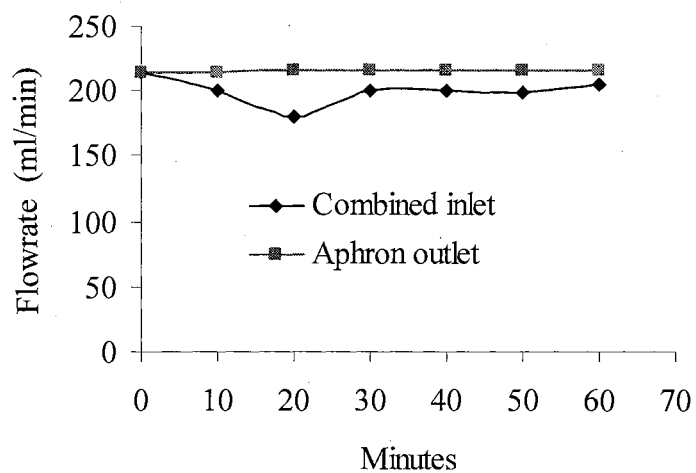


Figure 6.7. Total volumetric balance around the microbubble generator when gas flow rate was controlled by a rotameter. The combined inlet flow rate was calculated by adding the individual inlet gas and liquid flowrates.

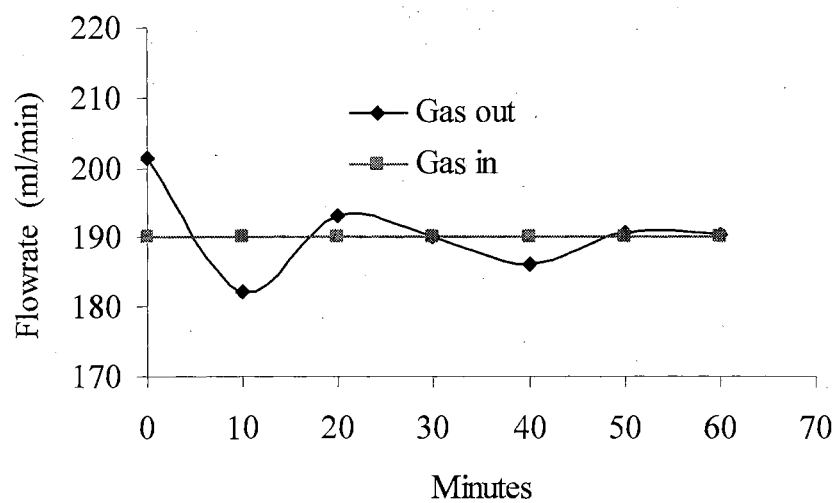


Figure 6.8. Total volumetric gas balance around the microbubblegenerator when inlet gas flow rate was controlled by a mass flow meter.

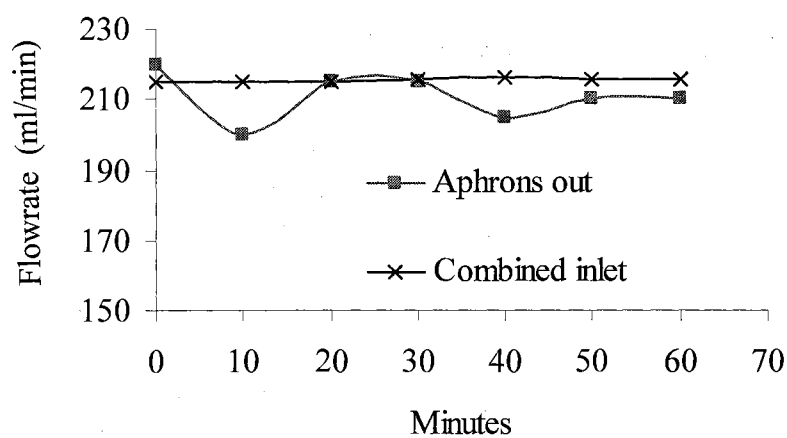


Figure 6.9. Total volumetric balance around the microbubble generator when inlet gas flow was controlled using a mass flow meter. The combined inlet flow rate was calculated by adding the inlet gas and liquid flow rates.

conditions. The maximum deviation was about 5%. Experiments conducted at inlet gas flow rates of 216, 300 and 400 ccm showed gas balances over 96% agreement in each case, the least being for 400 ccm (Figure 6.10). The percentage of inlet gas incorporated into the microbubbles for at inlet gas flow rates of 216, 300 and 400 ccm was about 94, 90 and 88% respectively.

#### **6.4.3 Effect of surfactant concentration**

Figure 6.11 shows the effect of surfactant concentration on the microbubble quality and the fraction of the total inlet gas incorporated into microbubbles. All experiments were conducted at an inlet gas flow rate of 190 ccm and a disc speed of 5950 rpm. Each data point shown in the figure was the average of seven data points collected over a sixty-minute period at 10-minute intervals. No appreciable change in quality was observed for the upper and lower ranges of the surfactant concentration and was constant at about 87%. The fraction of the total inlet gas incorporated into microbubbles varied between 0.92-0.95 for surfactant concentrations above 100 ppm. The value was only 0.82 at an 80-ppm surfactant concentration.

#### **6.4.4 Effect of salt addition**

The addition of 2.8 g/L of NaCl at different surfactant concentrations had no effect on the microbubble quality (Figure 6.12). This set of experiments was conducted at an inlet gas flow rate of 216 ccm and a disc speed of 5950 rpm. The gas fraction of the microbubbles (quality) was constant at about 86% for surfactant concentrations > 100 ppm. The total inlet gas incorporated into microbubbles increased from 75% to 93%

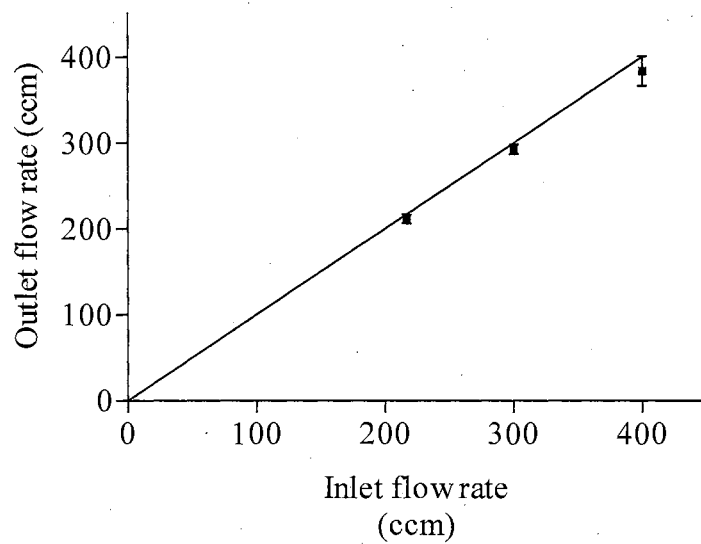


Figure 6.10. Volumetric gas balance for different gas flow rates.

Each data point is the average of 7 data points measured at 10 minute intervals. The line indicates an outlet flow/inlet flow ratio of unity.

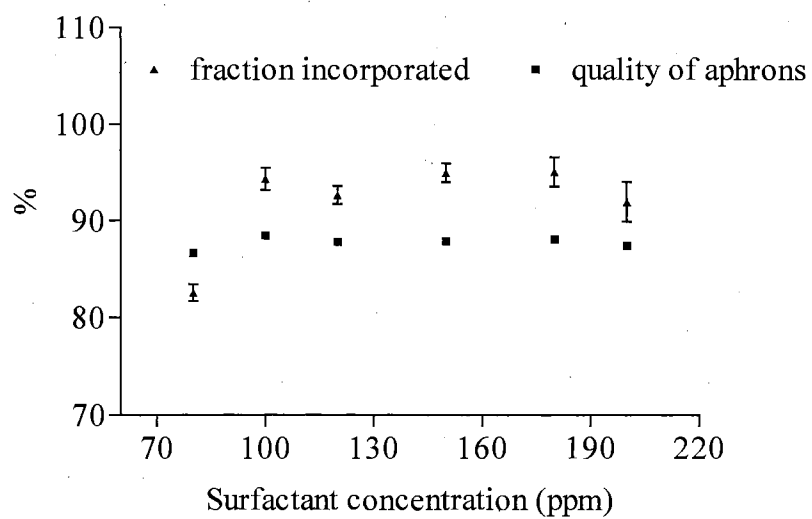


Figure 6.11. Effect of surfactant concentration on microbubble quality and gas incorporation. Each data point is the average of seven data points. The inlet gas flowrate was 216 ccm and the disc speed was 5950 rpm



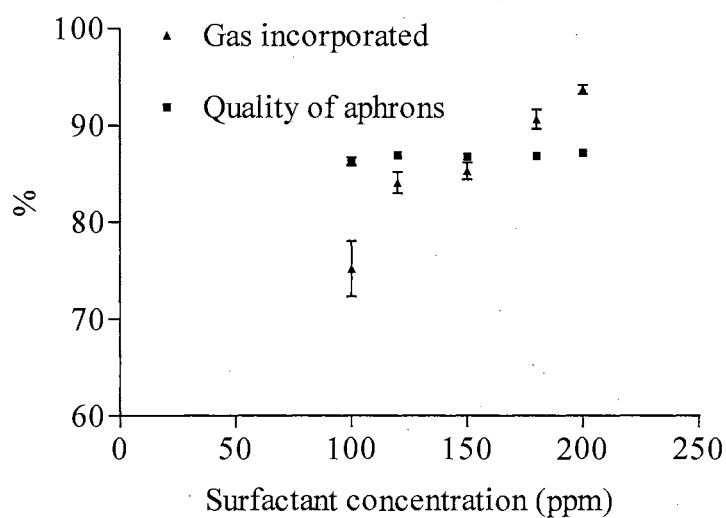


Figure 6.12. Effect of salt addition (2.8 g/L) on microbubble quality and gas incorporation at different surfactant concentrations. The inlet gas flow rate was 216 ccm and the disc speed was 5950 rpm. Each data point is the average of 7 data points.

when the surfactant concentration increased from 100 ppm to 200 ppm. The total gas incorporation was about 7-10% lower for surfactant concentrations up to 150 ppm as compared to the values obtained without the use of any salt (92-95%). Salt addition had negligible effect on the gas incorporation at surfactant concentrations of 180 and 200 ppm and the total inlet gas incorporated into microbubbles was about 90-93%.

#### **6.4.5 Effect of disc speed**

As shown in Figure 6.13, there was an increase in microbubble quality from 81% to 86% when the disc speed was increased from 4750 rpm to 5950 rpm. No significant microbubble production was observed at speeds lower than 4750 rpm. Similarly, the gas incorporation went up from 70% to 86%, when the disc speed was increased from 4750 to 5950 rpm. Effects of further increase in the disc speed could not be studied because of the limitations of the experimental apparatus.

#### **6.4.6 Effect of gas flowrate**

This set of experiments was conducted in the presence of salt (2.8 g/L) and surfactant concentration of 120 ppm and at a disc speed of 5950 rpm. As shown in Figure 6.14, increasing the inlet gas flow rate had a negative impact on both the quality and gas. The quality of microbubbles was about 86% at an inlet gas flow rate of 216 ccm and steadily dropped to 75% when the inlet gas was increased to 900 ccm. However, there was a negligible effect on the percentage of gas incorporated into microbubbles for an inlet gas flow rate up to 500 ccm and the value was steady at about 84%, except for a gas

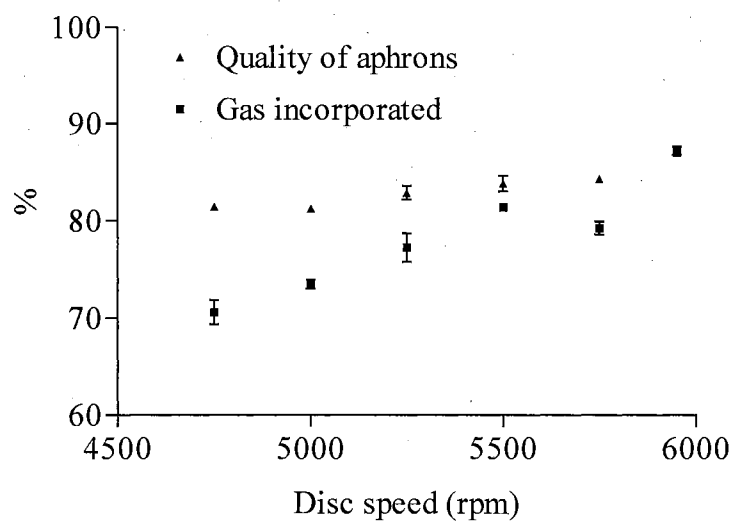


Figure 6.13. Effect of disc speed on microbubble quality and gas incorporation.

Each data point is the average of 2 data points. The inlet gas flow rate was 216 ccm with a 120 ppm surfactant concentration.

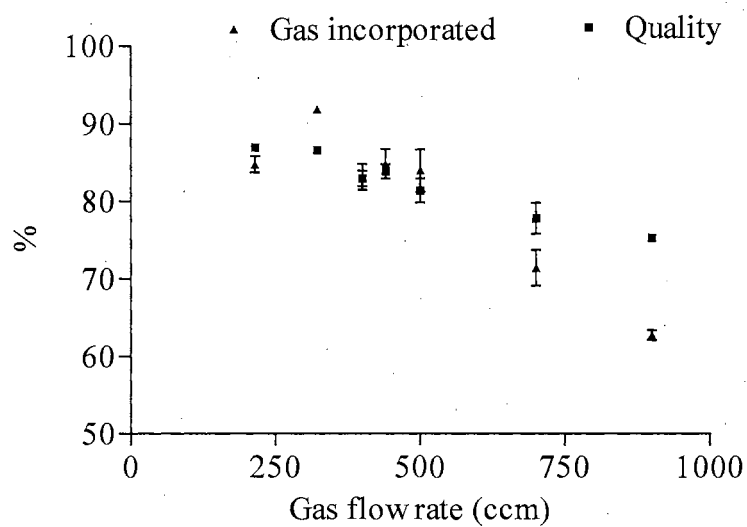


Figure 6.14. Effect of inlet gas flow rate on quality of microbubbles and gas incorporated. The experiment was run with salt addition (2.8 g/L) and surfactant concentration of 120 ppm and disc speed of 5950 rpm.

flow of 321 ccm for which it was 91%. The percentage dropped down to 71.5 and 62.8 at gas inlet flow rates of 700 and 900 ccm, respectively.

#### **6.4.7 Effect of gas/liquid ratio**

An inverted U shaped curve was obtained (Figure 6.15) when the ratio of inlet gas flow to liquid flow was plotted against the percentage of gas incorporated. The maximum gas incorporated was 91% at a ratio of 7, while the lowest value was about 62% for a gas/liquid ratio of 4.75.

### **6.5 Discussion**

The four baffle design for the microbubble generator significantly improved the quality of microbubbles as compared to two baffle designs reported in the literature (Sebba, 1985, Bredwell and Worden, 1998). The gas fraction of the microbubbles was consistently above 85% as compared to about 60-70% as reported earlier (Kaster et al., 1990, Bredwell and Worden, 1998, Hashim et al., 1998, Sebba, 1985). A higher quality of microbubbles is important because the liquid inlet flow rate would be lower for a given microbubble flow rate. The lower liquid flow rate will reduce the operational load on a cell-recycle system and increase the working life of the cell-recycle filter. This would likely have a positive impact on the economics of fermentation. The total gas incorporated into microbubbles is also critical since the unincorporated gas would be unutilized and wasted. The best percentage of gas incorporated using the modified design was approximately 95% at inlet gas flow rates of 216 ccm. No values from previous

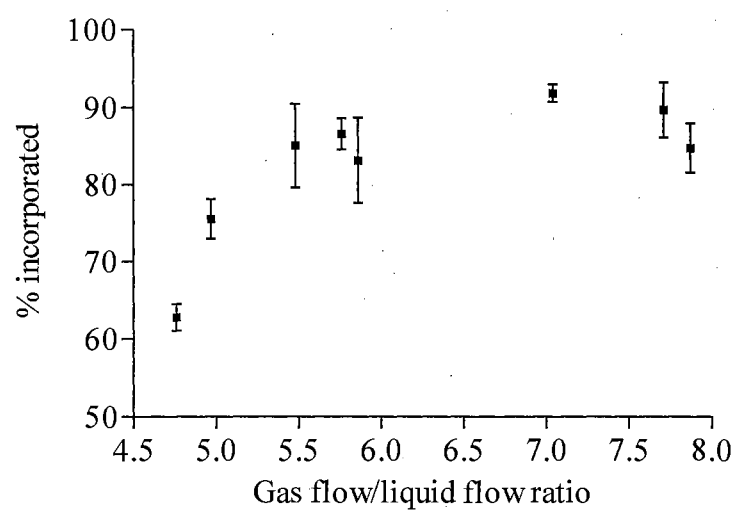


Figure 6.15. Effect of inlet gas flow/liquid flow ratio on percentage of incorporated gas. The experiment was conducted at 120 ppm surfactant concentration and salt addition (2.8 g/L) and a disc speed of 5950 rpm.

literature were available for comparison since most of the previous studies were done with either nitrogen or air. The percentage of gas incorporated into microbubbles is a critical consideration since it is endeavored to maximize the producer gas incorporation into microbubbles and minimize the amount of unincorporated gas. The recycle of unincorporated gas back to the microbubble generator needs to be studied for complete gas incorporation. The bubble size was measured using a Malvern mastersizer. The average microbubble diameter was close to the values reported in literature of 10-100  $\mu\text{m}$  (Jauregi et al., 1997). 95% of the bubbles had a diameter of 100  $\mu\text{m}$  or smaller, with 80% smaller than 76  $\mu\text{m}$ . Thus, the bubble size of the microbubble was significantly lower than the bubble size (3-5 mm) obtained with spargers (Bredwell and Worden, 1998). Thus, resistance 3 (described in section 6.1) can be lowered by the use of microbubbles. However, the mass transfer coefficients could not be evaluated (either with  $\text{N}_2$  or  $\text{O}_2$ ) because of equipment limitations (no dissolved  $\text{O}_2$  or  $\text{N}_2$  probe).

The overall material balance was less accurate when a rotameter was used for controlling the inlet gas flow rate. The inlet gas flow rate was measured at the start of the experiment and assumed to be constant throughout although slight fluctuations in position of the ball of the rotameter were observed. However, the gas balance was greater than 95% accurate when the rotameter was replaced by a mass flow meter to control the inlet gas flow.

Tween 20 was chosen as the surfactant in this study because of its nontoxic nature to many culture systems and relatively low cost and easy availability (Bredwell et al., 1997). However, the toxicity and inhibition of cell growth by Tween 20, specific to fermentation of producer gas by P7 must be investigated in the future. The surfactant concentrations

used in this study were about 1.5 to 3 times the critical micelle concentration for Tween 20 (CMC = 60 ppm). Critical micelle concentration (CMC) is the lowest surfactant concentration needed for the formation of colloidal structures (such as microbubbles). There was no effect on quality of microbubbles at the tested surfactant concentration levels. Experiments were not conducted for concentrations below 80 ppm since it has been reported that the dispersions formed are unstable at concentrations lower than the CMC because of the insufficient surfactant present to stabilize a large amount of surface area (Bredwell et al., 1997). Similarly, increasing the concentration above 3 times the CMC does not offer any significant benefits. However, the optimal surfactant concentration would also depend on the mass transfer coefficient and cell growth rates. The increased surfactant concentration will result in a thicker surfactant shell around the microbubble, thus lowering the overall mass transfer coefficient. The cell growth could also be negatively affected at high surfactant concentrations due to a possible inhibitory effect.

The addition of salt did not have any effect on the quality of microbubbles for the surfactant concentrations tested in this study. This is attributed to the fact that neutral salts like sodium chloride have a very little influence on the CMC of non-ionic surfactants. However, the cause of decreased fractional gas incorporation must be determined.

The critical speed for microbubble formation was 4750 rpm. The quality of microbubbles was independent of the disc speed, but the percentage of gas incorporated was directly proportional to the disc speed. Increasing the rotational disc speed produces stronger waves that strike the baffle surface and hence more gas is entrained in the bubble



per unit time. This explains the increase in gas incorporation with increase in disc speed. Therefore, the highest possible disc speed is favorable (5950 rpm in this case) for maximum gas incorporation.

There was a reduction in both the microbubble quality and gas incorporation with increase in the inlet gas flow rate. However, the effect was negligible for gas flow rates up to 500 ccm. The reduction is attributed to the insufficient disc speed and available shear area for formation of microbubbles. Although the gas fraction in the microbubbles reduced to 75% at high gas flow rates, it was higher than the values reported in the past (Kaster et al., 1990, Bredwell and Worden, 1998, Hashim et al., 1998, Sebba, 1985). Thus, a four-liter microbubble generator (with working liquid volume of only one liter) is capable of gas delivery in the form of microbubbles upto flow rates of 900 ccm. The gas flow rate of 900 ccm is about 4-5 times the gas flow rate used for a four-liter fermenter (based on inlet gas flow rate information in Chapters 3 and 4). Hence, the ratio (microbubble generator volume/reactor volume) of about 0.2-0.25 can be used for future potential scale-up and integration of the microbubble generator and the reactor for producer gas fermentations, although the optimal ratio can be determined by evaluation of the mass-transfer coefficients.

The optimal gas inlet/liquid inlet ratio was in the range of 7-7.7. Lower gas incorporation was observed at lower and higher ratios because of flooding of the microbubble generator with gas or liquid. The optimal ratio would be helpful in scale-up of the microbubble generator for gas transfer in commercial scale fermenters.

## **6.6 Conclusions**

A modified design for a microbubble generator has been discussed in this chapter. The four baffle design yielded a significant increase in the quality of microbubbles over the existing two baffle designs.

The microbubble generator was operated continuously for more than 90 minutes at steady state and accurate material balances for gas and liquid were established.

Future work will involve the estimation of mass transfer coefficients using a microbubble generator, and the integration of the microbubble generator with the bioreactor for producer gas fermentations.

## **CHAPTER 7**

### **CONCLUSIONS AND FUTURE WORK**

The development of low-cost, sustainable, and renewable energy sources has been a major focus in light of diminishing petroleum reserves. Unlike fossil fuels, ethanol obtained from renewable sources helps maintain and reduce global greenhouse gas emissions, in addition to several economic and social benefits. Therefore, there is a tremendous potential for conversion of underutilized low-cost biomass to liquid fuels such as ethanol and other useful products in lieu of traditional fossil fuels. Ethanol can be used as a supplement to gasoline or as an alternative transportation fuel in the future, despite the current low usage.

There is a need to produce ethanol via inexpensive routes, since the current wholesale ethanol prices cannot economically compete with gasoline, without incentives from the state and federal governments.

Almost all of the current commercial ethanol production in the United States is from the fermentation of sugar crops (sugar cane and sugar beet) and from starchy crops (maize, wheat and corn). Due to the relatively high cost of these raw materials, several processes are being investigated for the production of ethanol from underutilized low-cost biomass such as grasses, woodchips, or municipal waste.

The gasification of biomass to producer gas, followed by fermentation of the producer gas, is one such process that has a tremendous potential for commercial production of ethanol. Recent studies at Oklahoma State University have shown that about 90-94% of carbon present in switchgrass was converted to carbon in the producer gas, while the remaining 6-10% remained unutilized in the form of ashes and tars. The 6-10% unutilized carbon is lower than the 10-40% unutilized carbon (in the form of lignin) in traditional fermentation processes.

In view of no prior knowledge available on fermentation of biomass-generated producer gas, this research was targeted at investigating some of the critical process parameters including cell concentration, substrate utilization, and acid/alcohol production during fermentation of biomass-generated producer gas and comparing these parameters to those obtained previously by using clean bottled gases. A novel anaerobic bacterium, P7, was used as the biological catalyst and the fermentation studies were conducted using a four-liter bubble column bioreactor.

## **7.1 Key research findings**

*Integration of gasifier and bioreactor:* The successful implementation of generating producer gas from biomass and then fermenting the producer gas has been demonstrated for the first time. Following the introduction of producer gas, the cells stopped growing but did not die, after a 1.5-day delay. The delay was extended by two more days with better gas clean up. The gas clean up involved the use of a 10% acetone solution instead of 100% water. Thus, the diminishing cell OD in the continuous mode was due to cell washout and not due to cell death. The possibility exists that following the introduction of

producer gas, there is an alteration in the metabolic pathway(s) due to some trace species in the producer gas or the buildup of a metabolite in the medium. Although the cells stopped growing, they were metabolically active and capable of converting producer gas to ethanol. The cells began growing again if “clean” bottled gases were introduced following exposure to the producer gas. Ethanol was primarily produced once the cells stopped growing (ethanol is non-growth associated) with biomass-generated producer gas. The  $H_2$  utilization ceased shortly after exposure to producer gas. The decrease in hydrogen uptake after introduction of producer gas is likely explained by the inactivation or inhibition of hydrogenase. Previous studies have shown that nitric oxide (Hyman and Arp, 1988 and 1991), acetylene (Tibelius and Knowles, 1984, Sun et al., 1992) and oxygen (Maness et al., 2002) are strong inhibitors of hydrogenase, all of which have been identified as constituents in the biomass-generated producer gas. The pH rise with producer gas was not due to the dissolution of constituents of producer gas, but possibly due to the conversion of acetate to ethanol until the acetate was depleted.

*Effect of individual impurities:*  $O_2$  (up to 1900 ppm) and  $CH_4$  (4.5 vol%) had no effect on the cell OD during continuous fermentation.  $H_2$  utilization was unaffected after the introduction of  $O_2$  and  $CH_4$ . No detectable change in the concentrations of ethanol and butanol was observed with 1000 ppm  $O_2$ . Similarly, the concentrations of ethanol, acetate, butanol and butyrate remained steady after the introduction of 4.5 vol%  $CH_4$ . Although P7 is an anaerobic acetogen, it can tolerate and grow in the presence of  $O_2$  up to 1900 ppm. P7 can survive and recover from pH shocks (pH of about 6.7), even though the optimal pH range for growth and product formation is between 5 and 6.

*Design and assessment of a microbubble generation system:* The four baffle design for the microbubble generator significantly improved the quality of microbubbles as compared to the previous designs. The quality (fractional gas composition) of microbubbles was consistently above 85% and about 95% of the inlet gas was incorporated into microbubbles. Volumetric gas and liquid balances were established for a continuous microbubble generation system with about 95% agreement in the balance. The critical disc speed for aphron production for this particular microbubble generator was found to be 4750 rpm. The quality of microbubbles produced was independent of the disc speed between 4750-5950 rpm, but the percentage of gas incorporated into microbubbles was found to be directly proportional to the disc speed. Increasing the rotational disc speed produces stronger waves that strike the baffle surface and hence more gas is entrained in the bubble per unit time. This explains the increase in gas incorporation with increase in disc speed. The surfactant concentration (without salt addition) did not affect the quality or percentage of gas incorporation up to 100 ppm. Addition of salt (2.8 g/L NaCl) to the surfactant solution had negligible effect on the quality of microbubbles, but the percentage of gas incorporated was directly related to the surfactant concentrations up to 200 ppm. This is attributed to the fact that neutral salts like sodium chloride have a very little influence on the CMC of non-ionic surfactants. However, the cause of decreased fractional gas incorporation must be determined.

*Media optimization:* A successful screening design for identification of nutrients affecting cell growth was performed. The concentration of several nutrients was reduced to minimize media cost without affecting the cell OD. Cell OD was inversely proportional (at the levels tested in this study) to the concentration of sodium chloride,

ammonium chloride, potassium chloride, potassium chloride and calcium chloride in the fermentation media and directly proportional to the concentration of magnesium sulfate. Lowering the concentration of pyridoxine favored cell growth, while the reduction in p-amino benzoic acid negatively affected the cell OD. Vitamin B<sub>12</sub> and d-biotin can be eliminated from the media without affecting the cell OD. However, yeast extract present in the nutrient media, of which the composition is undetermined, could be a source of d-biotin. The key nutrients identified after the screening experiments for trace metals are nitrilotriacetic acid, manganese sulfate, zinc sulfate, nickel chloride, and sodium molybdate. The first three nutrients enhanced cell OD, while the latter two inhibited cell growth at higher levels, although the effect (positive and negative) was very small. Models were developed after the optimization study with over 99% confidence in the model reliability. Using the optimized concentrations obtained from the above experiments, a cost analysis for minerals, vitamins, and trace metals show a reduction of 78%, 87% and 0.5% in the final cost of the optimized fermentation media as compared to the original media.

Thus, to conclude, the following summarizes the significant findings in this study:

- H<sub>2</sub> utilization was observed for the first time on a 4-liter scale.
- Cells stopped growing after a 1.5 delay following introduction of producer gas, but did not die in both batch and continuous modes.
- Ethanol was primarily produced following introduction of producer gas, suggesting non-growth associated ethanol production.
- H<sub>2</sub> utilization stopped completely, shortly after introduction of producer gas.

- Cells began growing again if “clean” bottled gases were introduced following exposure to the producer gas.
- P7 is a robust organism and can tolerate pH shocks.
- O<sub>2</sub> (up to 1900 ppm) and CH<sub>4</sub> (4.5 vol %) did not affect the cell OD, pH, product formation and substrate utilization.
- Elimination of d-biotin and vitamin B<sub>12</sub> from the nutrient media did not affect the cell OD.
- The overall media cost was successfully reduced by about 75%.
- An improved microbubble generator was designed, capable of producing microbubbles of over 85% quality.
- Quality of microbubbles was independent of the disc speed, salt addition and surfactant concentration over the ranges studied.
- The fraction of gas incorporated into microbubbles was directly proportional to disc speed and surfactant concentration.

## 7.2 Future studies

*Cell recycle:* A cell recycle system must be incorporated in the product outlet loop to prevent loss of cells during the continuous mode, especially when cells stop growing when exposed to producer gas, and to increase the cell concentration inside the bubble column reactor. Since the product formation is directly proportional to the cell concentration in the reactor, a higher cell OD will result in higher product concentration. The cell recycle system would involve the use of two hollow fiber membrane filters connected in parallel with pressure gauges at the upstream and downstream ends. The use



of a dual filter system will enable a continuous recycle system. Upon fouling (indicated by higher upstream pressure) of one filter module, the flow of the fermentation broth can be switched through the clean filter module. The clogged filter module can be either cleaned by back flushing with liquid media or by a high-pressure nitrogen stream.

*Dual reactor set up:* Previous studies with P7 have indicated that cell growth and acetate formation are favored at a higher pH (of about 6), while solvent (ethanol) formation occurs at a lower pH (of about 5). Thus, by using a dual reactor system in series, in which the first reactor is operated at a pH of 6 and the second reactor is operated at a pH of 5, the cell concentration and ethanol production can be maximized. The gas flow would be counter current, with the unconverted gas from the second reactor being fed into the first reactor along with some additional fresh gas.

*Media optimization:* The final cost of the media directly influences the economics of production of ethanol. Currently, media components like yeast extract and MES buffer constitute about 90% of the total media cost. Hence, the use of low cost alternative nutrient sources such as soybean hydrolysate and buffers such as sodium bicarbonate to replace expensive additives like yeast extract and MES buffer must be investigated in the future. The next step in media optimization will involve the use of a full factorial design on the key nutrients identified by the initial screening design with cell OD and ethanol production as the response variables. A full factorial design will help identify individual factors and their interactions that influence the cell OD and ethanol production.

*Enzyme assays:* The effect of producer gas contaminants like nitric oxide, acetylene, ethane and ethylene, on key enzymes such as hydrogenase, CODH, formate dehydrogenase and ethanol dehydrogenase must be further explored. Future studies will

also involve a comprehensive analysis of the biomass generated producer gas to identify possible contaminants that might cause inactivation or inhibition of the enzymes discussed above.

## REFERENCES

- Abrini, H., Naveau, H., Nyns, E. J. (1994). *Clostridium autoethanogenum*, sp. nov., an anaerobic bacterium that produces ethanol from carbon monoxide. Arch Microb, **161**, 345-351.
- Ahmed, F. E. (2001). Toxicology and human health effects following exposure to oxygenated or reformulated gasoline. Toxicology Letters, **123**, 89-113.
- Bailey, J. E., Ollis, D. F. (1986). Biochemical engineering fundamentals. New York: McGraw-Hill, 2<sup>nd</sup> edition.
- Belgiorno, V., Feo, G. D., Rocca, C. D., Napoli, R. M. A. (2003). Energy from gasification of solid wastes. Waste Management, **23**, 1-15.
- Bjerknes, K., Sontum., P. C., Smistad, G., Agerkvist, I. (1997). Preparation of polymeric microbubbles: formulation studies and product characterization. International Journal of Pharmaceutics, **158**, 129-156.
- Blackburn, W. J., Teague J. M. (1998). Coordinating California's efforts to promote waste to alcohol production. Appl Biochem Biotech, **70-72**, 821-841.
- Blanch, H. W., Clark, D. S. (1997). Biochemical engineering. New York, Marcel Dekker.
- Bredwell, M. D., Telgenhoff, M. D., Worden, R. M. (1995). Formation and coalescence properties of microbubbles. Applied Biochemistry and Biotechnology, **51/52**, 501-509.
- Bredwell, M. D., Telgenhoff, M. D., Barnard, S., Worden, R. M. (1997). Effect of surfactants on carbon monoxide fermentations by *Butyribacterium methylotrophicum*. Applied Biochemistry and Biotechnology, **63-65**, 637-647.
- Bredwell, M. D., Worden, R. M. (1998). Mass transfer properties of microbubbles: experimental studies. Biotechnology Progress, **14**, 31-38.
- Bredwell, M. D., Srivastava, P., Worden, R. M. (1999). Reactor design issues for synthesis gas fermentations. Biotechnology Progress, **15**, 834-844.
- Bridgewater, A. V. (1994). Catalysis in thermal biomass conversion. Applied Catalysis, **116**, 5-47.

- Bridgewater, A. V. (2003). Renewable fuels and chemicals by thermal processing of biomass. Chemical Engineering Journal, 97, 87-102.
- Bryant, M. P. (1972). Commentary on the hungate technique for culture of anaerobic bacteria. American Journal of Clinical Nutrition, 25, 1324-1328.
- Burns, S. E., Yiacoimi, S., Tsouris, C. (1997). Microbubble generation for environmental and industrial separations. Separation and Purification Technology, 11, 221-232.
- Buschhorn, H., Durre, P., Gottschalk, G. (1989). Production and utilization of ethanol by the homoacetogen acetobacterium woodii. Applied. Environ. Microbiol., 55, 1835-1840.
- Cateni, B. G., Bellmer, D. D., Huhnke, R. L., Lelo, M. M., Bowser, T. J. (2000). Recirculation in a fluidized bed gasifier to minimize oxygen content in synthesis gas from biomass. ASAE Paper No. 006033, Annual International Meeting, Milwaukee, WI.
- Cateni, B.G., Bellmer, D. D., Huhnke, R. L., Bowser, T. J. (2003). Effect of switchgrass moisture content on producer gas composition and quality from a fluidized bed gasifier. ASAE Paper No. 036029, Annual International Meeting, Las Vegas, NV.
- Chang, I. S., Kim, B. H., Lovitt, R. W., Bang, J. S. (2001). Effect of CO partial pressure on cell-recycled continuous CO fermentation by *Eubacterium limosum* KIST612. Process Biochemistry, 37, 411-421.
- Chatterjee, S., Grethlein, A. J., Worden, R. M., Jain, M. K. (1996). Evaluation of support matrices for an immobilized cell gas lift reactor for fermentation of coal derived synthesis gas. Journal of Fermentation and Bioengineering, 81, 2, 158-162.
- Chum, H. L., Overend, R. P. (2001). Biomass and renewable fuels. Fuel Processing Technology, 71, 187-195.
- Ciriello, S., Barnett, S. M., Deluise, F. J. (1982). Removal of heavy metals from aqueous solutions using microgas dispersions. Sep. Sci. Technol., 17, 521-530.
- Clausen, E. C., Gaddy, J. L. (1993). Concentrated sulfuric acid process for converting lignocellulosic materials to sugars. United States Patent # 5,188,673.
- Cockshott, A. R., Sullivan, G. R. (2001). Improving the fermentation medium for Echinocandin B production. Part I: sequential statistical experimental design. Process Biochemistry, 36, 7, 647-660.
- Cowger, J. P., Klasson, K. T., Ackerson, M. D., Clausen, E. C., Gaddy, J. L. (1992). Mass-transfer and kinetic aspects in continuous bioreactors using *Rhodospirillum rubrum*. Applied Biochemistry and Biotechnology, 34/35, 613-624.

- Cummer, K. R., Brown, R. C. (2002). Ancillary equipment for biomass gasification. Biomass and Bioenergy, 23, 2, 113-128.
- Devi, L., Ptasiński, K. J., Janssen, F. J. J. G. (2003). A review of the primary measures for tar elimination in biomass gasification processes. Biomass and Bioenergy, 24, 2, 125-140.
- DOE Report. (1994). Bench-scale demonstration of biological production of ethanol from coal synthesis gas. Quarterly report, DE-AC22-92PC92118.
- Doukov, T., Seravalli, J., Stezowski, J. J., Ragsdale, S. W. (2000). Crystal structure of a methyltetrahydrofolate- and corrinoid-dependent methyltransferase. Structure with Folding & Design, 8, 8, 817-830.
- Dowel. (1981). Laboratory methods in anaerobic bacteriology. CDC laboratory manual, US Department of Public Health Service, HHS publication, Atlanta, CDC-81-8272.
- Drake, H. L. (1982a). Occurrence of nickel in carbon monoxide dehydrogenase from *Clostridium pasteurianum* and *Clostridium thermoaceticum*. Journal of Bacteriology, 149, 2, 561-566.
- Drake, H. L. (1982b). Demonstration of hydrogenase in extracts of the homoacetate-fermenting bacterium *Clostridium thermoaceticum*. Journal of Bacteriology, 150, 2, 702-709.
- Drake, H. L. (1994). Acetogenesis. Chapman and Hall. New York.
- Furman, A. H., Kimura, S. G., Ayala, R. E., Joyce, J. F. (1993). Biomass gasification pilot plant study. EPA Project Summary, EPA/600/SR-93/170, 1-2.
- Gaddy, J. L., Sitton, O. C. (1982). Ethanol production with an immobilized cell reactor. United States Patent # 4,355,108.
- Gaddy, J. L., Clausen, E. C. (1992). *Clostridium ljungdahlii*, an anaerobic ethanol and acetate producing microorganism. United States Patent # 5,173,429.
- Gaddy, J. L. (1997). *Clostridium* strain which produces acetic acid from waste gases. United States Patent # 5,593,886.
- Genthner, B. R. S., Bryant, M. P. (1982). Growth of *Eubacterium limosum* with carbon monoxide as the energy source. Appl. Environ. Microbiol., 43, 70-74.
- Gil, J., Aznar, M., Caballero, M., Frances, E., Corella, J. (1997). Biomass gasification in fluidized bed at pilot plant scale with steam-oxygen mixtures, product distribution of very different operating conditions. Energy and Fuels, 11, 6, 1109-1118.

- Gogate, P. R., Beenackers, A. C. M., Pandit, A. B. (2000). Multiple-impeller systems with a special emphasis on bioreactors: a critical review. Biochemical Engineering Journal, 6, 2, 109-144.
- Greene, D. L., Schafer, A. (2003). Reducing green house gas emissions from U.S. transportation. Prepared for the Pew Center on Global Climate Change, May 2003, 1-80.
- Grethlein, A. J., Worden, R. M., Jain, M. K., Datta, R. (1990). Continuous production of mixed alcohols and acids from carbon monoxide. Applied Biochemistry and Biotechnology, 24/25, 875-884.
- Grethlein, A. J., Jain, M. K. (1992). Bioprocessing of coal-derived synthesis gases by anaerobic bacteria. Tibtech, 10, 418-423.
- Grupe, H., Gottschalk, G. (1992). Physiological events in *Clostridium acetobutylicum* during shift from acidogenesis to solventogenesis in continuous culture and presentation of a model for shift induction. Applied and Environmental Microbiology, 58, 12, 3896-3902.
- Hashim, M. A., Gupta, B. S. (1998). The application of colloidal gas aphrons in the recovery of fine cellulose fibres from paper mill wastewater. Bioresource Technology, 64, 199-204.
- Hashim, M. A., Gupta, B. S., Kumar, S. V., Lim, R., Lim, S. E., Tan, C. C. (1998). Effect of air to solid ratio in the clarification of yeast by colloidal gas aphrons. Journal of Chemical Technology and Biotechnology, 71, 335-339.
- He, B. Q., Wang, J. X., Hao, J. M., Yan, X. G., Xiao, J. H. (2003). A study on emission characteristics of an EFI engine with ethanol blended gasoline fuels. Atmospheric Environment, 37, 949-957.
- Himmel, M. E., Adney, S. A., Baker, J. O., Elander, R., McMillan, J. D., Nieves, R. A., Sheehan, J. J., Thomas, S. R., Vinzant, T. B., Zhang, M. (1997). Fuels and Chemicals from Biomass, American Chemical Society, 1-45.
- Hohenstein, W. G., Wright, L. L. (1994). Biomass energy production in the United States: an overview, Biomass and Bioenergy, 6, 161-173.
- Houng, J. Y., Hsu, H. F., Liu, Y. H., Wu, J. Y. (2003). Applying the Taguchi robust design to the optimization of the asymmetric reduction of ethyl 4-chloro acetoacetate by bakers' yeast. Journal of Biotechnology, 100, 3, 239-250.
- Hu, S. I., Drake, H. L., Wood, H. G. (1982). Synthesis of acetyl coenzyme A from carbon monoxide, methyltetrahydrofolate, and coenzyme A by enzymes from *Clostridium thermoaceticum*. Journal of Bacteriology, 149, 440-448.

- Hwang, S., Hansen, C. L. (1997). Modeling and optimization in anaerobic bioconversion of complex substrates to acetic and butyric acids. Biotechnology and Bioengineering, 54, 5, 451-460.
- Hyman, M. R., Arp, D. J. (1988). Reversible and irreversible effects of nitric oxide on the soluble hydrogenase from *Alcaligenes eutrophus* H16. The Biochemical Journal, 254, 2, 469-475.
- Hyman, M. R., Arp, D. J. (1991). Kinetic analysis of the interaction of nitric oxide with the membrane-associated, nickel and iron-sulfur-containing hydrogenase from *Azotobacter vinelandii*. Biochemica et Biophysica Acta, 1076, 2, 165-172.
- Idris, A., Ismail, A. F., Noordin, M. Y., Shilton, S. J. (2002). Optimization of cellulose acetate hollow fiber reverse osmosis membrane production using Taguchi method. Journal of Membrane Science, 205, 1-2, 223-237.
- Ingram, L. O., Lai, X., Moniruzzaman, M., Wood, B. E., York, S. W. (1997). Fuels and chemicals from biomass, American Chemical Society, 57-73.
- Iranmahboob, J., Nadim, F., Monemi, S. (2002). Optimizing acid-hydrolysis: a critical step for production of ethanol from mixed wood chips. Biomass and Bioenergy, 22, 401-404.
- Jauregi, P., Gilmour, S., Varley, J. (1997). Characterization of colloidal gas aphrons for subsequent protein recovery. Chemical Engineering Journal, 65, 1-11.
- Jauregi, P., Varley, J. (1998). Colloidal gas aphrons: a novel approach to protein recovery. Biotechnology and Bioengineering, 59, 4, 471-481.
- Jauregi, P., Varley, J. (1999). Colloidal gas aphrons: potential applications in biotechnology, Tibtech October, 17, 389-395.
- Jenkins, K. B., Michelsen, D. L., Novak, J. T. (1993). Application of oxygen microbubbles for in-situ biodegradation of p-xylene contaminated groundwater in a soil column. Biotechnology Progress, 9, 394-400.
- Kadam, K. L., McMillan, J. D. (2003). Availability of corn stover as a sustainable feedstock for bioethanol production. Bioresource Technology, 88, 17-25.
- Kalil, S. J., Maugeri, F., Rodrigues, M. I. (2000). Response surface analysis and simulation as a tool for bioprocess design and optimization. Process Biochemistry, 35, 6, 539-550.

- Kaster, J. A., Michelsen, D. L., Velandar, W. H. (1990). Increased oxygen transfer in a yeast fermentation using a microbubble dispersion. Applied Biochemistry and Biotechnology, 24/25, 469-484.
- Kim, B. H., Bellows, P., Datta, R., Zeikus, J. G. (1984). Control of carbon and electron flow in *Clostridium acetobutylicum* fermentations: Utilization of carbon monoxide to inhibit hydrogen production and to enhance butanol yields. Applied and Environmental Microbiology, 48, 4, 764-770.
- Klasson, K. T., Ackerson, M. D., Clausen, E. C., Gaddy, J. L. (1992). Bioconversion of synthesis gas into liquid or gaseous fuels. Enzyme Microb. Technol., 14, 602-608.
- Klasson, K. T., Ackerson, M. D., Clausen, E. C., Gaddy, J. L. (1993). Biological conversion of coal and coal-derived synthesis gas. Fuel, 72, 12, 1673-1678.
- Kosaric, N., Velikonja, J. (1995). Liquid and gaseous fuels from biotechnology: challenge and opportunities. FEMS Microbiology Reviews, 16, 111-142.
- Krishnan, M. S., Taylor, F., Davison, B. H., Nghiem, N. P. (2000). Economic analysis of fuel ethanol production from corn starch using fluidized-bed bioreactors. Bioresource Technology, 75, 2, 99-105.
- Laurinavichene, T. V., Chanal, A., Wu, L. F., Tsygankov. (2001). Effect of O<sub>2</sub>, H<sub>2</sub> and redox potential on the activity and synthesis of hydrogenase 2 in *Escherichia coli*. Res. Microbiol., 152, 793-798.
- Liou, S., Tanner, R. S. (2002). Production of acids and alcohols from CO by clostridial strain P7. Presented at ASM 102<sup>nd</sup> General Meeting, Salt Lake City, UT, May 20, Abstract O-11.
- Liou, S., McGuire, J. E., Tanner, R. S. (2002). Conversion of synthesis gas to ethanol by Clostridial strain P7. Presented at ASM 102<sup>nd</sup> General Meeting, Salt Lake City, UT, May 20, Abstract O-10.
- Liu, H., Gibbs, B. M. (2003). Modeling NH<sub>3</sub> and HCN emissions from biomass circulating fluidized bed gasifiers. Fuel, 82, 13, 1591-1604.
- Ljungdahl, L. G., Andersen, J. R. (1975). Tungsten, a component of active formate dehydrogenase from *Clostridium thermoaceticum*. FEBS Letters, 54, 2, 279-282.
- Ljungdahl, L. G. (1986). Annual Review of Microbiology, 40, Annual Review Inc., Palo Alto, CA, 415-440.
- Lorowitz, W. H., Bryant, M. P. (1984). *Peptostreptococcus productus* strain that grows rapidly with CO as the energy source. Appl. Environ. Microbiol., 47, 961-964.



- Lynd, L., Kerby, R., Zeikus, J. G. (1982). Carbon monoxide metabolism of the methylotrophic acidogen *Butyribacterium methylotrophicum*. Journal of Bacteriology, 149, 255-263.
- Madhukar, G. R., Elmore, B. B., Huckabay, H. K. (1996). Microbial conversion of synthesis gas components to useful fuels and chemicals. Applied Biochemistry and Biotechnology, 57/58, 243-251.
- Maness, P. C., Weaver, P. F. (2001). Evidence of three distinct hydrogenase activities in *Rhodospirillum rubrum*. Applied Microbiology and Biotechnology, 57, 751-756.
- Maness, P. C., Smolinski, S., Dillon, A. C., Heben, M. J., Weaver, P. F. (2002). Characterization of the oxygen tolerance of hydrogenase linked to a carbon monoxide oxidation pathway in *Rubrivivax gelatinosus*. Applied and Environmental Microbiology, 68, 6, 2633-2636.
- Maness, P. C., Weaver, P. F. (2002). Hydrogen production from a carbon-monoxide oxidation pathway in *Rubrivivax gelatinosus*. International Journal of Hydrogen Energy, 27, 1407-1411.
- Marlatt, J. A., Datta, R. (1986). Acetone-butanol fermentation process development and economic evaluation. Biotechnology Progress, 2, 23-30.
- McCabe, W. L., Smith, J. C. (1956). Unit operations of chemical engineering. McGraw Hill book company, 2<sup>nd</sup> edition.
- McKendry, P. (2002a). Energy production from biomass (part 1): overview of biomass. Bioresource Technology, 83, 37-46.
- McKendry, P. (2002b). Energy production from biomass (part 3): gasification technologies. Bioresource Technology, 83, 55-63.
- McKendry, P. (2002c). Energy production from biomass (part 2): conversion technologies. Bioresource Technology, 83, 37-46.
- McLaughlin, S. B., Walsh, M. E. (1998). Evaluating environmental consequences of producing herbaceous crops for bioenergy. Biomass and Bioenergy, 14, 4, 317-324.
- Menon, S., Ragsdale, S. W. (1996). Unleashing hydrogenase activity in carbon monoxide dehydrogenase/acetyl-CoA synthase and pyruvate: ferredoxin oxidoreductase. Biochemistry, 35, 15814-15821.
- Menon, S., Ragsdale, S. W. (1997). Evidence that carbon monoxide is an obligatory intermediate in anaerobic acetyl-CoA synthesis. Biochemistry, 35, 37, 12119-12125.

- Nadim, F., Zack, P., Hoag, G. E., Liu, S. (2001). United States experience with gasoline additives. Energy Policy, 29, 1-5.
- Narvaez, I., Orio, A., Aznar, M., Corella. (1996). Biomass gasification with air in an atmospheric bubbling fluidized bed, effect of six operational variables on the quality of the produced raw gas. Ind. Eng. Chem. Res., 35, 2110-2120.
- Natarajan, E., Nordin, A., Rao, A. N. (1998). Overview of combustion and gasification of rice husk in fluidized bed reactors. Biomass and Bioenergy, 14, 5, 533-546.
- Nishiwaki, A. (1997). Analysis of a two-stage fermentor with cell recycling for continuous acetic acid production. Journal of Fermentation and Bioengineering, 83, 6, 565-570.
- Parekh, S. R., Cheryan, M. (1994). Continuous production of acetate by *Clostridium thermoaceticum* in a cell recycle membrane bioreactor. Enzyme Microb. Technol., 16, 104-109.
- Pezacka, E., Wood, H. G. (1984). The synthesis of acetyl-CoA by *Clostridium thermoaceticum* from carbon dioxide, hydrogen, coenzyme A and methyltetrahydrofolate. Arch. Microbiol., 137, 63-69.
- Phillips, J. R., Klasson, K. T., Clausen, E. C., Gaddy, J. L. (1993). Biological production of ethanol from coal synthesis gas, Medium development studies. Applied Biochemistry and Biotechnology, 39/40, 559-571.
- Phillips, J. R., Clausen, E. C., Gaddy, J. L. (1994). Synthesis gas as a substrate for the biological production of fuels and chemicals. Applied Biochemistry and Biotechnology. 45/46, 145-157.
- Picataggio, S. K., Zhang, M., Eddy, C., Deanda, K. A., Finkelstein, M. (1997). Recombinant zymomonas for pentose fermentation. United States Patent # 5,514,583.
- Plackett, R. L., Burman, J. P. (1946). The design of optimum multifactorial experiments. Biometrika, 33, 305-325.
- Poulopoulos, S., Philippopoulos, C. (2000). Influence of MTBE addition into gasoline on automotive gas exhaustions. Atmospheric Environment, 34, 4781-4786.
- Prince, R. C., Liu, C. L., Morgan, T. V., Mortenson, L. E. (1985). Formate dehydrogenase from *Clostridium pasteurianum*: Electron paramagnetic resonance spectroscopy of the redox active centers. FEBS Letters, 189, 2, 263-266.

- Qureshi, N., Meagher, M. M., Hutkins, R. W. (1999). Recovery of butanol from model solutions and fermentation broth using a silicate/silicone membrane. Journal of Membrane Science, 158, 115-125.
- Rajagopalan, S. (2001). Microbial conversion of syngas to ethanol. Ph.D dissertation, Oklahoma State University, Stillwater, Oklahoma.
- Rajagopalan, S., Datar, R. P., Lewis, R. S. (2002). Formation of ethanol from carbon monoxide via a new microbial catalyst. Biomass and Bioenergy, 23, 487-493.
- Rani, S. K., Swamy, M. V., Seenayya, G. (1994). High ethanol production by new isolates of *Clostridium thermocellum*. Biotechnology Letters, 18, 8, 957-962.
- Rani, S. K., Swamy, M. V., Seenayya, G. (1997). Increased ethanol production by metabolic modulation of cellulose fermentation in *Clostridium thermocellum*. Biotechnology Letters, 19, 8, 819-823.
- Rao, G., Mutharasan, R. (1987). Altered electron flow in continuous cultures of *Clostridium acetobutylicum* induced by viologen dyes. Applied and Environmental Microbiology, 53, 6, 1232-1235.
- Rao, G., Mutharasan, R. (1988). Altered electron flow in a reducing environment in *Clostridium acetobutylicum*. Biotechnology Letters, 10, 2, 129-132.
- Reed, T. B., Jantzen, D. (1979). Biomass gasification: principles and technology. Energy Technology Review, 67, 27-90.
- Renewable Fuels Association. (2003). Ethanol industry outlook 2003: Building a secure energy future, 1-14.
- Riesenberg, D., Guthke, R. (1999). High cell density cultivation of microorganisms. Appl. Microbiol. Biotechnol., 51, 422-430.
- Roy, D., Valsaraj, K. T., Kottai, S. A. (1992). Separation of organic dyes from wastewater using colloidal gas aphrons. Sep. Sci. Technol., 25, 573-578.
- Russell, W. K., Lindahl, P. A. (1998). CO/CO<sub>2</sub> potentiometric titrations of carbon monoxide dehydrogenase from *Clostridium thermoaceticum* and the effect of CO<sub>2</sub>. Biochemistry, 37, 10016-10026.
- Sadaka, S. S., Ghaly, A. E., Sabbah, M. A. (2002). Two phase biomass air-steam gasification model for fluidized bed reactors: Part II—model sensitivity. Biomass and Bioenergy, 22, 6, 463-477.

- Sanderson, M. A., Reed, R. L., McLaughlin, S. B., Wullschleger, S. D., Conger, B. V., Parrish, D. J., Wolf, D. D., Taliaferro, C., Hopkins, A. A., Ocumpaugh, W. R., Hussey, M. A., Read, J. C., Tischler, C. R. (1996). Switchgrass as a sustainable bioenergy crop, Bioresource Technology, 56, 1, 83-93.
- Schmidt, S. R., Launsby, R. G. (1994). Understanding industrial designed experiments. 4<sup>th</sup> edition, Air Academy Press, Colorado Springs, CO.
- Schroen, C. G. H. P., Woodley, J. M. (1997). Membrane separation for downstream processing of aqueous-organic bioconversions. Biotechnology Progress, 13, 276-283.
- Sebba, F. (1971). Microfoams- an unexploited colloid system. Journal of Colloid and Interface Science, 35, 4, 643-646.
- Sebba, F. (1985). An improved generator for micron-sized bubbles. Chemistry and Industry, February 4, 91-92.
- Sebba, F. (1987). Foams and Biliquid Foams- Aphrons, John Wiley and Sons, New York.
- Seravalli, J., Ragsdale, S. W. (2000). Channeling of carbon monoxide during anaerobic carbon dioxide fixation. Biochemistry, 39, 6, 1274-1277.
- Shanmugasundaram, T., Sundaresh, C. S., Kumar, G. K. (1993). Identification of a cysteine involved in the interaction between carbon monoxide dehydrogenase and corrinoid/Fe-S protein from *Clostridium thermoaceticum*, FEBS Letters, 326, 1-3, 281-284.
- Shenkman, R. S. (2003). Personal communication. Oklahoma State University, Stillwater, OK.
- Shuler, M. L., Kargi, F. (1992). Bioprocess engineering: Basic concepts. Prentice Hall, Englewood Cliffs, New Jersey.
- Slaff, G.F. (1984). Ph.D. thesis, University of Pennsylvania, University Microfilms International, Ann Arbor, MI.
- Sreekumar, O., Chand, N., Basappa, S. C. (1999). Optimization and Iteration of Media Components in Ethanol Production Using *Zymomonas mobilis* by Response Surface Methodology. Journal of Bioscience and Bioengineering, 88, 3, 334-338.
- Sun, J. H., Hyman, M. R., Arp, D. J. (1992). Acetylene inhibition of *Azotobacter vinelandii* hydrogenase: acetylene binds tightly to the large subunit. Biochemistry, 31, 12, 3158-3165.
- Sun, Y., Cheng, J. (2002). Hydrolysis of lignocellulosic materials for ethanol production: a review. Bioresource Technology, 83, 1-11.

- Szczodrak, J., Fiedurek, J. (1996). Technology for conversion of lignocellulosic biomass to ethanol. Biomass and Bioenergy, 10, 5/6, 367-375. Shenkman, R. M. (2003). Personal communication. Oklahoma State University, Stillwater, Oklahoma.
- Taliaferro, C. M., Horn, F. P., Tucker, B. B., Totusek, R., Morrison, R. D. (1975). Performance of three warm-season perennial grasses and a native range mixture as influenced by N and P fertilization. Agronomy Journal, 67, 289-292.
- Tanner, R. S., Miller, L. M., Yang, D. (1998). *Clostridium ljungdahlii* sp. Nov, an acetogenic species in clostridial rRNA homology group I. International Journal of Systematic Bacteriology, 43, 2, 232-236.
- Tanner, R. S. (2003). Personal Communication. Professor, Department of Botany and Microbiology, University of Oklahoma, Norman, Oklahoma.
- Tibelius, K. H., Knowles, R. (1984). Hydrogenase activity in *Azospirillum brasilense* is inhibited by nitrite, nitric oxide, carbon monoxide, and acetylene. Journal of Bacteriology, 160, 1, 103-106.
- Tolbert, V. L., Wright, L. L. (1998). Environmental enhancement of U.S. biomass crop technologies: research results to date. Biomass and Bioenergy, 15, 1, 93-100.
- Ugarte, D. D. L., Walsh, M. (2002). Synergism between agricultural and energy policy: The case of dedicated bioenergy crops. Presented at Southern Agricultural Economics Association Annual Meeting, Orlando, Florida, February 2-5, 2002, 1-10.
- US Department of Energy. (1997). Alternatives to traditional fuels. DOE-EIA-0585. Distribution category UC-950. Office of coal, nuclear, electric and alternate fuels. Washington DC.
- Vega, J. L., Holmberg, V. L., Clausen, E. C., Gaddy, J. L. (1989a). Fermentation parameters of *Peptostreptococcus productus* on gaseous substrates (CO, H<sub>2</sub>/CO<sub>2</sub>). Arch. Microbiol., 151, 65-70.
- Vega, J. L., Prieto, S., Elmore, B. B., Clausen, E. C., Gaddy, J. L. (1989b). The biological production of ethanol from synthesis gas. Applied Biochemistry and Biotechnology, 20/21, 781-797.
- Vega, J. L., Clausen, E. C., Gaddy, J. L. (1990). Design of bioreactors for coal synthesis gas fermentations. Resources, Conservation and Recycling, 3, 149-160.
- Vijjeswarapu, W. K., Chen, W. Y., Foutch, G. L. (1985). Performance of a cell recycling continuous fermentation system for the production of n-butanol by *Clostridium acetobutylicum*. Biotechnology and Bioengineering, Symposium No. 15, 471-477.

- Wheals, A. E., Basso, L. C., Alves, D. M. G., Amorim, H. V. (1999). Fuel ethanol after 25 years. Tibtech, 17, December, 482-487.
- Wood, H. G., Ragsdale, S. W., Pezacka, E. (1986). The Acetyl CoA pathway for autotrophic growth. FEMS Microbiology Rev, 39, 345-362.
- Worden, R. M., Grethlein, A. J., Zeikus, J. G., Datta, R. (1989). Butyrate production from carbon monoxide by *Butyribacterium methylotrophicum*. Applied Biochemistry and Biotechnology, 20/21, 687-698.
- Worden, R. M., Grethlein, A. J., Jain, M. K., Datta, R. (1991). Production of butanol and ethanol from synthesis gas via fermentation. Fuel, 70, 615-619.
- Worden, R. M., Bredwell, M. D., Grethlein, A. J. (1997). Engineering issues in synthesis gas fermentations. *Fuels and Chemicals from Biomass*, American Chemical Society, 320-335.
- Wright, L. L. (1994). Production technology status of woody and herbaceous crops. Biomass and Bioenergy, 6, 191-209.
- Xia, J., Sinclair, J. F., Baldwin, T. O., Lindahl, P. A. (1996). Carbon monoxide dehydrogenase from *Clostridium thermoaceticum*: Quaternary structure, stoichiometry of its SDS-induced dissociation and characterization of the faster migrating form. Biochemistry, 35, 1965-1971.
- Yang, X., Tsao, G. T. (1994). Mathematical modeling of inhibition kinetics in acetone-butanol fermentation by *Clostridium acetobutylicum*. Biotechnology Progress, 10, 532-538.
- Zervas, E., Montagne, X., Lahaye, J. (2001). Emission of specific pollutants from a compression ignition engine. Influence of fuel hydrotreatment and fuel/air equivalence ratio. Atmospheric Environment, 35, 1301-1306.

2

VITA

Rohit Pradeep Datar

Candidate for the Degree of

Doctor of Philosophy

Thesis: ANEROBIC FERMENTATION OF BIOMASS-GENERATED PRODUCER  
GAS TO ETHANOL

Major Field: Chemical Engineering

Biographical:

Personal Data: Born in Mumbai, India, On December 07, 1977, the son of Pradeep Datar and Manik Datar.

Education: Graduated from Sathaye College, Mumbai, India in May 1995; received Bachelor of Engineering degree in Chemical Engineering from University of Pune, Pune, India in May 1999. Completed the requirements for the Doctor of Philosophy degree with a major in Chemical Engineering at Oklahoma State University in December 2003.

Experience: Research Assistant, Chemical Engineering, Oklahoma State University from August 1999 to August 2003; Teaching Assistant, Chemical Engineering Process Modeling from August 2001 to December 2001; Research Intern, National Renewable Energy Laboratory from May 2002 to August 2002.

Professional Memberships: American Institute of Chemical Engineers.

**OKLAHOMA STATE UNIVERSITY  
INSTITUTIONAL REVIEW BOARD  
FOR HUMAN SUBJECTS RESEARCH**

**Date:**

**IRB#:**

**Proposal Title:** ANAEROBIC FERMENTATION OF BIOMASS GENERATED  
PRODUCER GAS TO ETHANOL

**Principal Investigator(s):** Randy Lewis Professor, Rohit Datar Student

**Reviewed and Processed as:** Exempt

**Approval Status Recommended by Reviewer(s):** Approved with Provisions

APPROVAL STATUS SUBJECT TO REVIEW BY FULL INSTITUTIONAL  
REVIEW BOARD AT NEXT MEETING.

APPROVAL STATUS PERIOD VALID FOR ONE CALENDAR AFTER WHICH A  
CONTINUATION OR RENEWAL REQUEST IS REQUIRED TO BE SUBMITTED  
FOR BOARD APPROVAL. ANY MODIFICATIONS TO APPROVED PROJECT  
MUST ALSO BE SUBMITTED FOR APPROVAL.

---

Comments. Modifications/Conditions for Approval or Reasons for Deferral or  
Disapproval are as follows:

Signature: \_\_\_\_\_

Chair of Institutional Review Board

Date: \_\_\_\_\_